2012

The Role of CD147 in Breast Cancer Progression

George Daniel Grass
Medical University of South Carolina

The Role of CD147 in Breast Cancer Progression

by

George Daniel Grass

A dissertation submitted to the faculty of the Medical University of South Carolina in partial fulfillment of the requirement for the degree of Doctor of Philosophy in the College of Graduate Studies.

Department of Regenerative Medicine and Cell Biology

2012

Approved by:

Chairman, Advisory Committee

Bryan P. Toole, Ph.D.

W. Scott Argraves, Ph.D.

David J. Cole, M.D.

Robert G. Gourdie, Ph.D.

Dennis K. Watson, Ph.D.

Acknowledgements

First of all, I would like to express my deepest gratitude to my mentor, Dr. Bryan Toole. Bryan gave me the opportunity to begin learning research techniques in his laboratory the summer before and all throughout my first two years of medical school. His strong advocacy allowed me to gain admission into the Medical Scientist Training Program, which would have been impossible without his support and guidance. I want to especially thank Bryan for his patience as I bombarded him with various project ideas over the years and his polite response of "Focus." I also would like to thank him for taking his time to mold me into a capable scientist and giving me the tools to succeed in academia in the future. Most of all, I would like to thank him for his friendship and the opportunity to experience great Australian cooking.

I would next like to thank my committee members, Dr. Scott Argraves, Dr. David Cole, Dr. Robert Gourdie and Dr. Dennis Watson. Their advice and insightful critiques during our many meetings improved my presentation skills and the quality of this dissertation.

I would like to thank past and current members of the Toole laboratory. First, I would like to thank Mark Slomiany for his mentorship during my initial transition into the laboratory. Next, I would like to thank Momka Bratoeva, Lauren Tolliver, Lu Dai, and Maria Guinea for their technical assistance with various aspects of this dissertation and for their friendship and support.

I want to acknowledge Dr. Perry Halushka and the many students that I have met in the MUSC MSTP for their support and guidance during this process.

Most of all, I thank my family for their encouragement and support. I would especially like to thank my beautiful wife, Kate, for her unwavering support during my research. I would not be where I am today without her love and sacrifice.

Table of Contents

Abbreviations

µM - Micromolar

2D – Two dimensional

3D- Three dimensional

AMPK – Adenosine monophosphate kinase

AnxA2 - Annexin II

AOBS – Acoustic optical beam splitter

AP-1/2-Activator protein 1/2

AP1B – Adaptor protein 1B

Arp2/3 – Actin-related proteins 2/3

ASCT2 – Sodium-dependent neutral amino acid transporter type 2

ATCC – American Type Culture Collection

B-gal – Beta galactosidase

BCA - Bicinchoninic acid assay

BCRP – Breast cancer resistance protein

BL – Basolateral

Bp- Base pair

BSA – Bovine serum albumin

cAMP – Cyclic adenosine monophosphate

CCL – Chemokine (C-C motif) ligand

cDNA – Complementary deoxyribonucleic acid

CGI- CpG island

cGMP- Cyclic guanosine monophosphate

CIE – Clathrin-independent endocytosis

CRP- C-reactive protein

CspA – Cyclosporine A

CT – Cycle threshold

Ctx-B – Cholera toxin-B

CXCL - Chemokine (C-X-C motif) ligand

Cyp - Cyclophilin

DIC – Differential interference contrast

DTT – Dithiothreitol

ECM- Extracellular matrix

EEA1 – Early endosomal antigen 1

EGF- Epidermal growth factor

EGFR- Epidermal growth factor receptor

EGR2- Early growth response protein 2

EMMPRIN- Extracellular Matrix Metalloproteinase Inducer

EMT- Epithelial-mesenchymal transition

EpCAM – Epithelial cell adhesion molecule

ER- Estrogen receptor

ErbB2 – Epidermal growth factor receptor 2

ERK- Extracellular signal-regulated kinase

ETS- E-twenty six

EV – Empty vector

FACS –Fluorescent activated cell sorting

FAK – Focal adhesion kinase

FBS – Fetal bovine serum

FGF – Fibroblast growth factor

FGFR – Fibroblast growth factor receptor

FRET- Fluorescence resonance energy transfer

GAP – GTPase activating protein

GDP – Guanosine diphosphate

GEF – GTP exchange factor

GLUT1 – Glucose transporter 1

GPCR- G-protein coupled receptor

Grb2 - Growth factor receptor-bound protein 2

GST – Glutathione S-transferase

GTP- Guanosine triphosphate

HA - Hyaluronan

HCC – Hepatocellular carcinoma

HCl – Hydrogen chloride

HG- High-glycosylated

HIF2α – Hypoxia-inducible factor 2 alpha

HNSCC – Head and neck squamous cell carcinoma

HRP – Horseradish peroxidase

HSP – Heat shock protein

IG- Immunoglobulin

IGSF- Immunoglobulin superfamily

IL- Interleukin

JNK – c-Jun-N-terminal kinase

kDa- Kilodalton

LAT1 – L-type amino acid transporter 1

LG- Low-glycosylated

MAPK – Mitogen-activated protein kinase

MCT – Monocarboxylate transporter

MDR – Multidrug resistance

MEGM – Mammary epithelial growth medium

MEK - Mitogen-activated protein kinase kinase

MHC- Major histocompatibility complex

miRNA- Micro RNA

mM – Millimolar

MMP- Matrix Metalloproteinase

MOI – Multiplicity of infection

mRNA – Messenger RNA

MT1-MMP – Membrane type 1 MMP

MWCO – Molecular weight cut-off

NaCl – Sodium chloride

NAD- Nicotinamide adenine dinucleotide

NAMPT- Nicotinamide phosphoribosyltransferase

NF-κβ- Nuclear factor kappa beta

nm – Nanometer

nM - Nanomolar

NO- Nitric oxide

oHA – Hyaluronan oligosaccharide

PBS – Phosphate buffer saline

PGC-1α- peroxisome proliferator-activated receptor -coactivator 1

PgP – P-glycoprotein

PI3K- Phosphatidylinositol 3-kinase

PIP_2 – Phosphatidylinositol-3,4-bisphosphate

PIP_3 – Phosphatidylinositol-3,4,5-triphosphate

PKC- Protein kinase C

PKG- Protein kinase G

PLA – Proximity ligation assay

PMSF - Phenylmethanesulfonylfluoride

PPAR – Peroxisome proliferator-activated receptor

PPIase – Peptidyl-prolyl *cis-trans* isomerase

qRT-PCR – Quantitative RT-PCR

RACK1- Receptor for activated protein kinase C1

RANKL- Receptor activator for NF-κβ

Rb - Recombinant

RBD – Ras-binding domain

RGD - Arginine-Glycine-Aspartic acid

RING-CH E3 – (really interesting new gene)-CH ubiquitin E3 ligase

RIPA – Radioimmunoprecipitation buffer

RNA – Ribonucleic acid

ROCK – Rho-kinase

RPMI – Roswell Park Memorial Institute Medium

RTK – Receptor tyrosine kinase

RT-PCR – Reverse transcription polymerase chain reaction

SCC- Squamous cell carcinoma

SCP-2- Sterol carrier protein 2

SDS-PAGE- Sodium dodecyl sulfate polyacrylamide gel electrophoresis

SEM – Standard error of the mean

SHC – Src homology 2-contaning adaptor protein

SHP-1- Src homology region 2 domain-containing phosphatase-1

siRNA- Small interfering RNA

SNP- Single nucleotide polymorphism

Sp1- Specificity protein 1

STAT3- Signal transducers and activators of transcription 3

TCF/LEF1 – T cell factor/lymphocyte enhancer factor 1

TCSF- Tumor cell-derived Collagenase-Stimulatory Factor

TF- Transcription factor

TGFβ- Transforming growth factor beta

TIMP – Tissue inhibitor of MMPs

TIRF – Total internal reflection fluorescence

TNFα- Tumor necrosis factor alpha

TSH – Thyroid stimulating hormone

TSK5 – Tyrosine kinase substrate with 5 SH3 domains

TYR – Tyrosine

UCH-L1 – Ubiquitin c-terminal hydrolase L1

uPA – Urokinase-type plasminogen activator

UTR- Untranslated region

VEGF –Vascular endothelial growth factor

VEGFR – Vascular endothelial growth factor receptor

WASP- Neural Wiskott-Aldrich syndrome protein

WAVE2 – Wiskott-Aldrich syndrome protein 2

ZEB-1/2 - Zinc finger E-box-binding homeobox 1/2

ABSTRACT

GEORGE DANIEL GRASS. The role of CD147 in Breast Cancer Progression

(Under the direction of BRYAN P. TOOLE)

In the U.S., approximately 40,000 women will die from breast cancer this year, while an additional 230,500 women will be newly diagnosed with invasive breast disease. Despite tremendous advancement leading to earlier detection and novel therapeutic approaches, recurrent metastatic breast cancer remains a major cause of mortality. Invasive breast cancer cells employ specialized actin-rich protrusions called invadopodia, which are enriched in proteases, to degrade the extracellular matrix and these structures correlate with metastasis *in vivo*. The multifunctional immunoglobulin superfamily protein emmprin (CD147) is highly enriched on the surface of malignant breast cancer cells and is associated with matrix metalloproteinase (MMP) induction and invasion. In this dissertation we found that CD147 regulates the activity of invadopodia in non-transformed breast epithelial cells and invasive breast cancer cells by regulating the expression and localization of membrane type-1 MMP (MT1-MMP). Furthermore, we discovered that up-regulation of CD147 regulates invasiveness by facilitating the assembly of multi-protein signaling complexes containing CD147, CD44 and EGFR. Assembly of these complexes leads to the activation of EGFR-Ras-MEK-ERK signaling cascades. We further found that Ras regulates CD147 expression and may participate in a complex feedback loop involving hyaluronan-CD44 interactions and ERK signaling. Lastly, we observed that sub-populations of cells with differential CD147 surface expression correlate with distinct functional phenotypes. Our work has begun to unravel

the complexity of CD147 function in breast cancer invasion and provides strong evidence that CD147 should be a therapeutic target in future studies.

Chapter 1: An Overview of CD147 Biology

Introduction

CD147 is a type I integral membrane protein belonging to the Ig superfamily that is variably glycosylated and expressed across several tissue types. The expression of CD147 is elevated on the surfaces of various cancer types, whereas the expression in most normal tissues is at much lower levels. CD147 was originally identified as a tumor-associated protein that stimulates matrix metalloproteinase (MMP) production in fibroblasts, but over the years it has become clear that CD147 is a molecule with pleiotropic biology. In addition to MMP induction, the role of CD147 in cancer progression has been associated with multi-therapy resistance, angiogenesis, migration, invasion and chaperoning of metabolic transporters to the cell surface.

CD147 Nomenclature and Gene and Protein Structure

Nomenclature

CD147 was identified and characterized independently under numerous names in various species and tissues using different experimental protocols: RET-PE2 (Finnemann et al., 1997), CE9 (Nehme et al., 1993) and OX-47 (Fossum et al., 1991) in rats, gp42 (Altruda et al., 1989) and basigin (Miyauchi et al., 1990) in mice, HT7 (Seulberger et al., 1990), neurothelin (Schlosshauer et al., 1995), and 5A11 (Fadool and Linser, 1993) in

chickens, the human leukocyte-activation associated antigen M6 (Kasinrerk et al., 1992), the blood group Ok^a antigen (Spring et al., 1997), the hepatoma-associated antigen HAb18G (Jiang et al., 2001) and matrix-metalloproteinase (MMP)-inducing factor, emmprin (Biswas et al., 1995) in humans. CD147 was first functionally characterized by Biswas and colleagues (Biswas, 1984; Ellis et al., 1989) using a co-culture system with lung carcinoma cells and fibroblasts, in which they identified a Tumor cell-derived Collagenase-Stimulatory Factor (TCSF) that was present on the cell surface and in conditioned media. In later years, in addition to collagenase (matrix metalloproteinase-1; MMP-1), TCSF was found to stimulate increases in both message and protein levels of MMP-2 and MMP-3 and was renamed to Extracellular Matrix Metalloproteinase Inducer (emmprin) (Biswas et al., 1995; Kataoka et al., 1993). It is now clear that all of the above designated proteins are in fact the same and are now commonly termed CD147 (Kanekura et al., 1991; Kasinrerk et al., 1992; Yan et al., 2005).

Gene Structure

The gene locus for CD147 is located at chromosome 19p13.3 in human (Kaname et al., 1993) and was originally thought to contain eight exons spanning over 10.8 kilobases (Guo et al., 1998), but new evidence suggests that the CD147 gene contains 10 exons that span 15,000 nucleotides (Belton et al., 2008; Liao et al., 2011). Interestingly, the CD147 gene displays many unique features including: a multi-exon 3'-untranslated region (3'-UTR), immunoglobulin (Ig)-like domains encoded by paired exons, and a junctional exon of the second Ig-like domain encoding the transmembrane domain and part of the cytoplasmic domain (Guo et al., 1998). The CD147 gene is flanked on the 5' end with a CpG island (CGI)-rich sequence in the promoter region, which was previously

described to lack CAAT or TATA boxes, but subsequent evidence suggests this promoter region may contain a TATA box (Liang et al., 2002). The mouse CD147 gene is located on chromosome 10 and is smaller in size compared to the human gene due to shorter intronic sequences interspersed between size-conserved exonic sequences (Cheng et al., 1994; Guo et al., 1998; Miyauchi et al., 1995).

Message and Protein Organization

Based on data in the Entrez Gene database, the CD147 gene is encoded into 4 variant transcripts, designated as CD147-1,2,3 and 4 (Figure 1-1). Recent findings have demonstrated that alternative splice variants of CD147 are formed: a tissue specific variant resulting in three Ig-like domains (CD147-1) was identified in the retina (Hanna et al., 2003; Ochrietor et al., 2003) as well as two other variants lacking the N-terminal Ig-like domain (CD147-3 and CD147-4) (Belton et al., 2008; Liao et al., 2011). However, CD147-2 is the most abundant, widely distributed and best characterized isoform and will be designated as CD147 hereafter. Sequence analysis of CD147 by several groups revealed that it is a single-chain type I transmembrane molecule and member of the Ig superfamily (IgSF). The mRNA transcript for CD147 encodes a 269 amino acid protein that is composed of a 21 amino acid signal sequence, a 186 residue-long extracellular portion consisting of two Ig-like domains at the N-terminus, a 21 amino acid transmembrane domain, and a 41 residue cytoplasmic domain at the C-terminus (Weidle et al., 2010).

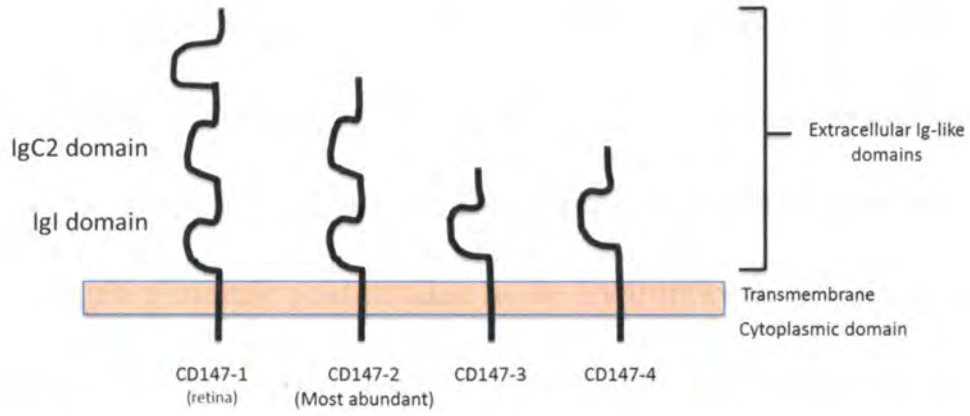

Figure 1-1. CD147 isoforms. CD147 alternative splice variant protein structures. CD147-2 is the most abundant and best characterized isoform and will be designated as CD147 hereafter.

Due to the presence of certain sequence motifs, CD147 has been described to have homology to both the major histocompatibility complex class II (MHC II) beta-chains and Ig variable domain (V); this has led some investigators to propose that CD147 may be an evolutionary intermediate between a primordial Ig form and MHC II-beta chain-like and V domain-containing molecules (Altruda et al., 1989; Fossum et al., 1991; Kanekura et al., 1991; Miyauchi et al., 1990; Miyauchi et al., 1991). In line with this, high resolution crystallography has revealed that CD147 contains a N-terminal IgC2 domain and a membrane proximal IgI domain that are organized in a unique manner, thus distinguishing CD147 from other IgSF proteins (Yu et al., 2008). The protein sequence shows varying conservation across several species, especially in the extracellular domains, but the linker sequence between the Ig-like domains, the cysteine residues, asparagine glycosylation sites, transmembrane domain, and cytoplasmic domain demonstrate strong homology (Fossum et al., 1991; Miyauchi et al., 1995; Schuster et al., 1996; Seulberger et al., 1990; Yu et al., 2008). Interestingly, the highly conserved regions of CD147 contain unique structural characteristics. The flexible 5-residue linker

domain has been shown to provide CD147 a great deal of domain mobility, possibly allowing the first IgC2 domain to alter its orientation to interact with ligands or adjacent binding partners (Yu et al., 2008). The transmembrane domain contains a uniquely-embedded charged glutamic acid residue in the hydrophobic-rich sequence as well as a leucine zipper motif (Yan et al., 2005). Proteins with these characteristics have been shown to oligomerize into multi-protein complexes and are often involved in cell signaling events: this is especially recognized in immune cell receptor complexes (Humphrey et al., 2005). Support for this homo- or hetero- oligomerization is found in a study identifying that polyleucine rich transmembrane domains with an embedded glutamate residue confer strong interactions between α-helices, possibly via hydrogen bonding (Zhou et al., 2001).

The predicted molecular weight from the sequence of CD147 is 27-29 kDa, yet many investigators discovered that CD147 migrates on sodium dodecyl-sulfate polyacrylamide gel electrophoresis (SDS-PAGE) between 31-65 kDa. Originally, discovered as a protein that carries a developmentally-regulated carbohydrate moiety, in conjunction with three conserved N-glycosylation sites, CD147 is classified as a glycoprotein. Studies with glycosylation inhibitors and specific lectins revealed that approximately 50% of the mass of CD147 is due to carbohydrate side groups bearing β1,6-branched, polylactosamine-type sugars, fucosylations, Lewis^x glycan epitopes, and sialylations (Kamada et al., 1987; Riethdorf et al., 2006; Tang et al., 2004a; Yang et al., 2011). CD147 glycoforms were previously characterized as low-glycosylated (LG) and high-glycosylated (HG) forms, representing ~32 kDa and ~45-65 kDa, respectively (Tang et al., 2004a). The LG-CD147 was found to contain a high-mannose carbohydrate,

whereas the HG-CD147 was enriched for branched polylactosamine chains. It is clear that CD147 is heterogeneously glycosylated across many tissue and cell types (Nakai et al., 2006) and even shows variations in glycosylation in cell lines derived from the same tissue of origin (Riethdorf et al., 2006). Currently, it is unclear whether different CD147 glycoforms have different biological functions.

Very little data exists on how CD147 glycosylation status is regulated. Currently the only published mechanistic data describes a role for caveolin-1 in regulating CD147 glycosylation. It was recognized that CD147 associates with caveolin-1 mostly on the cell surface via its membrane proximal IgI domain and that this association attenuates CD147 self-aggregation (Tang and Hemler, 2004). Further evaluation of this interaction, revealed that LG-CD147 preferentially associated with caveolin-1 and that the caveolin-1-CD147 interaction inhibited CD147-induced MMP induction (Tang et al., 2004a). The authors of these studies proposed that caveolin-1 associates with CD147 during its transit through the golgi and two divergent pathways regulate CD147 glycosylation status: 1) CD147 associates with caveolin-1 and is escorted to the cell surface forming caveolin-1-CD147 complexes possibly in membrane compartments adjacent to lipid rafts; 2) N-acetylglucosaminyltransferase V initiates the addition of β1,6-branched polylactosamine-type sugars on CD147, forming HG-CD147, which does not bind caveolin-1 and is thought to be the major active form of CD147 in relation to MMP induction. However, other studies have found that up-regulation of caveolin-1 increases MMP synthesis (Jia et al., 2006). Further clarification of this mechanism is needed as these authors previously published apparently contradictory data suggesting that HG-CD147 associated with caveolin-1and that the majority of the identified CD147-caveolin-1 complex was isolated

after cell surface biotinylation (Tang and Hemler, 2004). However, there may be a small sub-population of caveolin-1 in the golgi that regulates CD147 glycosylation distinct from caveolin-1 pools present on the cell surface. Alternatively, a less clarified mechanism has also suggested that hypoxia increases the HG-CD147 glycoform, which is independent of an increase in transcription (Floch et al., 2011).

Regulation of CD147 Expression

Transcriptional Regulation

As mentioned previously, prior characterization of the promoter region of CD147, consisting of 950 base pairs (bp) upstream of the transcription start site, revealed that it is enriched in a CGI and contained consensus binding sites for the transcription factor (TF) specificity protein 1 (Sp1) and activator protein 2 (AP-2) (Guo et al., 1998). Subsequent promoter analysis demonstrated that a fragment 471 bp upstream of the previously identified coding region was necessary to mediate CD147 transcription: deletion analysis of this fragment revealed that a 30 bp element from -142 to -112 bp, containing overlapping binding sites for Sp1, AP-1, early growth response protein 2 (EGR2), and transcription factor II (TFII), was sufficient to initiate CD147 transcription. Of these potential regulatory TFs, only Sp1 demonstrated binding to the 30 bp region and cooperated with Sp3 to augment CD147 transcription. Interestingly, this study also identified a negative regulatory element in the 5'-flanking segment consisting of the -1413 to -1024 bp region, though this regulatory region needs further evaluation (Liang et al., 2002). Further studies, demonstrated that a 66 bp region (-108 to -42) containing the

third Sp1 binding site, was the minimal essential element needed to regulate constitutive CD147 expression (Kong et al., 2011b). Though Sp1 appears to be the main transcriptional regulator of CD147, other studies also support a role for EGR2 (Dai et al., 2012). In addition to this first recognized promoter, a new study found that an alternative promoter located in the -656 to -473 bp region upstream of exon 1 regulated CD147-3/4 expression, which was distinct from the promoter regulating CD147-1/2 (Liao et al., 2011).

Due to the fact that Sp1 binds to CpG motifs present in CGIs, which can be epigenetically modified by methylation, Sp1-mediated transcriptional initiation can be regulated by altered binding affinity to methylated CpG motifs present in promoters (Deaton and Bird, 2011). In support of this, the CD147 promoter was found to be hypomethylated in cancer tissue compared to normal tissue, resulting in increased Sp1 binding and subsequently increased CD147 expression (Kong et al., 2011a). This evidence clearly supports the idea that CD147 expression is regulated via Sp1-mediated events. Although previous studies demonstrated that Sp1 is a ubiquitous TF that is a constitutive activator of housekeeping genes, accumulating evidence now suggests it is also involved in the regulation of inducible genes (Wierstra, 2008).

In addition to Sp1, CD147 has been shown to be regulated by Snail-1 (Snail) (Kuphal et al., 2005) and Snail-2 (Slug) (Wu et al., 2011a), TFs that orchestrate the epithelial-mesenchymal transition (EMT). The latter study by Wu et. al determined that Slug, but not Snail, binds to an E-box 2 domain located in a 306 bp region of the CD147 promoter (-644 to -338), which results in CD147 transcription. Interestingly, transforming growth factor-beta (TGF-β)-induced CD147 expression was attenuated by

knockdown of other EMT-related TFs, such as ZEB-1 and ZEB-2; this down-regulation of CD147 may be due to upstream regulation of factors that directly bind to the CD147 promoter rather than direct promoter activation. A possible association between the E-twenty six (ETS) TF family member PEA3 and CD147 may exist, but this study only demonstrated a co-staining pattern in tumor tissues (Davidson et al., 2003b). Treatment of ovarian cancer cells with signal transducers and activators of transcription 3 (STAT3) decoy oligodeoxynucleotides resulted in decreased CD147 expression, suggesting that STAT3 may have a role in regulating CD147 transcription (Zhang et al., 2010). In addition, a transcriptionally active fragment of Sterol-Carrier Protein 2 (SCP-2), which regulates cycling of endogenous cholesterol between membrane compartments, thus altering cholesterol metabolism, was found to increase CD147 transcription (Ko and Puglielli, 2007). This study identified a high affinity binding site in the -245 to -95 bp region and a low affinity binding site between the -392 to -242 bp region in the CD147 promoter. A recent study employing a 1 kb fragment upstream of the mouse CD147 coding sequence found an E2F binding site that mediated nitric oxide (NO)-induced repression of CD147 in cardiomyocytes, which was dependent on a cyclic guanosine monophosphate (cGMP)-dependent protein kinase G (PKG) pathway (Tarin et al., 2011). Thus, it is clear that many transcriptional regulators influence CD147 expression in various cellular contexts.

Control of CD147 expression by *cis*-regulatory elements and sequence variations/polymorphisms has also been described. Recently, the seed regions of let-7, a tumor-suppressive non-protein coding microRNA (miRNA) family, was shown to have complementary sequence to the 3'-UTR of CD147, with let-7b being the most

complementary (Fu et al., 2011a; Fu et al., 2011b). In addition, miRNA-492 was found to interact with the CD147 3'-UTR; interestingly, the efficiency to suppress CD147 expression was dependent on a single nucleotide polymorphism (SNP) located at the 4th nucleotide complementary to the miRNA-492 seed region (Wu et al., 2011b). It is thought that ~2-6 contiguous base pairs in the seed region of miRNAs are needed for effective miRNA-mRNA duplex formation and target suppression (Brodersen and Voinnet, 2009), hence the SNP in the miRNA-492 binding site may alter affinity to the CD147 3'-UTR resulting in differential suppression of CD147. Other SNPs located in the membrane-proximal IgI domain and 3'-UTR have been shown to alter CD147 expression in the equine genus (Koho et al., 2012), though the relevance in humans is currently unknown.

Regulators of CD147 Upstream of Transcription Factors

Many studies have identified factors upstream of the CD147 transcription initiators and repressors mentioned above. Some of the earliest studies identified an increase in CD147 expression after activation of lymphocytes with granulocyte macrophage colony-stimulating factor (GM-CSF), concanavalin-A or phytohemagglutinin (Kasinrerk et al., 1992; Paterson et al., 1987). Additionally, endothelial cells that invaded co-cultured brain tissue demonstrated increased CD147 expression (Risau et al., 1986). These earlier studies set the premise that CD147 may be an inducible molecule in both physiological and pathological contexts.

Over the years many soluble factors such as growth factors, cytokines and hormones have been shown to regulate CD147 expression (see Table 1-1). In breast

cancer cells, epidermal growth factor (EGF) and amphiregulin induced the expression of CD147 via a EGF receptor (EGFR) kinase activation pathway (Menashi et al., 2003; Xu et al., 2011). In addition, TGFβ induced CD147 expression via a phosphatidylinositol-3-kinase (PI3K) -Akt pathway in hepatocytes (Wu et al., 2011a).

Since CD147 most likely has a role in inflammation, ischemic injury, atherosclerosis, rheumatoid arthritis and tissue repair (Gabison et al., 2009; Yan et al., 2005), it is no surprise that it is regulated by inflammatory mediators. A coculture model between macrophages and breast or ovarian cancer cells demonstrated that cancer-associated CD147 is induced via a tumor necrosis factor alpha (TNFα)-c-Jun-N-terminal kinase 2 (JNKII)-nuclear factor kappa-light-chain-enhancer of activated B cells (NF-κβ) pathway (Hagemann et al., 2005). CD147 is regulated by hydrogen peroxide (Siwik et al., 2008) and the cytokine interleukin-18 (IL-18) in both cardiomyocytes (Reddy et al., 2010) and smooth muscle cells (Venkatesan et al., 2009). Preliminary evidence suggests that IL-1 may also regulate CD147 expression in corneal fibroblasts, though in other cell types this does not seem to be the case (Braundmeier et al., 2006; Gabison et al., 2009). Another cytokine that regulates CD147 expression is receptor activator of NF-κβ ligand (RANKL), an osteoclastogenic mediator involved in bone remodeling in physiologic and pathologic states (Rucci et al., 2010; Si et al., 2003). Furthermore, in support of CD147 involvement in inflammation, treatment of cells with C-reactive protein (CRP) induced CD147 transcription (Abe et al., 2006) and iron deficiency upregulated CD147 via a p38-NFκβ related pathway (Fan et al., 2011b). NO treatment negatively regulated CD147 expression in cardiomyocytes, but had no regulatory role in macrophages, indicating cell-type specific regulation (Tarin et al., 2011). A recent finding also suggested a role for

prostaglandin E2 in regulating CD147 expression and this may involve an interaction with the non-tyrosine kinase c-Src (Lee et al., 2011).

Regulation of CD147 by sex hormones has been suggested by studies involving analysis of the menstrual cycle, pregnancy, and peri-implantation events. These studies found that CD147 expression was induced by both estrogen and progesterone, with the latter possibly regulating post-transcriptional glycosylations of the core protein (Braundmeier et al., 2006; Noguchi et al., 2003; Xiao et al., 2002). Analysis of estrogen receptor (ER)-α or –β null mice demonstrated that CD147 is regulated by ERα in select tissues, whereas in others it is independent of estrogen signaling. Furthermore, the regulation of CD147 expression seemed to be at the translational level rather than transcriptional (Chen et al., 2010). Other hormones that have been shown to regulate CD147 expression include the peptides Thyroid-stimulating hormone (TSH) (Fanelli et al., 2003; Nehme et al., 1995) and Angiotensin II (Pons et al., 2011; Yang et al., 2010a). Also, somatostatin was shown to increase CD147 cell surface levels in intestinal epithelial cells (Saksena et al., 2009). Interestingly, these hormones signal through G protein-coupled receptors (GPCRs), suggesting CD147 can be modulated via this pathway.

Other pathways that have been shown to regulate CD147 expression include: the Protein Kinase C delta (PKCδ)-ERK pathway in activated macrophages (Wang et al., 2011b) and β6 integrin-Fyn kinase signaling in oral squamous cell carcinoma (Ramos and Dang, 2011). Elevated expression of the scaffold protein receptor for activated protein kinase C1 (RACK1) was shown to increase CD147 expression in breast cancer (Cao et al., 2010). Also, Notch1 signaling has been shown to regulate CD147 expression

in breast cancer, though the exact mechanism of regulation is currently unknown (Wang et al., 2011a). An additional mechanism regulating CD147 expression is a positive feedback mechanism. This was demonstrated by treating fibroblasts with a recombinant soluble form of the extracellular domain of CD147 (rbCD147), which in turn, increased CD147 transcription (Tang et al., 2004b).

Interestingly, CD147 also appears to be regulated by several molecules involved in cell metabolism. As mentioned above, CD147 is regulated by a transcriptionally-active fragment of SCP-2, a protein involved in cholesterol metabolism (Ko and Puglielli, 2007) as well as TSH, a hormone that regulates global metabolism (Fanelli et al., 2003; Nehme et al., 1995). In this latter case, TSH induced CD147 expression in thyroid cells via a cyclic adenosine monophosphate (cAMP)-related pathway, but interestingly this regulation was at the post-transcriptional level. Also, peroxisome proliferator-activated receptor alpha and gamma (PPARα/γ) TFs have been shown to regulate CD147 expression, with the latter suppressing CD147 translation in activated macrophages (Ge et al., 2007; Konig et al., 2010). In relation to this aforementioned regulatory network, up-regulation of PPARγ-coactivator 1 alpha (PGC-1α) resulted in elevated CD147 expression in skeletal muscle cells (Benton et al., 2008). Additionally, the adipocytokine, nicotinamide phosphoribosyltransferase (NAMPT), a key enzyme involved in generating nicotinamide adenine dinucleotide (NAD), has been shown to increase CD147 expression via an ERK-p38-NF-κβ pathway (Fan et al., 2011a). In a recent study, it was demonstrated that elevated glucose concentration induces CD147 transcription (Bao et al., 2010). This compilation of data strongly suggests that CD147 may be a protein

related to the cellular response of metabolic stress or aids in the general metabolism of the cell.

In addition to being regulated by soluble factors that activate various signaling pathways, CD147 expression and cellular localization is determined by protein binding partners. One of the most studied and best characterized binding partners of CD147 are the family of MonoCarboxylate Transporters (MCTs). MCTs are proton-coupled transporters that mediate transit of L-lactate, pyruvate, and ketone bodies across the plasma membrane (Halestrap, 2011a). Earlier studies indicated that CD147 is tightly associated with MCT1 and MCT4 via a transmembrane/cytoplasmic domain interaction (Kirk et al., 2000), which was later determined to be mediated mainly by hydrophobic interactions in the c-terminal aspect of the transmembrane domain rather than ionic interactions with the glutamate residue (Finch et al., 2009; Wilson et al., 2009). This was later followed up with a fluorescence resonance energy transfer (FRET) study demonstrating that CD147 and MCTs interact and form a heterotetramer complex consisting of two central oligomerized CD147 molecules associated with peripherally localized MCTs (Wilson et al., 2002).

As it is clear that CD147 and the MCT isoforms 1,3, and 4 associate (Halestrap, 2011a), other studies evaluated whether either interacting member regulated expression or localization of the other. Knockdown of MCT1 expression resulted in an alteration of the CD147 glycoforms expressed, with a proclivity to accumulate the high-mannose form of CD147 relative to the highly-complex branched glycoform (Deora et al., 2005); interestingly no changes in mRNA were found with MCT1 knockdown, indicating regulation at the post-transcriptional level. In addition to regulation of CD147 protein,

specific membrane localization to the basolateral (BL) membrane was determined by dominant BL signals in MCT3 and MCT4, whereas CD147 contains a dominant BL signal at leucine 252 (Deora et al., 2004) that directs MCT1 localization. MCT3 knockout mice supported this conclusion as well, as they demonstrated reduced CD147 trafficking to the basolateral membrane (Daniele et al., 2008). A similar study found that depletion of MCT4 in metastatic breast cancer cells resulted in an enrichment of the high mannose glycoform of CD147, which did not traffic to the cell surface and remained confined to the endoplasmic reticulum; this study also found that there was no difference in mRNA levels of CD147 (Gallagher et al., 2007). Also, knockdown of CD147 resulted in decreased MCT4 protein, but not message, and caused an enrichment of MCT4 in endolysosomes, possibly leading to increased MCT4 degradation. Other studies also found that a dual knockdown of MCT1 and MCT4 resulted in decreased CD147 expression and surface localization (Floch et al., 2011).

Additional studies have suggested that CD147 expression is necessary for MCT membrane localization and this seems to be independent of the charged glutamate residue imbedded in the CD147 transmembrane domain (Deora et al., 2005; Kirk et al., 2000; Manoharan et al., 2006). This is further supported by studies demonstrating that CD147-null mice were found to have decreased surface expression of MCT 1/3/4, even when MCT transcription was still present (Philp et al., 2003). A recent study demonstrated that the affinity of interaction between CD147 and MCT1 is moderate (~1 μM), approximately the same as for an antibody-antigen complex (Howard et al., 2010). This compilation of data strongly suggests that CD147 and MCTs regulate each other post-transcriptionally and act as co-chaperones.

Another protein class that regulates CD147 cell surface expression is the cyclosporine A-sensitive (CspA) cyclophilin protein family. Cyclophilins contain peptidyl-prolyl *cis-trans* isomerase (PPIase) activity, are known to regulate protein trafficking, and act as intercellular mediators in inflammatory events (Yurchenko et al., 2010). Earlier studies found that CD147 cell surface expression was decreased by treatment with the immunosuppressive drug CspA (Yurchenko et al., 2005) and that the proline 211 residue located near the CD147 transmembrane domain facilitates interaction with Cyclophilin 60 (Pushkarsky et al., 2005), which may be involved in escorting CD147 to the cell surface.

Membrane-type 1 MMP (MT1-MMP; MMP-14) has been shown to associate with CD147 at the cell surface and decreases cell surface CD147 by cleaving it in the linker region between the Ig-like domains (Egawa et al., 2006). Further analysis demonstrated that CD147 associated with both the pro and active forms of MT1-MMP (Niiya et al., 2009). Surface expression of MT1-MMP is tightly regulated by protease-mediate cleavage of the propeptide during transport from the golgi to the plasma membrane (Zucker et al., 2002). Thus, association of CD147 with the pro and active form of MT1-MMP may indicate a role in regulating cell surface expression of one another.

Studies evaluating the turnover of CD147 are scant. One study suggests that CD147 is ubiquitinated and degraded in the proteasome. They further suggested that this is regulated by the enzyme ubiquitin carboxyl-terminal esterase L1 (UCH-L1) and N-glycosylation (Wang et al., 2008), where decreased glycosylation increases CD147 ubiquitination and subsequent degradation. Furthermore, another study suggested that CD147 does not appreciably localize in lysosomal compartments following

internalization (Eyster et al., 2011). An opposing study suggests that CD147 is downregulated via a p53-mediated lysosomal pathway instead of a proteasomal degradation mechanism (Zhu et al., 2009). Thus, it remains unclear as to which pathway CD147 is primarily degraded.

It is apparent that CD147 is regulated by complex signaling networks in different physiological, pathological and tissue-specific contexts. The regulation of CD147 expression by various transcription factors, soluble mediators and binding partners underscores the complexity of CD147 function.

Table 1-1. Regulators of CD147 Expression and Localization.

Regulator	Pathway	Message/Protein/Both	Surface/Soluble	Cell Type
GM-CSF	-	-	↑ Surface levels	Lymphocyte
EGF/Amphiregulin	EGFR	↑Both	-	Breast cancer
TGFβ	PI3K/Akt	↑Both	-	Hepatocyte
VEGF-D	-	-	↑ Surface levels	Endothelial
TNFα	NF-κβ –JNKII	↑Message	-	Co-culture Breast/Ovarian cancer w/ macrophage
IL-18	PI3K/Akt-ERK; JNK/Sp1	↑Both	-	Smooth muscle; cardiac muscle
RANKL	-	↑Both	-	Breast Cancer
C-reactive protein		↑ Message	-	Macrophage
Iron deficiency	p38- NF-κβ	↑ Both	-	Macrophages
Nitric oxide	cGMP	↓ Message	-	Cardiac muscle
PGE_2 (decreased)	c-Src	↓ Protein	-	Endometrial and Stromal
Estrogen	-	↑ Message		Reproductive
ERα	-	↑ Message (tissue specific)		Reproductive
Progesterone	-	Post-transcription	-	Reproductive
TSH	cAMP	Post-transcription	-	Thyroid cells
Angiotensin II	COX-2-PGE_2; p38-ERK	↑ Both; message	-	Macrophages; RPE
Somatostatin	-	-	↑ Surface levels	Intestinal
SCP-2	-	↑ Message	-	-
PPARγ	NF-κβ	↓ Protein	-	Macrophage
PPARα		↑ Message	-	Hepatocytes
PGC-1α	-	↑ Protein	-	Skeletal muscle
RACK1	-	↑ Protein	-	Breast cancer
STAT3 (decreased)	-	↓ Protein	-	Ovarian cancer
NOTCH (decreased)	-	↓ Protein	-	Breast cancer
Glucose (high)	-	↑ Both	-	Monocytes
CD147	-	↑ Both	↑ Soluble CD147	Co-culture breast cancer w/ fibroblast
NAMPT	p38- NF-κβ	↑ Both	-	Macrophages
MCT1 (decreased)	-	Post-transcription	↓ Surface levels	Various cells
Cyclophilin 60	-	-	↑ Surface levels	Various cells
MT1-MMP	-	-	↑ Soluble CD147	Various cancers

See text for references.

CD147 Expression Patterns and Subcellular Localization

Expression in Normal and Cancer Tissue

Numerous investigators have indicated that CD147 is expressed in various tissues. Earlier studies identified that CD147 was expressed in many epithelia, neuronal, lymphoid and myeloid cell types (Arjonen et al., 2011; Fossum et al., 1991; Kanekura et al., 1991; Kasinrerk et al., 1992; Nakai et al., 2006), though with various glycoforms. A tissue array analysis of CD147 expression in various normal and cancer tissues demonstrated that a limited number of normal cells express CD147, whereas elevated expression of CD147 was recognized in the majority of malignant cancers compared to their benign counterparts (Riethdorf et al., 2006); squamous cell carcinoma (SCC), pancreatic, chromophobic kidney, hepatocellular, medullary breast adenocarcinoma and glioblastoma multiforme demonstrated the highest incidence of expression.

Expression of CD147 was found to have negative prognostic value for patients with serous ovarian carcinoma (Davidson et al., 2003a), breast cancer (Liu et al., 2010; Reimers et al., 2004), acute lymphoblastic leukemia (Beesley et al., 2005), clear cell renal cell carcinoma (Jin et al., 2006), hepatocellular carcinoma (Zhang et al., 2006), gastric carcinoma (Zheng et al., 2006), endometrial carcinoma (Ueda et al., 2007) lung adenocarcinoma (Sienel et al., 2008), differentiated thyroid carcinoma (Tan et al., 2008), colorectal cancer (Buergy et al., 2009), prostate cancer (Han et al., 2009), adenoid cystic carcinoma of salivary glands (Yang et al., 2010b) and pediatric medulloblastoma (Chu et al., 2011). In addition to relative expression levels in tumor tissue samples, specific localization of CD147 to plasma membrane was a strong prognosticator for survival in

lung adenocarcinoma in the absence of increased CD147 expression (Sienel et al., 2008). Similarly, a borderline relationship between overall survival and surface CD147 staining was identified in laryngeal SCC (Rosenthal et al., 2003).

Characterization of Cytoplasmic CD147

In support of the histological studies above, CD147 localization was originally identified on the cell surface with a proclivity to localize at cell-cell interfaces (Ellis et al., 1989; Hubbard et al., 1985; Schlosshauer et al., 1995). As imaging techniques have improved, it is becoming clearer that CD147 is also localized in the cytoplasm of various cells. The characterization of these cytoplasmic CD147-positive signals is just beginning. A novel study by Eyster *et al.* found that an Arf6-GTPase mutant expressed in HeLa cells led to enlarged vacuolar-type structures enriched with clathrin-independent endocytic (CIE) cargo; in this study, they found that CD147, CD44, CD98 and GLUT1 were novel cargo internalized via CIE (Eyster et al., 2009). Interestingly, they found that CD147, CD44 and CD98 rapidly joined the recycling tubular endosomes via the juxtanuclear endocytic recycling compartment; this rapid transit, in contrast to other CIE cargo, may be due to the dynamic processes each of these proteins take part in, such as nutrient uptake and ECM remodeling. Additional studies found that CD147 did not sort to late endosomes and therefore did not appear to be degraded by lysosomes; cell surface expression of CD147 was minimally affected by up-regulation of membrane-associated RING-CH E3 ubiquitin ligases, which reduced surface expression of other CIE cargo members (Eyster et al., 2011). Other studies have recognized that CD147 requires clathrin-dependent sorting to localize to the basolateral membrane, but is independent of the adaptor protein AP1B (Castorino et al., 2011; Deborde et al., 2008). Thus, it appears

that CD147 may recycle from the cell surface rapidly and in some cells this may or may not rely on clathrin.

Characterization of Extracellular Vesicle-associated CD147

In addition to cytoplasmic vesicular localization, CD147 has also been identified in extracellular vesicles. In the initial characterization of CD147 in cancer, it was recognized that it was also present in tumor-conditioned media (Ellis et al., 1989). Subsequent studies suggested that CD147 was released from the cell surface in a full length soluble form (Taylor et al., 2002) or a 22-kDa proteolytic cleavage product (Egawa et al., 2006) not associated with vesicles; whereas another study demonstrated that CD147 was associated with an ERK-dependent released microvesicle, but the vesicle degraded releasing CD147 into the media (Sidhu et al., 2004). Microvesicle-associated CD147 was shown to be released from ovarian cancer cells and this elicited an angiogenic phenotype in endothelial cells (Millimaggi et al., 2007). Since lipid rafts may be a point of origin for microvesicles (Muralidharan-Chari et al., 2010), preceding CD147 accumulation in lipid rafts may lead to enrichment of CD147 in microvesicles.

Other studies have found that CD147 localizes in exosomes, which arise from inward budding of endosomal membranes forming a late-endosome-associated multivesicular body (MVB). Those MVBs that do not fuse with lysosomes, may act as a temporary storage compartment that can later fuse with the plasma membrane releasing exosomes (Stoorvogel et al., 2002). CD147 has been found in exosomes derived from the malignant ascites of ovarian cancer patients (Keller et al., 2009) and in bladder cancer (Welton et al., 2010). In addition, CD147 is enriched in exosomes released by

cardiomyocyte progenitor cells, which stimulated endothelial cell migration (Vrijsen et al., 2010). Currently, the exact mechanism regulating the release of CD147 from the cell surface or how vesicle-associated CD147 functions in various aspects of cell biology is unknown.

The Multi-functional Nature of CD147 Biology

CD147 Function Identified in Knockout Models

It is clear that CD147 is a ubiquitously expressed molecule attributed with many biological functions in physiologic and pathologic contexts. Two of the earliest credited functions of CD147 include a MMP-inducer on tumor cells (Ellis et al., 1989) and a cell recognition molecule involved in neuronal-glial patterning and aggregation (Fadool and Linser, 1993). Subsequently, more understanding of the role of CD147 in cell biology came from knock-out mice and mutant *Drosophila* strains.

Mice lacking the CD147 gene display a variety of adverse phenotypes. Experiments revealed that the majority of CD147-null embryos died around the time of initial blastocyst implantation, though different unknown modifier regions surrounding the CD147 gene may attenuate this death rate (Chen et al., 2004), and the few that implanted subsequently died at post-implantation (Igakura et al., 1998). In the rare event that an embryo successfully implanted, the offspring were small in size and usually died before one month due to difficulty of breathing attributed to interstitial pneumonia. It was also noted that the surviving male CD147-null mice were sterile due to spermatogenesis arresting in meiosis I and female null mice have problems with

fertilization (Igakura et al., 1998; Kuno et al., 1998). Further studies revealed that CD147-null mice have abnormalities in spatial learning, memory, and sensory perception to painful stimuli and noxious odors (Igakura et al., 1996; Naruhashi et al., 1997). Additionally, CD147-null animals displayed an exacerbated mixed lymphocyte reaction, an assay that measures susceptibility to graft rejection via incompatibilities in major histocompatibility complex antigens (Igakura et al., 1996) and when challenged with ligation of the ureter they demonstrated less fibrosis, matrix remodeling, and infiltration of macrophages (Kato et al., 2011).

Other studies with CD147-null mice found delayed entrance into dark compartments, which led to subsequent studies describing retinal dysfunction as early as five weeks leading to blindness (Hori et al., 2000; Ochrietor et al., 2001; Ochrietor et al., 2002). In light of this identified vision impairment, earlier studies demonstrating neurological deficits may be due to preceding vision abnormalities, since the mice used in the behavioral studies were 3-5 months old (Naruhashi et al., 1997), whereas functional retinal abnormalities were identified as early as eye opening (Ochrietor et al., 2002). One of the main mechanisms suggested to contribute to retinal pathology in CD147-null mice is a disturbed metabolic interface between cellular constituents regulating retinal physiology; this is attributed to reduced MCT surface expression (Ochrietor and Linser, 2004; Philp et al., 2003). As mentioned previously, CD147 participates in a co-chaperone relationship with MCT1, MCT3, and MCT4 and this was further confirmed *in vivo* with a studying identifying a similar relationship across a diverse set of specific tissue and cell types (Nakai et al., 2006). These results in conjunction with the various *in vitro* studies strongly support a role of CD147 in regulating MCT surface expression.

Evaluation of CD147 function in other model systems revealed additional biological roles. Up-regulation of CD147 in High five insect cells causes a drastic change in cytoskeletal organization characterized by an induced elaborate microfilament and microtubule network, which seemed to be independent of cell contact or conditioned media from CD147-upregulated cells (Curtin et al., 2005). Depletion of CD147 in *Drosophila* has also revealed several other interesting phenotypes. For instance, CD147-null fruit flies are embryonic lethal and flies manipulated to lack CD147 only in the eye demonstrate that CD147 regulates cell architecture. These studies found that the absence of CD147 in photoreceptors leads to misplacement of nuclei, rough endoplasmic reticulum and mitochondria, possibly due to perturbed interactions with integrins; interestingly these phenotypes could be rescued with the mouse CD147 gene. Additional phenotypes identified in CD147-depleted flies include misplaced epithelial glia cells surrounding photoreceptors, altered synaptic vesicle release, and a greatly reduced presence of glial capitate projections induced by CD147-associated photoreceptors (Curtin et al., 2007). Other studies further identified that CD147 may act in a cell-cell interaction module in the neuromuscular junction by regulating synaptic cytoskeletal architecture and vesicle dynamics (Besse et al., 2007). A study screening mutations in CD147 identified that specific residues in the extracellular domains and transmembrane domain are vital for proper function (Munro et al., 2010), yet other studies also suggest a prominent role for the conserved YEKRRK sequence in the cytoplasmic tail of CD147 for function (Besse et al., 2007). These studies suggest that CD147 has a role in regulating the cytoskeleton, cell-cell interaction modules, and vesicle distribution,

implying that CD147 may have an essential role in linking organization on the plasma membrane with cytoplasmic vesicular networks.

The Role of CD147 in Cancer Progression

Tumor cells co-opt many physiological processes and use them to their advantage as they attempt to survive, expand, and spread to other tissue compartments. CD147 is highly enriched on the surfaces of many cancer types and plays a role in many aspects of cancer progression. The following section will review the pleiotropic roles of CD147 in relation to the various mechanisms of tumor evolution and maintenance.

Cancer Migration and Invasion

Cellular migration and invasion defined as cell motility and migration through or within a barrier, respectively, constitutes an essential biological mechanism used in many diverse physiological and pathological situations by various cell types. In epithelial cancer, cells depart from the primary tumor bulk by utilizing diverse migratory and invasive mechanisms (Yilmaz and Christofori, 2009). In order for cancer cells to successfully metastasize and colonize distant sites, several obstacles must be surmounted: they must detach from neighboring cells, break down the local basement membrane, activate programs to resist anoikis, migrate and invade through surrounding tissue, gain entry into the circulation via lymphatic or endothelial channels, survive mechanical or immune-mediated destruction in transit through the circulation, extravasate into a new tissue microenvironment, adapt their metabolic phenotype to different surrounding nutrient gradients, and recruit supportive stromal cells to the new microenvironment to

generate a macroscopic tumor (Chaffer and Weinberg, 2011). Many of the initial steps of the metastatic cascade are believed to involve transitions in cellular programs that support an increased migratory capacity. Cancer cells have been shown to utilize diverse modes of movement, including mesenchymal, amoeboid and collective migration (Sahai, 2005).

Mesenchymal Movement

Single cell mesenchymal movement in epithelial cells is believed to be initiated during the epithelial-mesenchymal transition (EMT). Established hallmarks of EMT include: 1) down-regulation of characteristic cell junctional proteins, 2) increased expression and nuclear translocation of several EMT-promoting transcription factors, including β-catenin and the T cell factor/lymphocyte enhancer factor 1 (TCF/LEF1) complex, Snail, and Twist, 3) alterations in cytoskeletal arrangements and protein expression, 4) loss of cell polarity, 5) and up-regulation of proteases (Teng et al., 2007). Recently, EMT programs were classified into 3 distinct groups: 1) EMT involved in embryonic implantation and development, 2) EMT involved in wound repair/tissue regeneration, and 3) EMT involved in cancer invasion and metastasis; though, these are separate biological processes, they most likely have many interrelated signaling networks (Kalluri and Weinberg, 2009). Recent evidence also suggests that the EMT program may endow cells with a stem-like quality, which has been demonstrated to promote increased tumorigenicity, invasiveness and therapy resistance (Dave et al., 2012).

Interestingly, CD147 has been shown to regulate biological processes in each of these EMT classifications (Gabison et al., 2009; Igakura et al., 1998; Zucker et al., 2001). CD147 has been shown to be regulated by the EMT-promoting TF Snail in melanoma

cells (Kuphal et al., 2005) and may be involved in an EMT-like process during embryonic stem cell differentiation (Ullmann et al., 2008). A role for CD147 in EMT was recently identified in hepatocytes where up-regulation of CD147 initiated a TGF-β signaling cascade resulting in Slug up-regulation, cadherin switching and morphological changes (Wu et al., 2011a). Whether CD147 is involved in EMT in other cell types is unknown. A direct link has also been suggested between EMT and resistance to anoikis, a cell death process initiated upon detachment from a supportive ECM potentiating survival signals (Onder et al., 2008). Up-regulation of CD147 in breast cancer cells confers resistance to anoikis (Yang et al., 2006) facilitating survival during matrix detachment in invasion.

Amoeboid Movement

Amoeboid cellular movement acts as another mechanism of single cell motility. This migratory mechanism is characterized by a plastic rounded morphology and intermittent actomyosin-regulated blebbing with little dependence on protease activity (Sanz-Moreno and Marshall, 2009). It is clear that cell migratory phenotypes exist as a fluxing continuum between different forms of membrane protrusion and contraction states, which are regulated by diverse signaling and physical matrix cues (Friedl and Wolf, 2009). Recently, it was demonstrated that the interplay between mesenchymal and amoeboid movement is regulated by the signaling activity differences in the Rho protein family members. Guanine nucleotide phosphate (GTP)-bound proteins are regulated by GTP exchange factors (GEFs) and GTPase activating proteins (GAPs), which promote activation and inactivation, respectively (Vigil et al., 2010). Inasmuch, amoeboid

movement is promoted when Rho-kinase (ROCK) signaling activates a Rac GAP and mesenchymal movement is stimulated with increased Rac activity, which in turn suppresses amoeboid motility; this study strongly supports the notion that cancer cells interconvert their migratory phenotypes (Sanz-Moreno et al., 2008).

A new mechanistic study provides evidence that CD147 can inhibit phosphorylation of Annexin II (AnxA2), which leads to attenuation of ROCK-mediated suppression of mesenchymal motility. Furthermore, they also found that up-regulation of CD147 increased Rac activity and Wiskott-Aldrich syndrome protein family member 2 (WAVE2) expression and membrane localization, which led to actin polymerization, lamellipodia formation and a mesenchymal morphology (Zhao et al., 2011). In a separate study in cardiomyocytes, CD147-induced functions were also shown to be dependent on Rac1 activity (Venkatesan et al., 2010). These studies suggest that CD147 may play a role in modulating the interconversion of individual cell migratory phenotypes via regulation of Rac signaling events.

Cellular Protrusions Involved In Cell Migration/Invasion

Filopodia

It has been suggested that concomitant with the mesenchymal transition and migratory phenotype, cells also utilize finger-like projections called filopodia to probe and explore the surrounding microenvironment (Yilmaz and Christofori, 2009). Filopodia are protrusions extending from the plasma membrane, usually originating from lamellipodia, that are composed of parallel actin filaments bundled by cross-linking proteins (Arjonen et al., 2011). Filopodia formation may serve as a precursor for cell-

ECM adhesion, thus promoting cell migration (Faix et al., 2009). Increased presence of filopodia formation promotes migration (Zhang et al., 2004) and increased filopodia have been seen at the invasive front of colorectal cancer cells, indicating that filopodia may facilitate the invasion process (Vignjevic et al., 2007). In support of this, a subset of filopodia have been found to have invasive characteristics in 3D culture and may have a role in invadopodia (see below) and mesenchymal invasion (Li et al., 2010). Knockdown of CD147 in prostate cancer cells resulted in a ~50% decrease in filopodia formation (Zhu et al., 2011) and up-regulation of CD147 in insect cells resulted in similar protrusive structures (Curtin et al., 2005). Fascin, the major actin-bundling protein in filopodia may interact with CD147 in promoting aggressive cancer types (Tsai et al., 2007), though further research is needed to elucidate possible molecular interactions between the two.

Invadopodia

In the early 80's investigators identified that Rous sarcoma virus (v-src)-transformed cells cultured on 2D substrata form ventral protrusions located at points of cell-ECM contact, which are enriched in actin and tyrosine phosphorylated proteins. Subsequently, these protrusions were found to degrade the ECM at cell contact points and thus were termed invadopodia (Chen et al., 1985). Other investigators found that similar protrusions could be formed in osteoclasts, macrophages, dendritic cells, endothelial cells, and vascular smooth muscle cells, yet these structures are termed podosomes. Recently, it has been suggested that the term 'invadopodia' be reserved for cells with transformed properties and the term 'podosome' for normal cells (Murphy and Courtneidge, 2011). Due to the presence of these degradative protrusions in both normal

and tumorigenic cells, much effort is focused on their potential roles in regulating physiological and pathological invasive processes.

Over the past couple of decades, it has become clear that invadopodia contain an actin-rich core inundated with modulators of actin polymerization (Albiges-Rizo et al., 2009). Many proteins orchestrate the dynamic reconstruction of the actin cytoskeleton, but recent findings have identified key players in invadopodia formation. Invadopodia construction has been characterized into initiation, assembly and maturation stages. Briefly, in the initiating stage the cancer cell attaches to the ECM and tyrosine kinase substrate with 5 SH3 domains (Tsk5) is recruited to phosphatidylinositol-3,4-bisphosphate (PIP_2)-enriched membranes via a Src-dependent mechanism (Oikawa et al., 2008), which leads to subsequent interaction with cortactin. Also, PIP_3 may serve as an initiating site of invadopoda formation by activating Akt signaling (Yamaguchi et al., 2011). In the assembly stage, this protein complex then recruits N-WASP, Arp2/3 and cofilin to initiate actin polymerization (Oser et al., 2009), which is regulated by various kinases, soluble mediators and actin polymerization modulators. In the maturation stage, proteases, including soluble and membrane-type MMPs, become enriched at the invadopodial tips and microtubules and vimentin filaments cooperate in the elongation of invadopodia (Schoumacher et al., 2010). MT1-MMP appears to be a vital component of invadopodia degradation machinery, as several investigators have demonstrated decreased invadopodia activity following attenuation of MT1-MMP activity (Hu et al., 2011; Nakahara et al., 1997; Sakurai-Yageta et al., 2008). MT1-MMP trafficking to invadopodia has been attributed to a diverse group of proteins, including caveolin-1 (Yamaguchi et al., 2009), cortactin (Clark et al., 2007) and the conserved octameric

exocyst complex (Liu et al., 2009; Sakurai-Yageta et al., 2008). Delivery of these proteases to invadopodia facilitates ECM degradation and promotes the invasion process. Active trafficking in invadopodia is also supported by electron micrographs demonstrating vesicles within invadopodia (Schoumacher et al., 2010) and a proclivity for the golgi to localize in close proximity to invadopodia (Baldassarre et al., 2003). See a recent article by Murphy *et al.* for a complete review on invadopodia dynamics (Murphy and Courtneidge, 2011).

Coupled with the dynamic stages described above, invadopodia may be regulated by various growth factors (e.g EGF) and signaling inputs (e.g. ERK) (Ayala et al., 2007; DesMarais et al., 2009; Eckert and Yang, 2011; Mader et al., 2011), reactive oxygen species (Weaver, 2009), pH gradients (Busco et al., 2010; Magalhaes et al., 2011), matrix composition and orientation (Alexander et al., 2008) and lipid raft integrity (Caldieri et al., 2009; Yamaguchi et al., 2009). Thus, it is clear that myriad factors seem to converge and dictate the tendency of invadopodia to form and actively degrade the underlying ECM barrier. Evidence for EMT involvement in invadopodia was identified when non-transformed breast epithelial cells stably-expressing Twist or Snail, EMT-promoting TFs, formed invadopodia and may be involved in metastasis *in vivo* (Eckert et al., 2011). Very strong evidence supporting a role of invadopodia in metastasis *in vivo* was recently demonstrated using intravital multiphoton imaging; in this study N-WASP deficient cells demonstrated defects in migration, invasion, intravasation and dissemination, which seemed to be MMP-mediated (Gligorijevic et al., 2012). Additionally, knockdown of Tsk5 in zebrafish neural crest cells resulted in attenuated EMT-like migration, suggesting

that regulators of invadopodia may also be involved in development processes (Murphy et al., 2011).

As imaging techniques have advanced, high resolution characterization of invadopodia dynamics is now possible in 2D and 3D models. Total internal reflection fluorescence (TIRF) microscopy, a technique that permits high resolution evaluation of events occurring directly at the cell membrane with little cytosolic noise, revealed that an invadopodial core attaches to the ECM, which then projects out multiple filament-like processes (Artym et al., 2010); culture of cells in a 3D dermis-based matrix demonstrated a similar invasive superstructure (Tolde et al., 2010). Culture of invasive cancer cells on a native basement membrane isolated from rat peritoneum demonstrated that invasive cells initially form invadopodia that degrade the underlying ECM, these invadopodia further elongate to1-7μm in length and after a period of 5-7 days the whole cell has infiltrated through the basement membrane defect (Schoumacher et al., 2010). A new linear invadopodia configuration was identified when cells were cultured in a collagen I model; these invadiopodial structures formed along the collagen fibrils and demonstrated proteolytic activity in 3D (Juin et al., 2012).

It is evident that many physical and biological inputs are integrated spatiotemporally to determine the configuration(s) of protrusions that a motile cell will employ. As it is clear that distinct protrusions are formed in various cells, many studies have recognized that similar protein constituents are involved in the dynamics of each of these protrusions (Linder et al., 2011). For instance, invadopodia rely on filopodia-associated proteins for function and vice versa (Li et al., 2010; Schoumacher et al., 2010). Hence these protrusive structures may represent a hybrid structure that has different

functional capacities in various biological/physical contexts (Ridley, 2011; Yilmaz and Christofori, 2009).

Protease Induction

In the mid to late 80's, Chitra Biswas' laboratory attempted to characterize a factor present on lung carcinoma cell membranes that stimulated collagenase production from co-cultured fibroblasts (Biswas, 1984; Biswas and Nugent, 1987). Later studies found that this cell surface factor was CD147, which was identified as a protein with diverse molecular weights both in the membrane fractions and conditioned media (Ellis et al., 1989). Additional studies revealed that MMP-inducing activity via CD147 could be achieved by cell-cell contact or via shedding from the cell surface. Subsequent studies found that CD147 could induce the synthesis of MMP-1, MMP-2, MMP-3, MMP-9, MMP-14, and MMP-15 (Yan et al., 2005). In addition to induction in fibroblasts, CD147 has been shown to increase MMP production in endothelial cells, macrophages, tumor cells, and non-immortalized epithelial cells (Weidle et al., 2010). Supplemental to MMP induction, CD147 also participates in the activation of the urokinase-type plasminogen activator (uPA) system; in this study, up-regulation of CD147 or treatment with CD147-enriched membranes were able to stimulate the uPA system in breast cancer, oral squamous and endothelial cells (Lescaille et al., 2012; Quemener et al., 2007).

Several mechanisms have been proposed to explain how CD147 induces MMPs, yet the exact mechanism on how this occurs is currently unknown. Current variables that have been described to influence the ability of CD147 to induce MMPs include:

glycosylation status, dimerization/oligomerization, and association with various protein binding partners leading to activation of cell signaling pathways.

Glycosylation

Earlier experiments demonstrated that CD147 cDNA expressed in bacteria resulted in a non-glycosylated form around 29 kDa, which had no MMP-inducing activity when added to fibroblasts. These studies also suggested that lower glycosylated forms of rbCD147 (30-45 kDa) were unable to induce MMP synthesis (Guo et al., 1997). Following studies further demonstrated that deglycosylated endogenous CD147 had no MMP-inducing activity and was able to attenuate the ability of HG-CD147 to induce MMPs (Sun and Hemler, 2001). Conversely, others have demonstrated that non-glycosylated CD147 (Attia et al., 2011; Belton et al., 2008) or a peptide corresponding to the IgC2 domain with a single N-acetylglucosamine (GlcNac) or chitobiose unit (Kawakami et al., 2011) was capable of stimulating MMP production. Studies in atherosclerosis and muscle differentiation proposed that different CD147 glycoforms induce a differing MMP repertoire (Attia et al., 2010; Sluijter et al., 2005), though further exploration of this phenomenon is needed. A recent study found that multiple colorectal cancer cell lines contained synonymous mutations in codons that correspond to glycosylation sites in the extracellular domain of CD147, though the significance of these alterations is unknown (Zheng et al., 2011). Clearly, the relationship between CD147 glycoforms and MMP induction warrants further intense investigation.

Homo-Dimerization/Oligomerization

CD147 was first found to homo-oligomerize in several avian tissues, in which the authors proposed that CD147 can potentially interact both in *cis* and *trans* fashion forming a macromolecular complex (Fadool and Linser, 1996). Subsequent studies found that CD147 forms homo-oligomers only in a *cis*-like manner and that the IgC2 domain was sufficient for this dimerization while N-glycosylation appeared to play no role (Yoshida et al., 2000). Since tumor-associated CD147 and soluble CD147 can induce MMP synthesis in neighboring cells, this implies that a counter-receptor may participate in *trans*-interactions between these cells (Yan et al., 2005). Studies using immobilized CD147 fusion protein determined that CD147 may be a receptor for itself, similar to other IgSF members, and that this association was dependent on the IgC2 domain. Additionally, treatment of cells with a monoclonal antibody demonstrated to specifically bind multimerized CD147 inhibited MMP induction, implying oligomerized CD147 may facilitate MMP induction (Sun and Hemler, 2001). Subsequent cross-linking studies between the Ig-like domains of rbCD147 and fibroblasts followed by MALDI-MS/MS sequencing identified CD147 as a receptor for rbCD147 (Belton et al., 2008). Other studies using crystallographic approaches have found that Ig-like domains in CD147 dimerize in both *cis* and *trans* fashion (Yu et al., 2008) possibly through β-strand domain swapping (Luo et al., 2009). A systematic mutational analysis of the ectodomain of CD147 revealed that multiple mutations in the Ig-like domains inhibited dimerization/oligomerization and subsequently MMP induction (Cui et al., 2012).

Though the above studies demonstrate that the CD147 N-terminus can interact homophilically between homo/hetero-typic cell types, surface plasmon resonance (Hanna

et al., 2003) and FRET analysis (Wilson et al., 2002) suggest otherwise. In contrast, a new study also suggests that CD147-3 binding to the IgI domain of CD147-2 attenuates induction of MMP synthesis and invasion, though this relevance is questionable as CD147-3 has been identified as a nonsense-mediated decay gene, thus additional studies are needed for further clarification (Liao et al., 2011). The above studies suggest that CD147 may self-associate in a *cis* or *trans* orientation on the cell surface, which results in MMP induction.

Heterophilic Protein Interactions

The protein structure and binding characteristics of CD147 suggest a role in being a component of protein-protein interactions. As described previously, CD147 contains an unusual glutamate residue as well as a leucine zipper motif in its transmembrane domain (Jian-Li and Juan, 2007); both of these characteristics have been associated with multi-protein complex assembly (Humphrey et al., 2005; Zhou et al., 2001). Other single span transmembrane proteins, such as discoidin domain receptors (Noordeen et al., 2006), erythropoietin receptors (Ruan et al., 2004) and E-cadherin (Huber et al., 1999) utilize leucine zipper motifs in dimerization. Additionally, further studies indicate that the IgC2 domain may also interact with IgI/V-like domains on other IgSF proteins (Yu et al., 2008) and CD147 may associate with proteins with attached oligomannose moieties (Heller et al., 2003). In addition to these mentioned characteristics, differential glycoforms of CD147 provide prodigious advantages to participate in diverse protein-protein interactions.

The most characterized binding partner of CD147 that regulates MMP induction is caveolin-1. As mentioned previously, caveolin-1 is thought to decrease CD147-induced MMP production by decreasing cell-surface clustering and further complex glycosylations, though these appear to be independent of each other (Tang et al., 2004a; Tang and Hemler, 2004). Conversely, studies evaluating MMP synthesis in a lung injury model and hepatocellular carcinoma progression suggest that an inverse relationship exists between caveolin-1 and CD147 (Barth et al., 2006; Jia et al., 2006), though this could be due to different cell models and experimental evaluation.

Another protein that has been shown to interact with CD147 and regulate MMP induction is Annexin II (AnxA2). AnxA2 is a multifunctional protein that regulates cytoskeleton organization, lipid raft dynamics, and endo/exo-cytic trafficking events (Gerke et al., 2005). A recent study found that CD147 and AnxA2 might cooperate in hepatocellular carcinoma migration and invasion by regulating MMP production (Zhao et al., 2010).

Earlier studies found that CD147 interacted with $\alpha_3\beta_1$ and $\alpha_6\beta_1$ integrins at cell-cell contacts, but not at focal adhesions sites; interestingly, it appears that LG-CD147 was the glycoform primarily associated with integrins (Berditchevski et al., 1997). Later studies found that these CD147-integrin interactions contributed to cancer invasiveness by inducing MMP synthesis in hepatoma cells via a PI3K signaling pathway (Dai et al., 2009). A recent study identified that Asp^{179} in the IgI domain of CD147 interacts with the metal ion-dependent adhesion site in the βA domain of the integrin β_1 subunit, this interaction was shown to lead to focal adhesion kinase (FAK) signaling events, which regulated *in vivo* tumor growth. This CD147- β_1 interaction was facilitated by manganese

and was attenuated by competing RGD containing ligands (Li et al., 2012). Interestingly, CD147 also interacts with caveolin-1 via this IgI domain (Tang and Hemler, 2004), though whether competing interactions between integrins, caveolin-1 or RGD-containing ligands influences CD147 function is unknown.

Angiogenesis

As the primary tumor bulk expands, nutrient availability becomes a limiting variable governing the success of further tumor growth. Nutrient, oxygen and metabolic waste transport through endothelial cell channels recruited by tumor cells is a major mechanism that can supply adequate nutrient supply to a primary or newly colonized tumor bed. CD147 has been shown to promote increased angiogenesis by upregulating soluble vascular endothelial growth factor (VEGF) protein and secretion in breast tumor cells and cancer cell-fibroblast cocultures; this induction of VEGF was also seen *in vivo* (Tang et al., 2005). Further characterization of this effect revealed that CD147 specifically increased the soluble $VEGF_{121}$ and $VEGF_{165}$ splice variants along with VEGF receptor 2 (VEGFR-2) via induction of hypoxia-inducible factor 2α (HIF-2α) in normoxic conditions (Bougatef et al., 2009). Similar findings were also observed in melanoma cells, where CD147 may be involved in a VEGF autocrine signaling mechanism promoting migration, invasion and proliferation (Bougatef et al., 2010). CD147 also appears to be involved in VEGF secretion during Kaposi sarcoma-associated herpesvirus' induction of a tumor-associated fibroblast phenotype (Dai et al., 2012). The exact mechanism of how CD147 induces VEGF production is not known, but analysis of

tumor-endothelial cross-talk revealed that tumor-derived CD147-associated microvesicles induce invasiveness, MMP production, and tubule formation in endothelial cells (Millimaggi et al., 2007). Thus, CD147 may mediate VEGF signaling and angiogenic events either by cell-cell contact, soluble or vesicle-associated CD147 mechanisms.

To date, a relationship between CD147 and VEGF has been demonstrated in breast cancer (Tang et al., 2005; Tang et al., 2006), liver cancer (Jia et al., 2007), renal cancer (Liang et al., 2009), osteosarcoma (Zhou et al., 2011), bladder cancer (Xue et al., 2011), colorectal cancer (Zheng et al., 2011), pancreatic cancer (Zhang et al., 2007), glioblastoma (Liang et al., 2005), gastric cancer (Zheng et al., 2006), melanoma (Bougatef et al., 2010; Chen et al., 2006a; Voigt et al., 2009) and head and neck SCC (HNSCC) (Newman et al., 2008a). Additionally, a recent study suggested a potential use of CD147 expression to stratify patients and their response to anti-VEGF therapies such as bevacizumab (Newman et al., 2009). CD147 takes part in tumor angiogenesis in several cancer types and induces VEGF production autonomously in tumor cells and in a paracrine fashion between tumor cells and fibroblasts and endothelial cells. In addition, to angiogenesis, CD147 also contributes to vasculogenic mimicry, a process in which malignant tumor cells form non-endothelial-lined channels and behave like blood vessels (Millimaggi et al., 2009).

Multi-therapy Resistance

Broad, combined and targeted chemotherapy regimens are limited in their efficacy by the development of tumor drug resistance. Tumor drug resistance can be

achieved in numerous ways. Cancer cell autonomous mechanisms include: alteration of metabolic and morphologic phenotype, amplification of the target, acquired mutation in the target via positive selection during drug exposure, bypassing signaling pathway(s) being targeted, increased repair and detoxification mechanisms, augmented capability to efflux drugs via cell membrane transporters and enhanced activation of cell survival/anti-apoptotic signaling pathways. Additionally, many of these drug-resistant characteristics can be modulated in the tumor tissue by stromal, endothelial and immune cell influences as well as the physical matrix/tissue barriers surrounding the vicinity of the growing tumor (Garraway and Janne, 2012).

CD147 expression has been correlated with a multidrug resistance (MDR) phenotype in several cancer types (Kuang et al., 2008; Yang et al., 2003) possibly by regulating expression of the MDR1 gene product, P-glycoprotein (P-gp) drug efflux pump (Li et al., 2007a). Subsequent studies revealed that reduction of CD147 expression led to increased accumulation of chemotherapy drugs in cancer cells (Yang et al., 2007). A growing amount of evidence also indicates that CD147 is increased upon chemotherapy exposure (Li et al., 2007b; Qin et al., 2011) and may associate with P-gp during this event (Wang et al., 2008). In the previously mentioned studies, CD147 has been associated with resistance to doxorubicin, paclitaxel, cisplatin, 5-fluorouracil, vincristine, and all-trans retinoic acid; therefore CD147-mediated drug resistance cannot be due solely to Pgp regulation. In support of this, a recent study found that CD147 regulates breast cancer resistance protein (BCRP) expression and plasma membrane presence (Qin et al., 2011), a protein that has a differing substrate profile than Pgp (Lemos et al., 2008). Additionally, CD147 has been shown to regulate the expression of

X-linked inhibitor of apoptosis, a protein related to chemotherapy resistance. Recently, a study employing laser capture microdissection identified CD147 expression as the most discriminatory protein in stratifying tamoxifen therapy resistance in breast cancer tumor samples (Umar et al., 2009) and CD147 expression in bladder cancer is associated with poor survival following cisplatin-based therapy (Als et al., 2007).

In addition to the regulation of drug efflux pumps, CD147 has also been shown to potentiate drug resistance by inducing the synthesis of hyaluronan (HA) (Toole and Slomiany, 2008). HA is a large non-sulfated extracellular sugar composed of repeating N-acetylglucosamine and glucuronic acid units, which can act as a scaffold for other ECM constituents in the construction of the interstitial milieu. HA engages cell surface receptors, including its main receptor CD44, and is believed to promote the formation of multi-protein cell surface complexes by creating a stabilizing pericellular scaffold (Ghatak et al., 2005; Toole, 2004). Disruption of HA-CD44 interactions leads to internalization of CD44 and respective binding partners, including metabolic and drug transporters (Slomiany et al., 2009a; Slomiany et al., 2009b).

The involvement of CD147 in resistance to radiation therapy is just beginning to emerge. A relationship between CD147 expression following brachytherapy for cervical carcinoma was identified, where patients with elevated CD147 tissue staining post-therapy demonstrated poorer survival (Ju et al., 2008). The exact mechanisms underlying this putative association of CD147 and radio-resistance are currently unknown, but may depend on altered control of reactive oxygen species (Xie et al., 2011).

CD147-induced Cell Signaling Pathways

It is clear that CD147 has various roles in diverse cell types in physiological and pathological contexts, though the signaling pathways activated in each setting are not completely clear. The first activated signaling pathway identified by exogenous CD147 treatment was the mitogen activated protein kinase (MAPK) p38-associated pathway, which led to MMP-1 synthesis in fibroblasts (Lim et al., 1998). Following studies found that full length soluble CD147 released from breast cancer cells induces a phospholipase A_2/5-lipoxygenase pathway resulting in arachidonic acid metabolism in fibroblasts (Taylor et al., 2002). Other studies have indicated that CD147 also regulates MAPK signaling pathways, including ERK and JNK (Qian et al., 2008; Xu et al., 2007). CD147 associates with the heparan sulfate-containing protein syndecan-1, resulting in CypB-mediated ERK activation (Pakula et al., 2007) and can also interact with a osteopontin peptide-CypC complex to elicit Akt 1/2 signaling (Mi et al., 2007). Other studies have demonstrated that CD147-integrin interactions lead to focal adhesion kinase (FAK)-PI3K related pathways (Dai et al., 2009; Tang et al., 2008). A recent study found that CD147 was a regulator of the canonical Wnt/β-catenin pathway in lung cancer. Specifically, up-regulation of CD147 led to an EMT-like phenotype, nuclear accumulation of β-catenin and additional tumorigenic characteristics (Sidhu et al., 2010). Co-culture of tumor cells and fibroblasts revealed a novel mechanism involving fibroblast growth factor (FGF) signaling and CD147 (Liu et al., 2011). In this study it was proposed that early in tumor progression CD147 expression may be low and tumor growth is dependent on fibroblasts and FGF signaling, whereas later stages of tumor growth have elevated CD147

expression with a concomitant reduction in FGFR signaling allowing the tumor to become independent of fibroblasts for further progression.

In inflammatory scenarios, CD147 can stimulate ERK and NF-κβ signaling (Kim et al., 2009; Schmidt et al., 2008) and inflammatory cytokines/chemokines IL-1, IL-6 and IL-8, CCL3, CCL20, CXCL2 and CXCL5 (Chen et al., 2009; Dean et al., 2009).

As mentioned above, CD147 can also interact with CD44 (Slomiany et al., 2009b), though no activated pathways have been ascribed to this interaction. Since CD147 has been shown to regulate HA synthesis (Edward et al., 2011; Ghatak et al., 2005; Kato et al., 2011; Marieb et al., 2004; Qin et al., 2011), it is possible that CD147-induced HA-CD44 interactions may activate similar pathways that HA alone induces. In this manner, CD147-mediated HA-CD44 interactions have led to activation of PI3K and ERK signaling pathways (Marieb et al., 2004). Whether the other aforementioned CD147-induced signaling pathways are intertwined with HA-CD44 signaling complexes is unknown.

In conjunction with inducing activation of 'linear' signaling pathways, CD147 also appears to be involved in autocrine signaling loops. For instance, TGFβ has been shown to increase CD147 expression and in turn CD147 increased TGFβ signaling leading to an EMT phenotype (Wu et al., 2011a). In melanoma, CD147 may stimulate an autocrine VEGF-VEGFR2 signaling loop (Bougatef et al., 2010) and VEGF-D may potentiate this by increasing CD147 expression at the plasma membrane (Papiewska-Pajak et al., 2010). During inflammatory or wound healing processes CD147 may also participate in an autocrine loop consisting of interleukin signaling (Gabison et al., 2009;

Venkatesan et al., 2009). A positive feedback loop for CD147 itself has also been identified (Tang et al., 2004b). Finally, the influence of CD147 in regulating HA synthesis also raises the question of whether CD147-induced HA-CD44 interactions also mediate autocrine signaling events, seen with up-regulation of HA alone (Misra et al., 2005).

Though no kinase motif has been identified in CD147, other studies have emphasized that interactions in the extracellular Ig-like domains activate downstream signaling pathways. CD147 dimerization/oligomerization has been shown to be a major factor in regulating ERK phosphorylation (Cui et al., 2012) and association with integrin β1 is associated with FAK signaling (Li et al., 2012). The short cytoplasmic tail contains partially conserved serine residues (Weidle et al., 2010) and our own preliminary analysis suggests that Serine 246 may be a putative Casein Kinase 1 phosphorylation site, though this needs further clarification. Whether the cytoplasmic domain has a role in signaling is not known, currently one study suggests that this may not be the case in CypA-CD147-induced signaling (Pushkarsky et al., 2007). Another study in activated T cell suggests that a membrane-localized CD147 cytoplasmic tail was sufficient to mediate the signaling effect mediated by CD147 (Ruiz et al., 2008).

The Role of CD147 in Metabolic Processes of the Cell

As described previously, CD147 is an inducible molecule governed by many diverse stimuli. CD147 has been demonstrated to be regulated by TSH, an active fragment of SCP-2, PPAR proteins, PGC1-α and NAMPT, which are all direct regulators of cell metabolic processes. In addition, exposure of cells to glucose, butyrate or pectin increases CD147 expression (Kirat et al., 2009). CD147-depleted oral SCC cells demonstrated a differential gene expression pattern with most of these genes being related to cellular metabolism (Kuang et al., 2008).

The strongest evidence, thus far, for CD147 being involved in cellular energetics is the observed associations between CD147 and monocarboxylate transporter (MCT) family members MCT1/2/3/4, which are proton-linked transporters that facilitate the movement of pyruvate, lactate, and ketone bodies across cell membranes (Halestrap, 2011b). CD147 has been shown to be an essential chaperone needed for surface expression of these MCTs, since overexpressed MCTs don't traffic to the plasma membrane unless CD147 is co-expressed (Gallagher et al., 2007; Kirk et al., 2000; Philp et al., 2003). The role of MCTs in lactic acid flux has been exploited by cancer cells as they utilize these transporters to maintain metabolic homeostasis.

Otto Warburg observed that cancer cells exhibited increased glycolysis to generate adenosine triphosphate (ATP), even in the presence of abundant oxygen supply; this process has now been coined the 'Warburg effect' (Warburg, 1956). A number of studies have gone on to demonstrate that accumulation of lactate is associated with poor prognosis in several cancer types and is strongly associated with highly invasive

phenotypes (Kennedy and Dewhirst, 2010). In addition to genetic/epigenetic heterogeneity in the tumor, metabolic heterogeneity is also present. For example, tumors contain cell populations localized in oxygenated and hypoxic regions and evidence of metabolic symbiosis between lactate-producing and lactate-utilizing cells has been demonstrated *in vivo* with MCT inhibitors (Sonveaux et al., 2008). Thus it appears that many cancers rely on glycolysis to generate ATP to synthesize the biomass needed for various anabolic reactions during proliferation (Vander et al., 2009).

Multiple studies have identified that inhibition of CD147 expression in various cancer types results in perturbed MCT-mediated lactic acid flux across the plasma membrane (Baba et al., 2008; Floch et al., 2011; Schneiderhan et al., 2009; Slomiany et al., 2009b; Su et al., 2009); in some studies this led to highly decreased ATP levels and cell death. A recent study has provided very strong evidence that one of the main functions of CD147 in tumorigenesis is the escorting of MCTs to the cell surface, which is vital for highly glycolytic and aggressive cancers (Floch et al., 2011). An elegant study employing cell surface crosslinking in the midst of different detergent conditions followed by mass spectrometry analysis identified that CD147 associates in a super metabolic complex on the cell surface. Specifically, CD147 was found to complex with the following: MCTs (lactate and pyruvate transporters), CD98hc (a multifunctional chaperone for nutrient transporters), L-type amino acid transporter 1 (LAT1), ASCT2 (neutral amino acid transporter) and epithelial cell adhesion molecule (EpCAM). The organization of the complex is proposed to consist of a CD147-MCT complex with direct linkage of CD147-to CD98, which associates with the other amino acid transporters and EpCAM (Xu and Hemler, 2005). Finally, this study identified that CD147 and CD98

regulated the surface expression of one another and that depletion of either one resulted in increased activation of the cellular energy sensor AMP kinase.

In addition to association with MCTs on the cell surface, CD147 has also been shown to associate in the inner mitochondrial membrane with MCT1, lactate dehydrogenase and cytochrome oxidase in a lactate oxidation complex (Hashimoto et al., 2006). This mitochondrial complex may aid in the utilization of lactate transferred between glycolytic and respiring cancer cell populations or aid in the consumption of cell autonomous lactate produced in the cytosol, thus maintaining redox balance (Hussien and Brooks, 2011).

CD147 has also been proposed to regulate Grp75 (mortalin) expression (Kuang et al., 2008), a 70 kDa heat shock protein (Hsp70) family member involved in the cellular response to glucose deprivation, mitochondrial import, vesicular trafficking and regulation of p53 activity (Wadhwa et al., 2002).

Clearly, CD147 appears to be involved in multiple aspects of cellular metabolism. This is supported by elevated expression of CD147 on many metabolically active cell types, such as lymphoblasts (Spring et al., 1997), brown adipocytes ((Nehme et al., 1995), inflammatory and malignant cancer cells (Muramatsu and Miyauchi, 2003). It may be inferred from the studies above that diminished CD147 expression may result in impaired lactate, pyruvate and amino acid transport across cell membranes, thus leading to an altered metabolic phenotype and may explain how CD147 inhibits starvation-induced autophagy (Gou et al., 2009).

Hypothesis

It is hypothesized that CD147 induces breast cancer invasion by regulating invadopodial dynamics via the assembly of multi-protein signaling complexes.

Rationale

CD147 expression is associated with an invasive phenotype in a wide array of cancer types, including breast cancer. CD147 is a predominant marker in breast cancer micrometastases (Klein et al., 2002; Reimers et al., 2004) and is enriched in malignant pleural effusions and circulating tumor cells (Davidson et al., 2004; Pituch-Noworolska et al., 2007), suggesting a prominent role for CD147 in tumor progression. The role of CD147 in invasion has been demonstrated in several model systems, including a study *in vivo* in which CD147-transfected breast cancer cells injected into mammary fat pads of nude mice were found to be more locally invasive than control transfected cells and in several animals metastasized to the liver, spleen, mediastinum, lymph nodes, and mesentery (Zucker et al., 2001). The mechanism mostly attributed to CD147-induced invasion is the induction of proteases, including soluble and membrane-type MMPs, though the mechanism regulating this process have not been fully elucidated.

Cancer cells employ multiple mechanisms to migrate, degrade and invade through the ECM. Invadopodia, actin-based proteolytic superstructures, have gained much attention for their role as vital organelles in cellular invasion (Murphy and Courtneidge, 2011) both *in vitro* and *in vivo*. The purpose of this project was to further characterize the mechanism(s) by which CD147 facilitates breast cancer invasion by evaluating the role of CD147 in invadopodia activity and potential related signaling pathways.

Chapter 2: Regulation of Invadopodia Formation and Activity by CD147

Abstract

A defining feature of malignant tumor progression is cellular penetration through the basement membrane and interstitial matrices that separate various cellular compartments. Accumulating evidence supports the notion that invasive cells employ specialized structures termed invadopodia to breach these structural barriers. Invadopodia are actin-based, lipid raft-enriched membrane protrusions containing membrane-type-1 matrix metalloproteinase (MT1-MMP) and several signaling proteins. CD147 (emmprin; basigin), an immunoglobulin superfamily protein that is associated with tumor invasion and metastasis, induces the synthesis of various matrix metalloproteinases in multiple systems. In this study we show that up-regulation of CD147 is sufficient to induce MT1-MMP expression, invasiveness, and formation of invadopodia-like structures in non-transformed, non-invasive, breast epithelial cells. We also demonstrate that CD147 and MT1-MMP are in close proximity within these invadopodia-like structures and co-fractionate in membrane compartments with the properties of lipid rafts. Moreover, manipulation of CD147 levels in invasive breast carcinoma cells causes corresponding changes in MT1-MMP expression, invasiveness, and invadopodia formation and activity. These findings indicate that CD147 regulates invadopodia formation and activity, most likely via assembly of MT1-MMP-containing complexes within lipid raft domains of the invadopodia.

Introduction

Focal penetration through the basement membrane is a defining event in the transition from a dysplastic carcinoma *in situ* to an invasive and malignant cancer. Invasive cancers most likely utilize various mechanisms to breach the surrounding extracellular matrix (ECM) scaffolds that segregate different tissue compartments (Friedl and Wolf, 2003). Cellular protrusions directly abutting and penetrating the ECM have been observed in multiple cancers as invasion progresses (Rowe and Weiss, 2008) and very similar, ventrally-localized, membrane superstructures called invadopodia are seen when invasive cells are cultured on 2D substrata (Artym et al., 2006). A recent study demonstrated a direct role for invadopodia in promotion of metastasis (Eckert et al., 2011). Invadopodia are composed of actin filaments and modulators of actin polymerization, including cortactin (Artym et al., 2006; Clark et al., 2007), and are enriched in kinases, cell-adhesion molecules, and matrix metalloproteinases (MMPs), notably membrane-type 1 MMP (MT1-MMP), a crucial enzyme for basement membrane and interstitial matrix degradation (Frittoli et al., 2010; Poincloux et al., 2009). A coordinated step-wise model for invadopodia formation has been described, in which cortactin-actin puncta form initially at sites of matrix attachment, followed by delivery and accumulation of MT1-MMP at the invadopodia-ECM interface (Artym et al., 2006; Oser et al., 2009; Schoumacher et al., 2010). Importantly, multiple studies have demonstrated that cancer cells primarily employ MT1-MMP targeted to invadopodia to degrade underlying ECM, which is orchestrated by a number of diverse proteins that integrate various signals to induce focalized MT1-MMP localization and matrix degradation (Artym et al., 2006; Clark et al., 2007; Frittoli et al., 2010; Liu et al., 2009; Murphy and Courtneidge, 2011).

Interestingly, a recent study found that MT1-MMP and other major invadopodia constituents localize in detergent-resistant membrane fractions characteristic of lipid raft domains (Yamaguchi et al., 2009). Thus, an emerging model describes invadopodia as dynamic cellular depots where diverse cell signaling inputs, vesicular trafficking, and protease activity converge in spatially-defined membrane compartments at the leading edge of an invasive cancer cell.

Emmprin/basigin/CD147 is a single pass integral membrane protein, belonging to the Ig superfamily, that is variably glycosylated across different tissue types. It is usually expressed at low levels in most normal tissues, but is highly up-regulated during dynamic cellular events, such as tissue remodeling and cancer progression (Gabison et al., 2009; Nabeshima et al., 2006; Yan et al., 2005). Emmprin was originally identified as a cell surface factor that induces MMP production in stromal cells (Ellis et al., 1989; Kataoka et al., 1993), but later studies revealed that emmprin is identical to basigin-2 (Biswas et al., 1995; Liao et al., 2011), and is multifunctional; it is now widely known as CD147. CD147 induces several MMPs at both the message and protein level, including MMP-1, MMP-2, MMP-3, MMP-9, MT1-MMP, and MT2-MMP, though there is variation in the particular MMPs induced in different systems (Nabeshima et al., 2006; Yan et al., 2005). Furthermore, CD147 has been shown to induce MMPs in tumor cells themselves as well as in stromal cells (Caudroy et al., 2002; Sun and Hemler, 2001). CD147 is a predominant marker in breast cancer micrometastases (Klein et al., 2002; Reimers et al., 2004) and is enriched in malignant pleural effusions and circulating tumor cells (Davidson et al., 2004; Pituch-Noworolska et al., 2007), suggesting a prominent role for CD147 in tumor progression. The role of CD147 in invasion has been demonstrated in

several model systems, including a study *in vivo* in which CD147-transfected breast cancer cells injected into mammary fat pads of nude mice were found to be more locally invasive than control transfected cells and in several animals metastasized to the liver, spleen, mediastinum, lymph nodes, and mesentery (Zucker et al., 2001).

In this study we show that up-regulation of CD147 is sufficient to induce many features of invadopodia in non-transformed breast epithelial cells and that manipulation of CD147 levels in invasive breast carcinoma cells causes corresponding changes in the formation and activity of invadopodia.

Materials and Methods

Cell culture

The human breast adenocarcinoma cell line MDA-MB-231 was obtained from American Type Culture Collection (ATCC) and was cultured in RPMI 1640 (R-8755) with 2.38 g/L HEPES, 2 g/L sodium bicarbonate, and 10% FBS (pH 7.4). The spontaneously immortalized human breast epithelial cell line MCF-10A was obtained from ATCC. The immortalized human mammary epithelial cell line HMLE was a generous gift from Dr. Robert Weinberg (MIT, Cambridge, MA). Low passage MCF-10A and HMLE cells were maintained in Mammary Epithelial Cell Growth Medium (MEGM) with BulletKit supplements (Lonza). All cells were cultured in a humidified 95% air/5% CO_2 incubator at 37°C.

Antibodies and Reagents

The following primary antibodies were obtained for these studies: CD147 (BD Pharmingen); Alexa Fluor 488-conjugated CD147 (Biolegend); cortactin (clone 4F11) and MT1-MMP/ hinge-region polyclonal (Millipore); MT1-MMP monoclonal (Epitomics); caveolin-1 (BD Biosciences); rabbit and mouse EEA1 (AbCam); and β-actin (Sigma). Alexa Fluor-488 goat anti-mouse, Alexa Fluor-488 goat anti-rabbit, Alexa Fluor-647 goat anti-rabbit, Alexa Fluor-555 goat anti-mouse, Alexa Fluor-555 goat anti-rabbit, and Alexa 647-phalloidin were purchased from Invitrogen. Goat anti-mouse HRP and goat-anti-rabbit HRP (Chemicon) were used as secondary antibodies for immunoblotting. Western blotting detection reagent (enhanced chemiluminescence) was purchased from Pierce. Recombinant TIMP-1 and TIMP-2 were purchased from Chemicon and were used at concentrations indicated in the figure legends. A function blocking antibody targeting the catalytic domain of MT1-MMP (LEM-2/15.8) and the IgG control antibody were obtained from Millipore.

Recombinant adenovirus infections

Recombinant human CD147 adenovirus and control β-galactosidase (β-gal) adenovirus were constructed and used as described previously (Li et al., 2001).

RT-PCR

Total RNA was isolated using the RNeasy Mini kit (Qiagen) and quality control and quantification was performed with the Agilent 2100 Bioanalyzer (Agilent Technologies, Inc., Santa Clara, CA) and Agilent RNA 6000 Pico LabChip kits. cDNA was synthesized from equal total RNA using iScript cDNA synthesis kit (Biorad) according to the

procedures of the manufacturer. The primers designed for targeting the genes included the following: CD147 sense, 5′ GGAATAGGAATCATGGCGGCTGCG 3′; CD147 antisense, 5′GAGCCTCAGGAAGAGTTCCTCTGGC 3′; MT1-MMP sense, 5' CCATTGGGCATCCAGAAGAGAGC 3'; MT1-MMP antisense, 5' GGATACCCAATGCCCATTGGCCA 3'; GAPDH sense, 5′ ATGTTCGTCATGGGTGTGAA 3′; GAPDH antisense, 5′ GGTGCTAAGCAGTTGGTGGT 3′. The PCR was performed in a DNA thermal cycler (Thermo Hybrid PCR Express Thermo Cycler,) under conditions of 95°C for 2 minutes; 30 cycles each at 95°C for 30 seconds, 59°C for 30 seconds, and 72°C for 60 seconds; followed by 72°C for 5 minutes.

RNAi

Control non-silencing siRNA and target-specific pooled CD147 siRNAs (#35298) were purchased from Santa Cruz Biotechnology and used according to manufacturer's protocol. For all experiments, cells were transfected with siRNA 72 hrs before each experiment.

Matrigel invasion assay

Matrigel invasion inserts (8 μm pores) for 24-well tissue culture plates were purchased from BD Biosciences. Briefly, the matrigel inserts (upper and lower chambers) were re-hydrated for 2 hrs at 37°C with serum culture medium (MDA-MB-231) or non-supplemented MEGM (MCF-10A/HMLE). $4.0x10^5$ MDA-MB-231 cells treated with siRNA (72 hrs) or adenoviruses (24 hrs) were detached and seeded in the upper chamber of the inserts and cultured for 24 hrs at 37°C. $8.0x10^4$ MCF-10A or HMLE cells, non-

treated or treated with adenoviruses, were placed in the upper chamber in non-supplemented MEGM, while medium in the lower chamber was replaced with complete growth medium containing 20 nM EGF, and cultured for 36 hrs at 37°C. After incubation, the cells were fixed in 3.7% paraformaldehyde for 15 minutes at room temperature, the chambers were rinsed with PBS and stained with 0.2% crystal violet for 10 minutes, followed by extensive washing. After scraping off the cells at the top of the matrigel membrane with a Q-tip, the cells that passed through the 8 μm pores in the membrane were visualized by imaging with a phase contrast microscope (Leica DFC320). Cells were counted in 4 separate fields for 3 independent experiments.

Gelatin degradation assay for invadopodia

This assay was performed as described previously with minor modifications (Artym et al., 2009). Briefly, gelatin was conjugated with 568 Alexa Fluor dye (Molecular Probes) using the manufacturer's protocol. Glass coverslips (18 mm) were acid washed with 1 M HCl for 12-16 hours and washed extensively with water. 70% Ethanol-sterilized coverslips were coated with 50 μg/ml poly-L-lysine for 20 minutes at room temperature, washed with PBS, and fixed with ice cold 0.5% glutaraldehyde for 15 minutes followed by extensive washing. The coverslips were then inverted on an 80 μL drop of fluorescent gelatin matrix (0.2% gelatin and Alexa Fluor-gelatin at an 8:1 ratio) and incubated for 15 minutes at room temperature. The coverslips were washed with PBS and the residual reactive groups in the gelatin matrix were quenched with 5 mg/ml sodium borohydride in PBS for 10 minutes followed by further washing in PBS. The coated coverslips were placed in 12-well plates, sterilized in 70% ethanol for 10 minutes, washed in PBS, and equilibrated in serum free medium and switched to serum medium

30 minutes before the addition of cells. For invadopodia assays, $5.0x10^4$ cells were plated on the coated coverslips and incubated at 37°C for 5-6 hrs (MDA-MB-231) or 15 hrs (MCF-10A). Cells were fixed-permeabilized with 3.7% paraformaldehyde/0.1% Triton X-100 for 10 minutes, washed with PBS, blocked in 3% BSA in PBS for 1 hour, and incubated with appropriate primary and secondary antibodies in 3% BSA in PBS. Actin filaments were visualized with Alexa 647-phalloidin.

In Situ Proximity Ligation Assay

Interaction of CD147 and MT1-MMP was detected in situ using the Duolink II secondary antibodies and detection kit (Olink Bioscience, Uppsala, Sweden) according to manufacturer instructions. Briefly, primary antibodies targeting CD147 (BD Pharmingen) and MT1-MMP (Millipore) were applied using standard procedures. Oligonucleotide-conjugated Duolink secondary antibodies were then added, followed by Duolink Ligation solution. The oligonucleotides ligate together in a closed circle only when the secondary antibodies are in close proximity (<40 nm) (Soderberg et al., 2006). Finally, polymerase was added, which amplified any existing closed circles, and detection was achieved with complementary, fluorescently labeled oligonucleotides. Specificity of the reaction was determined by treating cells with a single primary antibody followed by Duolink secondary antibodies, which results in no signal amplification due to absence of a second oligonucleotide needed for ligation and subsequent closed circle amplification.

Microscopy and image analysis

Images were captured with a Leica Total Confocal System SP5 Acoustic Optical Beam Splitter Confocal (TCS SP5 AOBS) microscope using a 63X/1.4 N.A. oil objective in the

Josh Spruill Molecular Morphology & Imaging Center in the Department of Regenerative Medicine and Cell Biology (MUSC, Charleston, SC). Images were acquired at high confocality (pinhole = 1 Airy unit) to achieve the thinnest possible optical slices at the matrix-cell interface. Potential overlaps in emission spectra were eliminated by sequential scanning and tuning of the AOBS. Differential interference contrast (DIC) microscopy was performed using the Leica SP5 Confocal System. 3-dimensional (3D) volumetric reconstruction of invadopodia-producing cells was carried out using the 3D reconstruction software Amira 5.2 (Visage Imaging, San Diego, CA). Image processing and compilation were performed using Canvas Software (Deneba Systems Inc.) and Adobe Photoshop.

To assess the ability of cells to form invadopodia and degrade matrix, at least 10 randomly chosen fields were imaged per trial and evaluated for foci of degraded matrix, which appear as dark "holes" in the bright fluorescent matrix field. A cell degrading at least one hole under the cell or near the cell edge was counted as a cell able to degrade matrix. Invadopodia, defined as actin puncta that colocalize with cortactin, were manually counted and analyzed for underlying matrix degradation and graphed as number of invadopodia per cell or percentage of cells with invadopodia over degraded matrix. Quantification of matrix degradation area per cell was analyzed as described previously (Liu et al., 2009) and was reported as normalized degradation, which is total area of degraded matrix relative to the area of the whole cell. Briefly, the area of degraded matrix in the cell field was measured using ImageJ 1.43s software. Areas of degraded matrix in the bright fluorescent field were converted to 8 bit grayscale files, automatically thresholded into black dots on a white background, followed by automatic

outlining of the dots. The area of each individual cell was measured by manually outlining the cell boundary using the β-actin channel. Data was collected in an Excel spreadsheet and was used to calculate degradation area per cell area.

Detergent-resistant membrane fractionation

Detergent-resistant membrane domains (e.g. lipid rafts) were isolated from MCF-10A cells as described previously (Thankamony and Knudson, 2006) with minor modifications. Briefly, cells cultured on gelatin-coated D150 plates were washed with ice cold PBS 3 times. Cells were lysed in 500 µl lysis buffer (25 mM Tris-HCl, pH 7.5, 150 mM NaCl, 1 mM DTT, 10% sucrose, 1% Triton X-100, and protease inhibitors) on ice for 30 minutes. The cells were mechanically disrupted by passaging 20 times through a 3-inch 22-guage needle. The lysates were mixed directly with iodixanol stock solution (60% solution of Optiprep iodixanol) to yield a 40% (v/v) iodixanol-lysate solution, which was placed at the bottom of an ultracentrifuge tube. Equal volumes of 35%, 30%, 25%, 20% and 0% Optiprep in lysis buffer without Triton X-100 were carefully overlaid above the iodixanol-lysate solution. The samples were centrifuged at 160,000 x g for 8 hours at 4°C in a SW41-Ti rotor (Beckman Coulter). Equal fractions were carefully collected from the top of the tube and equivalent aliquots of each fraction were subjected to immunoblotting using antibodies recognizing proteins of interest.

Immunoblot analysis

Whole cell lysates were prepared for immunoblotting using a RIPA buffer modified to contain 1 mM PMSF, 10 µg/ml aprotinin and leupeptin, 2 mM sodium orthovanadate, and 10 mM sodium fluoride. Protein content was determined by BCA assay (Pierce;

Rockford, IL), and aliquots were solubilized in SDS sample buffer, resolved on Pierce 4-20% reducing polyacrylamide gels, transferred to nitrocellulose (Osmonics, Westborough, MA) with a Pierce apparatus, and stained with antibody.

Results

Up-regulation of CD147 is sufficient for induction of invasiveness in non-transformed breast epithelial cells

We first evaluated endogenous CD147 protein levels expressed by non-transformed MCF-10A cells, a spontaneously immortalized, phenotypically normal, human breast epithelial cell line, and the resulting expression of CD147 after treatment of these cells with recombinant CD147 adenovirus or β-galactosidase (β-gal) adenovirus (as control). We found that an MOI of 2 was effective in expressing CD147 protein expression to a moderate degree (Fig. 2-1A), within the range observed previously in invasive cancer cells; an MOI of 2 was used for the following experiments. It should be noted, however, that the ~38kDa form of CD147 was increased to a greater extent than the ~52kDa form, as observed previously when using recombinant CD147 adenovirus (Li et al., 2001). The 38kDa and 52kDa forms of CD147 have been shown previously to differ in their degrees of glycosylation of the same ~27 kDa protein core (Li et al., 2001; Tang et al., 2004a)

We then evaluated the effect of increased CD147 on invasion of reconstituted basement membrane, Matrigel. We found that the β-gal-treated MCF-10A cells were non-invasive whereas increased CD147 expression induced their ability to invade (Fig. 2-1B, C). To ensure that this effect was not restricted to MCF-10A cells, we examined the

effect of increased CD147 on invasiveness in HMLE cells, another immortalized, non-transformed, human breast epithelial cell line; these cells also express low endogenous levels of CD147 (not shown). In similar fashion to the MCF-10A cells, up-regulation of CD147 induced invasion by these cells as compared with β-gal adenovirus treated cells (Fig. 2-1B, C). These results suggest that up-regulating CD147 is sufficient to induce an invasive cellular phenotype in non-transformed breast epithelia.

Up-regulation of CD147 is sufficient for induction of matrix-degrading invadopodia-like structures in non-transformed breast epithelial cells

Parental MCF-10A cells normally do not form invadopodia (Sung et al., 2009). Thus we next investigated whether the CD147-induced increase in invasion is associated with invadopodia formation and activity. Initially, we found that untreated and control β-gal virus-treated cells cultured on thin fluorescent matrices were unable to degrade the underlying matrix, whereas CD147-adenovirus-treated cells degraded the matrix significantly; moreover the areas of degradation appeared as discrete spots in the matrix (Fig. 2-2A, left panels). To evaluate whether this matrix degradation is due to invadopodia activity, we probed the cells for cortactin and actin; we observed that only cells with increased CD147 demonstrated significant co-localization of cortactin and actin in a punctate manner (Fig 2-2A), which is indicative of invadopodia formation. CD147 up-regulation increased the percentage of cells degrading matrix to approximately 40%, compared to less than 5% in the control groups (Fig. 2-2B, left panel); the areas of matrix degradation corresponded to areas of actin-cortactin co-localization in ~30% of

cells examined (Fig. 2-2C, left panel), indicating induction of active invadopodia by CD147 in these cells. We further evaluated the degradation areas and number of invadopodia present in each of the cell groups and found that CD147 up-regulation resulted in a greater area of matrix degradation per total cell area compared to parental and β-gal-treated cells (Fig. 2-2B, right panel). Moreover, whereas the parental and β-gal-treated cells had essentially no invadopodia, cells with increased CD147 expression had an average of ~6 invadopodia per cell (Fig. 2-2C, right panel).

In order to visualize the induction of invadopodia more clearly, we compiled a volumetric 3D-reconstruction of serial confocal images of MCF-10A cells treated with CD147 adenovirus, using Amira 3D image software. In Figure 2-3, panel A depicts the 3D environment for a single cell, where the fluorescent matrix appears as red, the actin cytoskeleton is blue, and cortactin is labeled in green. Approximately six invadopodia are penetrating through to the bottom of the matrix (Fig. 2-3B) and a cross-section through the cell-matrix interface demonstrates co-localization of actin and cortactin in these protrusions (Fig. 2-3C); supplementary videos illustrate protrusion of several of these invadopodia-like structures through the underlying matrix (supplementary material: Movies 1 and 2).

These observations indicate that CD147 plays an important role in the induction of invadopodia formation and activity.

CD147-induced, invadopodia-mediated, matrix degradation is dependent on membrane-type MMPs

Although multiple MMPs effectively degrade components of the ECM and mediate invasiveness in vitro, several studies show that invadopodia utilize membrane type MMPs, particularly MT1-MMP, to degrade the ECM (Artym et al., 2006; Frittoli et al., 2010; Liu et al., 2009; Poincloux et al., 2009; Rowe and Weiss, 2008). Since CD147 induces both soluble and membrane type MMPs in various systems (Nabeshima et al., 2006; Yan et al., 2005), we employed the MMP inhibitors, TIMP-1 and TIMP-2, to distinguish which class of MMP was responsible for CD147-induced, invadopodia-mediated matrix degradation. TIMP-1 selectively inhibits the activity of soluble MMPs whereas TIMP-2 is an inhibitor of both soluble and membrane-bound MMPs (Hotary et al., 2006). As expected, TIMP-2 inhibited most CD147-induced matrix degradation whereas TIMP-1 did not (Fig. 2-4A, B). These results show that cells expressing increased levels of CD147 utilize MT-MMPs to facilitate invadopodia-mediated matrix degradation.

Since the major membrane type-MMP associated with invadopodia formation and activity is MT1-MMP, we next evaluated whether increased CD147 in MCF-10A cells induces MT1-MMP expression. We found that MCF-10A cells express low amounts of MT1-MMP, but treatment with CD147 adenovirus increases MT1-MMP as well as CD147 protein levels (Fig 2-4C). CD147 induced expression of both the active form (~50 kDa) and pro-form (~63 kDa) of MT1-MMP when the cells were cultured on gelatin (Fig. 2-4C), the conditions employed for invadopodia formation. However, when the

CD147-upregulated cells were grown on polystyrene, only the ~63 kDa MT1-MMP pro-form was detected (data not shown).

To evaluate further whether the invasive phenotype of CD147-upregulated cells was due to MT1-MMP activity, we treated the cells with a function blocking antibody targeting the catalytic domain of MT1-MMP. We found that the MT1-MMP blocking antibody significantly decreased both CD147-induced matrix degradation and Matrigel invasion compared to cells treated with a control IgG antibody (Figures 2-4D and E).

CD147 associates with MT1-MMP in CD147-induced invadopodia-like structures and in membrane sub-fractions with the properties of lipid rafts

Since the data above support regulation of MT1-MMP expression by CD147, we investigated whether CD147 co-localizes with MT1-MMP and whether co-localization occurs within the induced invadopodia-like structures. We found that the two proteins co-localize over a subset of foci of degraded matrix (Fig 2-5A; yellow arrows), but also co-localize in foci that do not coincide with matrix degradation (Fig 2-5A; red arrows). Corresponding staining of β-gal-infected cells showed relatively weak staining for MT1-MMP or CD147 (Fig. 2 Supplemental 1). Previous studies have shown that CD147 and MT1-MMP are present in endocytic compartments, as well as in the plasma membrane (Eyster et al., 2009; Jiang et al., 2001). Thus, we evaluated whether sub-populations of CD147 and MT1-MMP were present in a vesicular compartment within MCF-10A cells over-expressing CD147, and found that distinct sub-populations of CD147 and MT1-MMP are co-localized in EEA1-positive vesicles (Fig. 2-5B). These results, together with

those in Fig. 2-5A, indicate that sub-populations of CD147 and MT1-MMP are present in vesicular compartments distinct from the populations that are localized in invadopodia. These findings are consistent with FACS analyses (data not shown), which showed that up-regulation of CD147 induced ~30% increase in cell surface MT1-MMP compared to a total increase in MT1-MMP expression of ~80% (from Western blots), implying that a significant fraction of induced MT1-MMP remains inside the cells.

Recent studies have shown that invadopodia are highly enriched in lipid raft domains and are dependent on these raft domains for invadopodia initiation and degradative activity (Yamaguchi et al., 2009). Independent studies have shown that CD147 (Schwab et al., 2007; Tang and Hemler, 2004) and MT1-MMP (Annabi et al., 2001; Yamaguchi et al., 2009) are at least in part localized in membrane compartments similar to lipid rafts. Thus, we examined whether CD147 influences MT1-MMP localization into lipid rafts. Using a detergent-based lipid raft isolation protocol we showed that up-regulation of CD147 in MCF-10A cells results in an enrichment of both CD147 and MT1-MMP in the raft fractions (light fraction) compared to β-gal-treated cells (Fig. 2-5C). Notably, most of the CD147 in the raft fractions was the lower molecular weight form of ~38kDa. These results, in conjunction with earlier findings (Yamaguchi et al., 2009), imply that up-regulation of CD147 leads to enrichment of MT1-MMP within specialized regions of the plasma membrane, most likely within invadopodia. However some of these lipid raft domains might reside in the membranes of intracellular vesicles, as discussed above.

CD147 regulates invadopodia function in invasive breast cancer cells

Multiple cell models have been used to study invadopodia dynamics, but the majority of these studies have utilized the invasive human breast cancer cell line MDA-MB-231 (Artym et al., 2006; Hu et al., 2011; Liu et al., 2009; Yamaguchi et al., 2009). Thus, we also evaluated whether CD147 regulates invadopodia dynamics in MDA-MB-231 cells. Figure 2-6A shows the endogenous level of CD147 expression in MDA-MB-231 cells and the resulting expression of CD147 after treatment of these cells with recombinant CD147 adenovirus or β-gal adenovirus as control. We found that an MOI of 2 was effective in up-regulating CD147 protein expression to a moderate degree (Fig 2-6A), within the range observed in various invasive cells; this MOI was used for the following experiments. As with the MCF-10A cells, the ~38kDa form of CD147 was increased to a greater extent than the ~52kDa form. The MDA-MB-231 cells express MT1-MMP and invade Matrigel to a moderate level. However, up-regulation of CD147 in these cells was accompanied by increased MT1-MMP expression (Fig. 2-6B) and increased Matrigel invasiveness (Fig. 2-6D) as compared to controls. Bands corresponding to pro-form and active form of MT1-MMP were induced. We also treated MDA-MB-231 cells with pooled target-specific siRNAs. Dose-dependent down-regulation of CD147 was observed and was accompanied by corresponding partial decreases in MT1-MMP message and protein levels (Fig. 2-6C), as well as invasiveness in Matrigel (Fig. 2-6D).

We next determined whether changes in CD147 expression in MDA-MB-231 cells led to corresponding changes in invadopodia formation and activity. Cells treated with β-gal adenovirus showed a moderate number of invadopodia and degradation spots in the fluorescent matrix field, in similar numbers to those reported in earlier studies (Artym et

al., 2006). However, when cells were treated with CD147 adenovirus there was an increase in the percentage of cells degrading the matrix, concomitant with an increase in the percentage of cells with invadopodia (Fig. 2-7A-C). Up-regulation of CD147 resulted in an increase in invadopodia number from ~4 per cell to ~8 per cell (Fig. 2-7C, right panel), coincident with large increases in degradation area per cell (Fig 2-7B, right panel). Partial down-regulation of endogenous CD147, using pooled siRNAs (Fig. 2-6C), resulted in corresponding partial decreases in the percentage of cells degrading matrix, cells with invadopodia, number of invadopodia per cell, and area of matrix degradation per cell, whereas cells treated with control siRNA were comparable to β-gal-treated cells (Fig 2-7A-C).

Co-localization of CD147 and MT1-MMP in invasive breast cancer cells

In similar manner to our experiments with CD147-treated MCF-10A cells (Fig. 2-5A), parental MDA-MB-231 cells displayed CD147 and MT1-MMP that co-localized over foci of degraded matrix (Fig 2-8A; yellow arrow/asterisk) and non-degraded matrix (Fig. 2-8A; red arrow/asterisk). These results were confirmed with a monoclonal antibody against MT1-MMP from Epitomics Inc. (Fig. 2 Supplemental 2)

To further evaluate the observed co-localization of CD147 and MT1-MMP, we performed a proximity ligation assay (PLA), which can detect endogenous protein-protein interactions that occur within 40 nm (Soderberg et al., 2006). Probing for CD147 and MT1-MMP in MDA-MB-231 cells using the proximity ligation method revealed that endogenous CD147 and MT1-MMP associate closely (Figure 2-8B). In a control

experiment using only CD147 primary antibody followed by secondary PLA probes and amplification, no interaction was observed; additional field images demonstrated that CD147-MT1-MMP interactions occur throughout the cell population (Fig. 2 Supplemental 3). Furthermore, we confirmed the specificity of the reaction by performing DIC microscopy, which demonstrated that the interactions occurred only in association with cells and did not represent non-specific staining of the culture substratum (Figure 2-8B, right panels; Fig. 2 Supplemental 3). We found approximately 12-15 CD147-MT1-MMP interactions per cell and, when the proximity ligation method was combined with the gelatin degradation assay, these CD147-MT1-MMP interactions were found over areas of both degraded and non-degraded matrix (Fig. 2-8C), similar to the results in Fig. 2-8A. These data strongly support close interactions of sub-populations of CD147 and MT1-MMP in actively degrading invadopodia, as well as in other areas of the cell such as EEA1-positive vesicles (Fig. 2-5B).

Discussion

Cancer cells employ various strategies to compromise the ECM scaffolds that inhibit their spreading through different tissue compartments. A major mechanism used by many cancer cell types to degrade the surrounding ECM is the formation of specialized actin-enriched membrane protrusions called invadopodia. The proteolytic activity of invadopodia has been mainly attributed to the localization of MT1-MMP at the cell surface in specialized membrane domains with the properties of lipid rafts, a process that is orchestrated by a diverse group of interacting molecules (Frittoli et al., 2010; Murphy

and Courtneidge, 2011; Poincloux et al., 2009). Here we have made several novel findings indicating that CD147 has a major mechanistic role in invadopodia formation and activity, and consequently in invasion.

CD147 expression is associated with many malignant phenotypes, including chemo- and radio-therapy resistance, aerobic glycolysis, anchorage-independent growth, angiogenesis, invasion and increased metastatic potential. Among the best characterized functions of CD147 is induction of MMPs, including MT1-MMP (Nabeshima et al., 2006; Yan et al., 2005). The exact mechanisms by which CD147 induces MMPs is not known, but current evidence indicates that homophilic CD147 interactions mediate this induction (Sun and Hemler, 2001; Tang et al., 2004b) and result in various downstream signaling events that promote MMP synthesis and other activities (Ghatak et al., 2005; Lim et al., 1998; Tang et al., 2008; Venkatesan et al., 2010; Yang et al., 2006). In agreement with earlier studies, we demonstrated that up-regulation or down-regulation of CD147 increases or decreases, respectively, the levels of MT1-MMP and invasiveness. In addition, we have demonstrated that modulation of CD147 expression correspondingly alters invadopodia function.

Most strikingly, we found that up-regulating CD147 expression in non-transformed breast epithelia was sufficient to induce an invasion program similar to that seen in already invasive cancer cells, which was characterized by Matrigel invasion and formation of MT-MMP-dependent, actively degradative invadopodia. This suggests that up-regulation of CD147 enriches the cell surface with active pools of MT1-MMP that subsequently degrade the matrix, as depicted in the gelatin degradation assays (Fig. 2-2A). Though the mechanisms are not fully understood, earlier reports have demonstrated

that CD147 interacts with actin (Schlosshauer et al., 1995) and that manipulation of CD147 expression results in reorganization of the actin cytoskeleton (Qian et al., 2008) and formation of actin-rich lamellipodia in Drosophila cells (Curtin et al., 2005); whether these findings are related to the mechanism of invadopodia formation is not known. In addition to its interactions with the actin cytoskeleton, CD147 interacts with several other invadopodia-enriched molecules, such as integrins (Berditchevski et al., 1997) and CD44 (Slomiany et al., 2009), that mediate attachment of ECM components to the cell surface and influence cytoskeleton remodeling. Recent evidence also suggests that CD147 can up-regulate various transcription factors leading to multiple downstream signaling events associated with ECM remodeling and invasion (Venkatesan et al., 2010). Thus, CD147-regulated invadopodia formation may be due in part to interactions with other ancillary invadopodia-associated proteins.

Another established function of CD147 is in lactate transporter trafficking to the cell surface, where CD147 is an essential chaperone needed to display sub-classes of lactate transporters on the cell surface (Halestrap and Meredith, 2004). Though it is currently unknown whether CD147 is also involved in trafficking of MMPs to the cell surface, our data demonstrate that endogenous CD147 and MT1-MMP are in close proximity and that sub-populations of this complex occur in actively degrading invadopodia whereas other sub-populations are present in EEA1-positive endocytic vesicles. These results suggest the possibility that CD147-MT1-MMP complexes may cycle between these two compartments. Other investigators have shown that CD147 associates with both the pro and active forms of MT1-MMP (Egawa et al., 2006; Niiya et al., 2009). In addition, we found that up-regulation of CD147 in non-transformed MCF-10A epithelial cells results

in enrichment of both CD147 and MT1-MMP in membrane compartments with characteristics similar to lipid raft domains, supporting previous observations that invadopodia formation and activity are dependent on these domains (Yamaguchi et al., 2009). These results are compatible with the idea that CD147 may play a role in subcellular trafficking or surface presentation of MT1-MMP. However, further work is required to determine whether CD147 is involved at multiple steps during initiation and maturation of invadopodia or whether it aids solely during the degradation process.

Of interest also is our observation that a relatively low-glycosylated form of CD147 was induced by treatment with recombinant CD147 adenovirus and that this form was the major form targeted to the lipid raft domains (Figure 2-5C). The results of some previous studies suggest strongly that high levels of glycosylation are necessary for induction of MMP production (Guo et al., 1997; Tang and Hemler, 2004), whereas others have demonstrated robust MMP production after treatment with non-glycosylated CD147 (Belton et al., 2008) or CD147 substituted only with the disaccharide, chitobiose (Kawakami et al., 2011). Clearly, further investigation is required to elucidate the role of glycosylation in CD147 activities within different contexts.

Mechanisms of regulation of endogenous CD147 expression are not well established, although several growth factors and cytokines have been shown to increase CD147 levels in a variety of contexts (Hagemann et al., 2005; Menashi et al., 2003; Reddy et al., 2010; Rucci et al., 2010). Previous studies have shown that Src is a critical regulator of invadopodia formation (Murphy and Courtneidge, 2011), and a recent study showed that the Src family kinase, Fyn kinase, induces emmprin expression (Ramos and Dang, 2011). We have also found that CD147 is elevated in cells over-expressing wild-type or

constitutively active Src (G.D.G, unpublished data), suggesting that Src may act at least in part via induction of CD147.

In the present study, we provide evidence that increased CD147 alone is sufficient to induce the formation of actively degradative invadopodia-like structures in non-transformed epithelial cells and that CD147 may regulate localization of MT1-MMP in lipid raft domains. Furthermore, we have demonstrated that CD147 and MT1-MMP are in close proximity to each other and these interacting pools are present in part within active invadopodia. Since CD147 is enriched on the surface of numerous malignant cancer cell types, it represents a plausible molecular target to evaluate for future cancer therapies, especially with respect to invasion and metastasis.

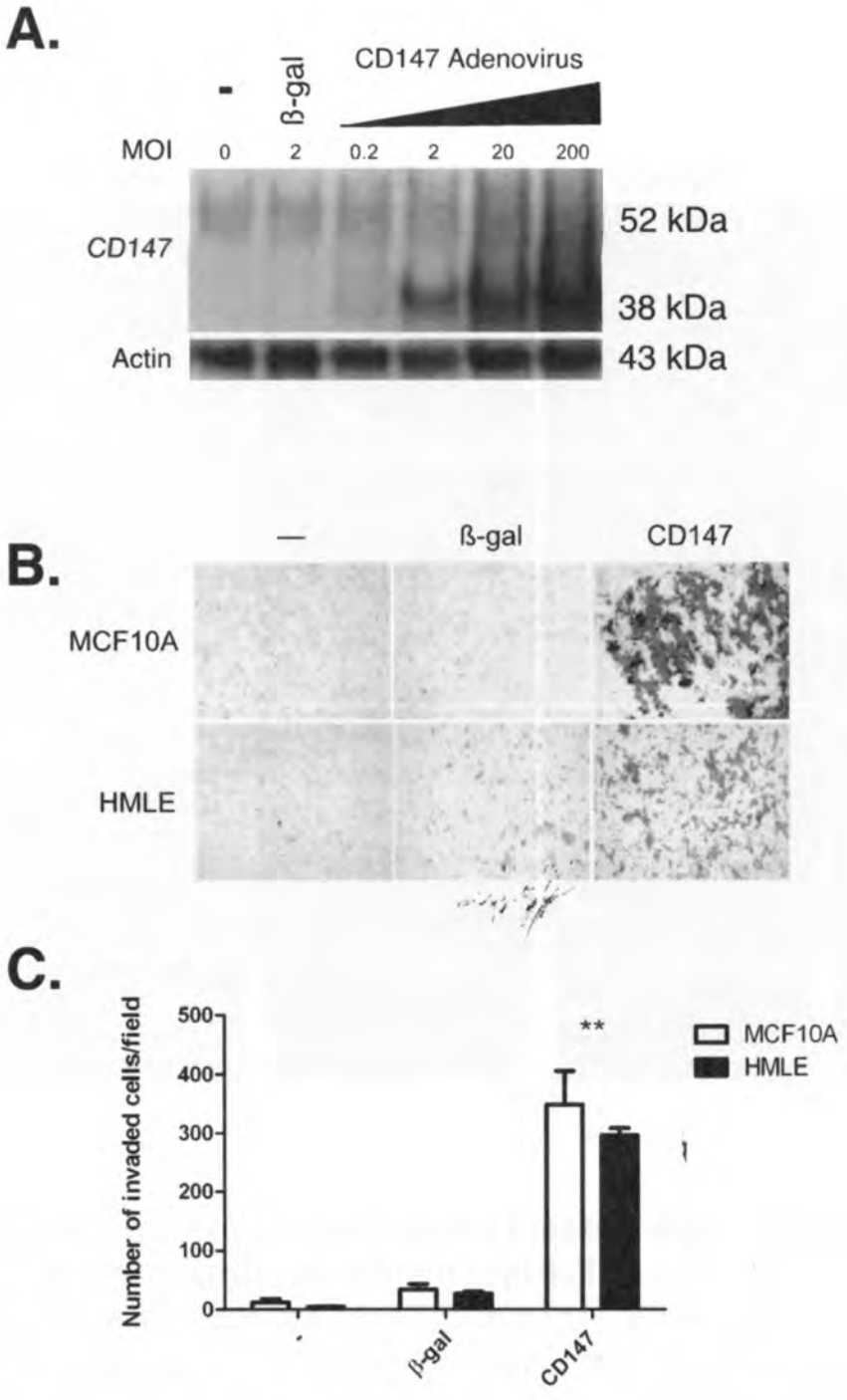

Figure 2-1. Up-regulation of CD147 in non-transformed breast epithelial cells increases invasion. (A) Western blot showing endogenous CD147 protein expression in MCF-10A cells and increased CD147 expression after up-regulation with increasing MOI of CD147 adenovirus. An MOI of 2 was used in all subsequent experiments. (B) MCF-10A or HMLE cells that were untreated or infected with β-gal or CD147 adenovirus were plated on Matrigel-coated invasion chambers and analyzed for invasion. (C) Quantitation of invasion; columns represent means +/- SEM of numbers of cells invaded per field in 3 independent experiments. ** $P < 0.01$.

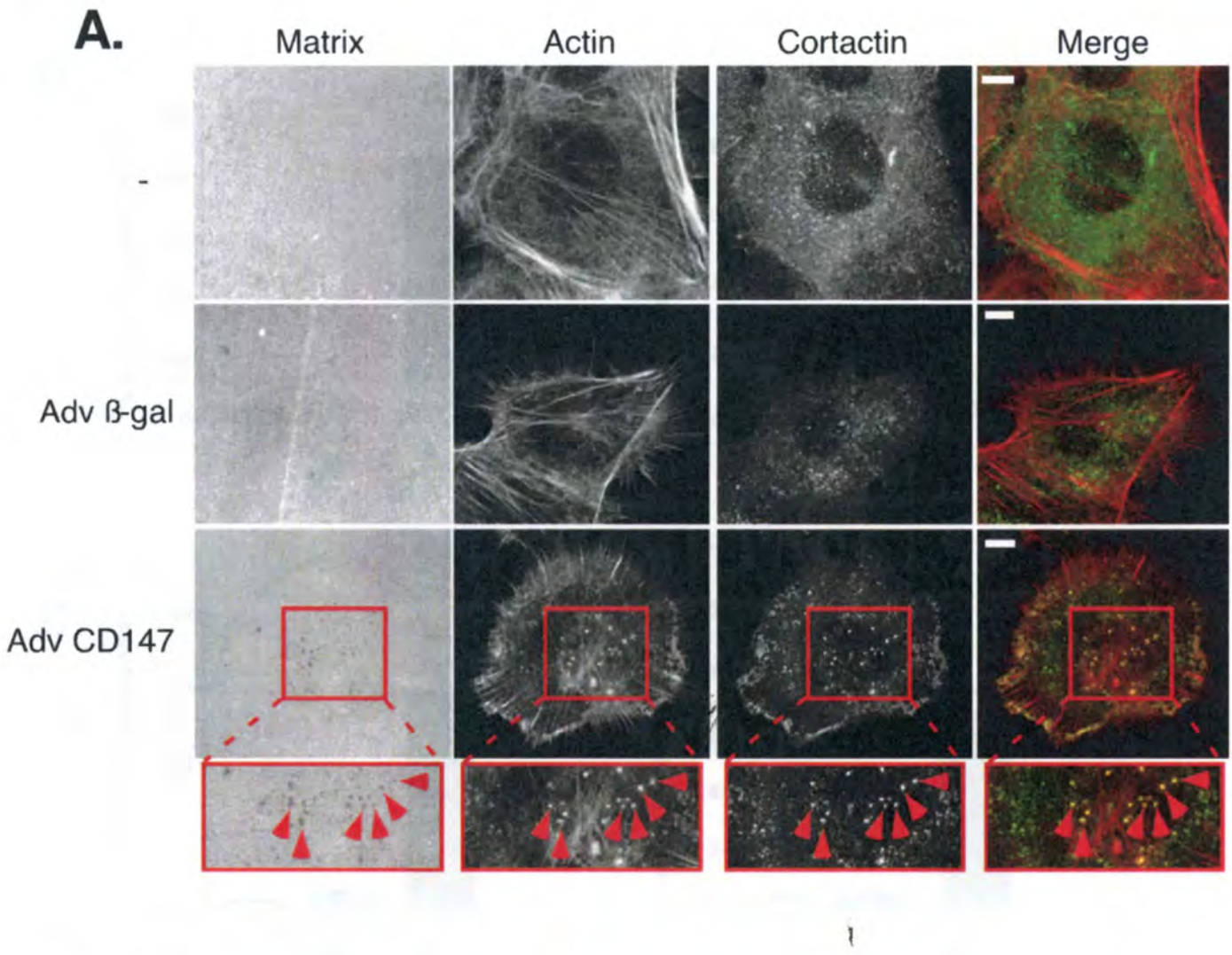

Figure 2-2. CD147 induces the formation of matrix-degrading invadopodia-like structures in non-transformed breast epithelial cells. MCF-10A cells, non-infected or infected with β-gal or CD147 adenovirus, were cultured on a fluorescent gelatin matrix for 15 hours. (A) Representative micrographs of non-infected, β-gal, and CD147 adenovirus-infected cells cultured on fluorescent matrix. After fixation, cells were immunolabeled for cortactin (primary 4F11 antibody followed by secondary Alex Fluor-488 antibody) and Alexa Fluor 647-phalloidin. Actin and the gelatin matrix were pseudo-colored to red and blue, respectively; this allows easier visualization of colocalization (yellow) of actin (red) and cortactin (green). Invadopodia-mediated matrix degradation appears as dark black foci in the bright fluorescent matrix field. *Boxed insets*, higher magnifications of examples of invadopodia (arrowheads), identified by colocalization of cortactin and actin punctae over areas of degraded matrix. Scale bar, 10 μm. Each experiment was repeated at least three times.

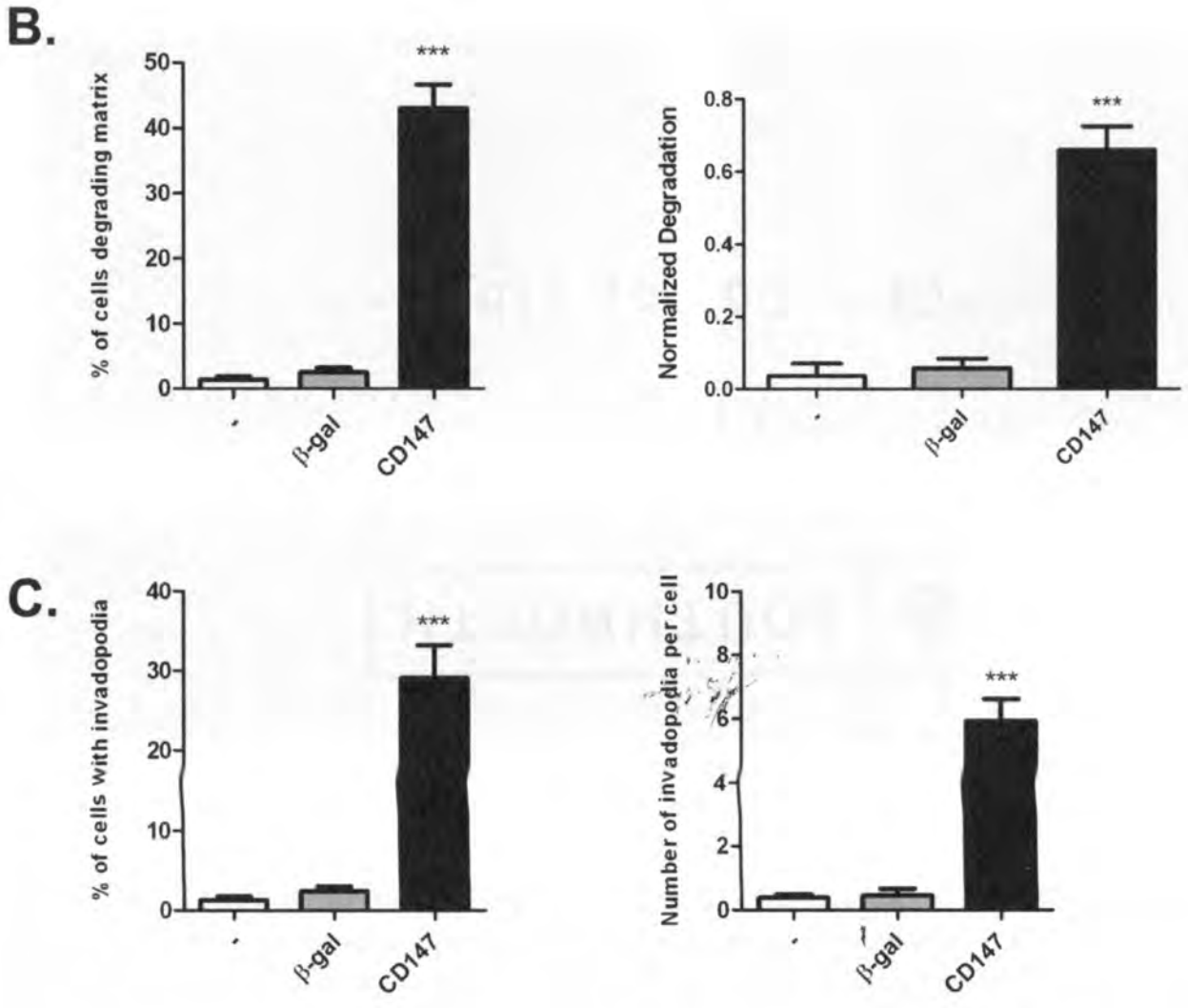

Figure 2-2 (continued). CD147 induces the formation of matrix-degrading invadopodia-like structures in non-transformed breast epithelial cells. (B-C) Quantification of invadopodia characteristics: (B) Left panel: Percentage of cells degrading matrix. Right panel: Normalized degradation, calculated as area of degradation/total cell area defined by actin channel. (C) Left panel: Percentage of cells with active invadopodia, defined as cortactin-actin aggregates over degraded matrix. Right panel: Number of invadopodia/cell. Each parameter was calculated by evaluating 10 random fields containing at least 15 cells/field over 3 independent experiments. Columns, mean; Bars, SEM. *** (p-value <0.001).

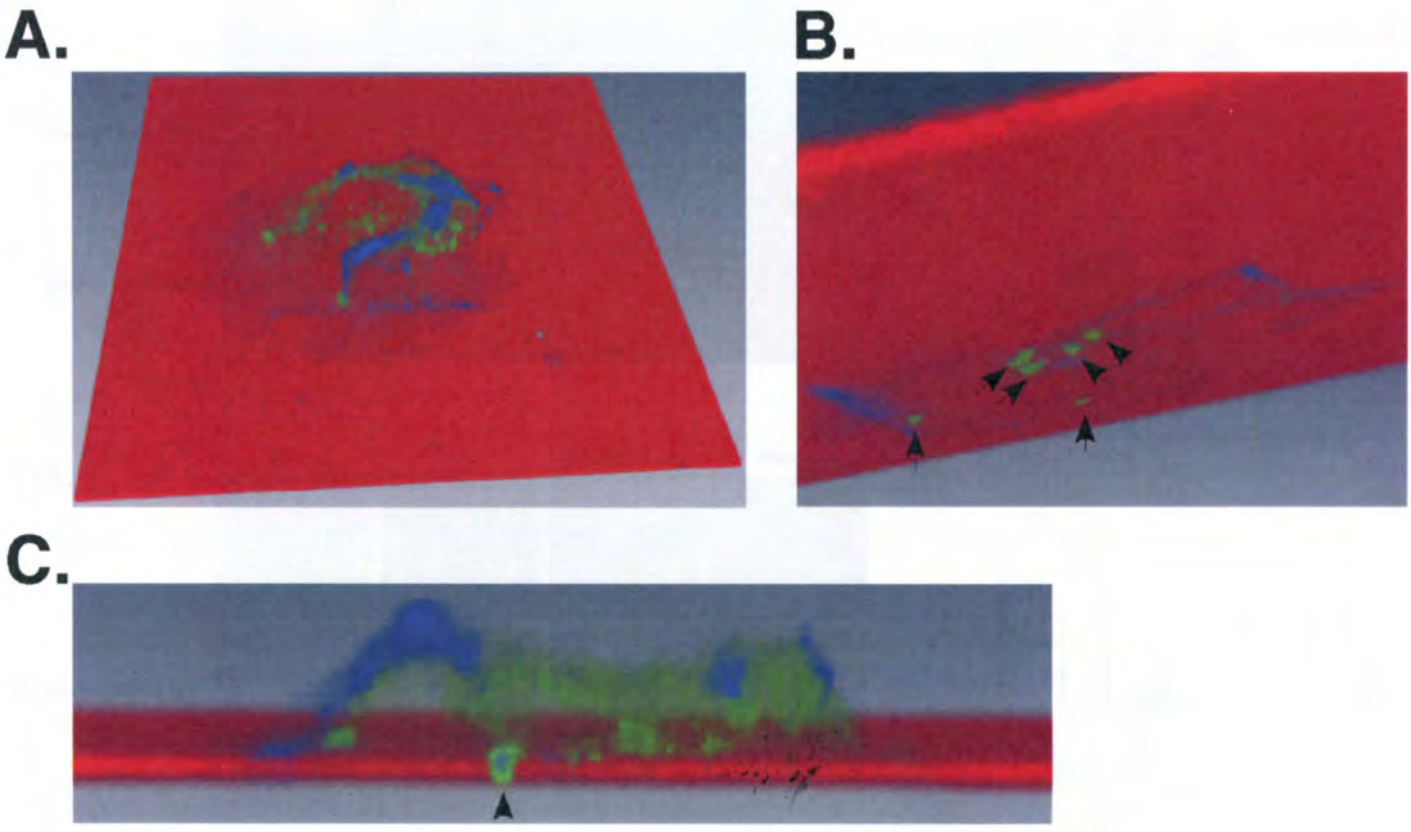

Figure 2-3. Three-dimensional volumetric reconstruction of CD147-induced invadopodia-like structures penetrating the underlying matrix. CD147 adenovirus-infected MCF-10A cells cultured on a fluorescent-gelatin matrix were analyzed with confocal microscopy. Leica SP5 confocal software was employed to obtain an optimal image stack from single cell images and was further processed with Amira software to reconstruct a 3D volumetric image of a cell producing invadopodia-like protrusions that are penetrating the underlying fluorescent matrix. Cells were stained with Alexa-phalloidin (blue) to image actin filaments and cortactin (green) to identify invadopodia; fluorescent matrix is depicted in red. A) Overhead view of a single cell cultured on fluorescent matrix; B) View underneath the fluorescent matrix showing ~6 invadopodia (arrows) penetrating the matrix; C) Magnified cross-section through cell demonstrating one of the invadopodia-like protrusions (actin and cortactin positive; arrowhead) penetrating the fluorescent matrix.

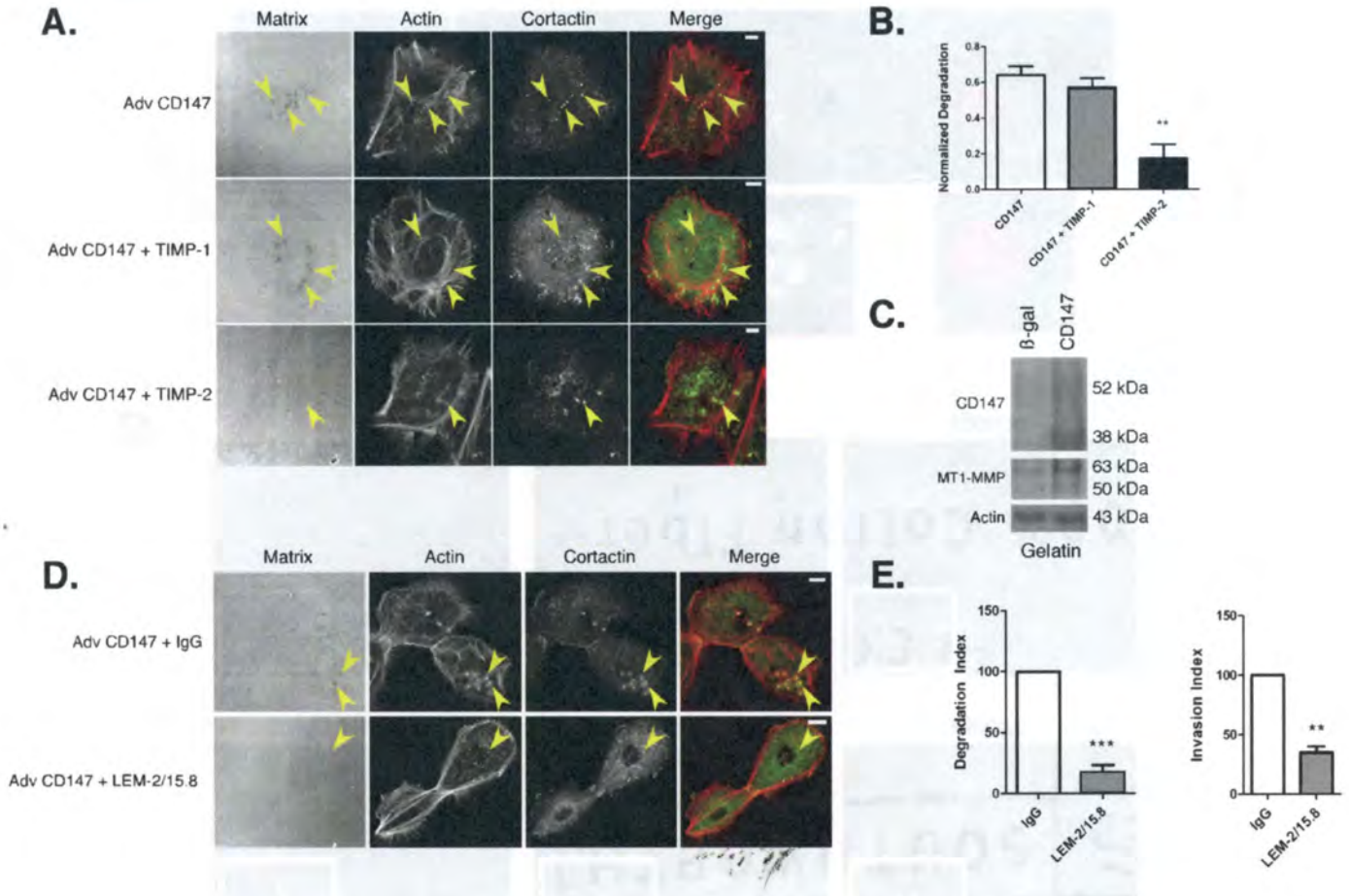

Figure 2-4. CD147-induced, invadopodia-mediated, matrix degradation is dependent on membrane-type MMPs. (A-B) MCF-10A cells infected with CD147 adenovirus were pre-treated with the protease inhibitors, TIMP-1 (0.5 μg/ml) and TIMP-2 (0.5 μg/ml) for 30 minutes and then plated on fluorescent matrices for 12 hours in the presence of these inhibitors. A) Representative micrographs of matrix degradation in control and CD147 up-regulated cells in the presence of protease inhibitors. Scale bar, 10 μm. B) Quantitation of normalized degradation area, expressed as means +/- SE. ** $p < 0.01$. Experiment was repeated 3 times. C) Western blot of CD147 and MT1-MMP in aliquots of lysates obtained from MCF-10A cells that were cultured on gelatin and untreated or treated with control (β-gal) or CD147 adenovirus. Actin was used as a loading control; n=3. (D-E) MCF-10A cells infected with CD147 adenovirus were pre-treated with function-blocking antibody against MT1-MMP (LEM-2/15.8; 12 μg/ml) or control IgG and then plated on fluorescent matrices for 12 hours in the presence of the blocking antibody or IgG. D) Representative micrographs of matrix degradation in control and CD147 up-regulated cells in the presence of blocking antibody or IgG. Scale bar, 10 μm. E) Left panel: Quantitation of normalized degradation area. Right panel: Quantitation of invasion through Matrigel. Expressed as means +/- SE. **$p < 0.01$; ***$p<0.001$; experiments were repeated 3 times.

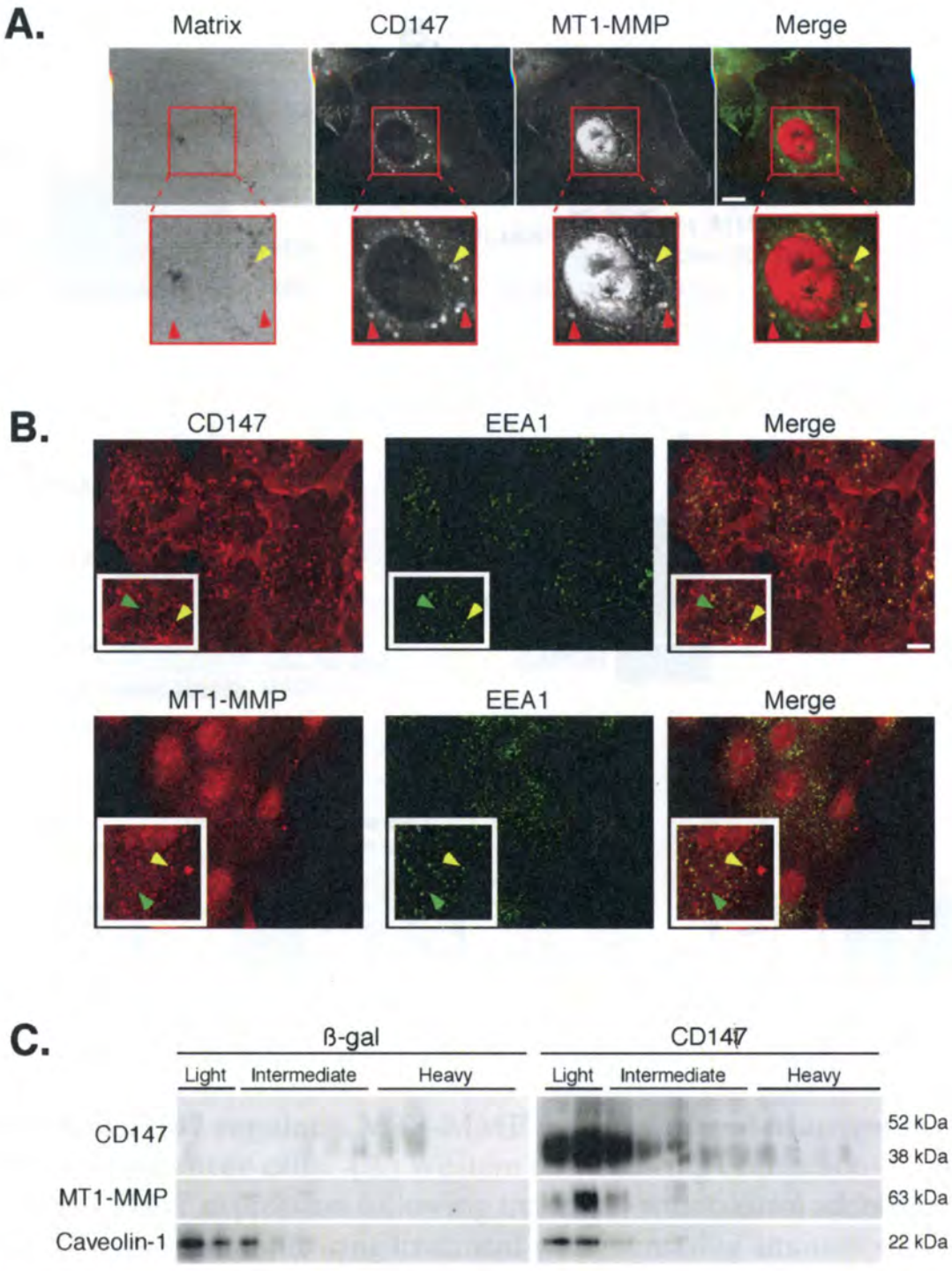

Figure 2-5. CD147 associates with MT1-MMP in invadopodia-like structures and in membrane sub-fractions with the properties of lipid rafts. A) Representative micrographs of CD147 and MT1-MMP colocalizing over degraded matrix in CD147-overexpressing MCF-10A cells. Yellow arrows indicate colocalization of CD147 (green) and MT1-MMP (red) over foci of degraded matrix; red arrows indicate colocalization of CD147 and MT1-MMP over areas not showing degraded matrix. Scale bar, 10 μm. B) Representative micrographs showing co-localization of CD147 (top panels) or MT1-MMP (bottom panels) with EEA1-positive vesicles. Yellow arrows indicate co-localization of proteins; green arrows indicate lack of co-localization. Scale, 10 μm C) MCF-10A cells infected with β-gal or CD147 adenovirus were plated on gelatin-coated plates overnight and were subjected to detergent-resistant membrane isolation. *Light* fraction represents the gradient interface (0-20%) where detergent-resistant membrane domains such as lipid rafts localize. n=2

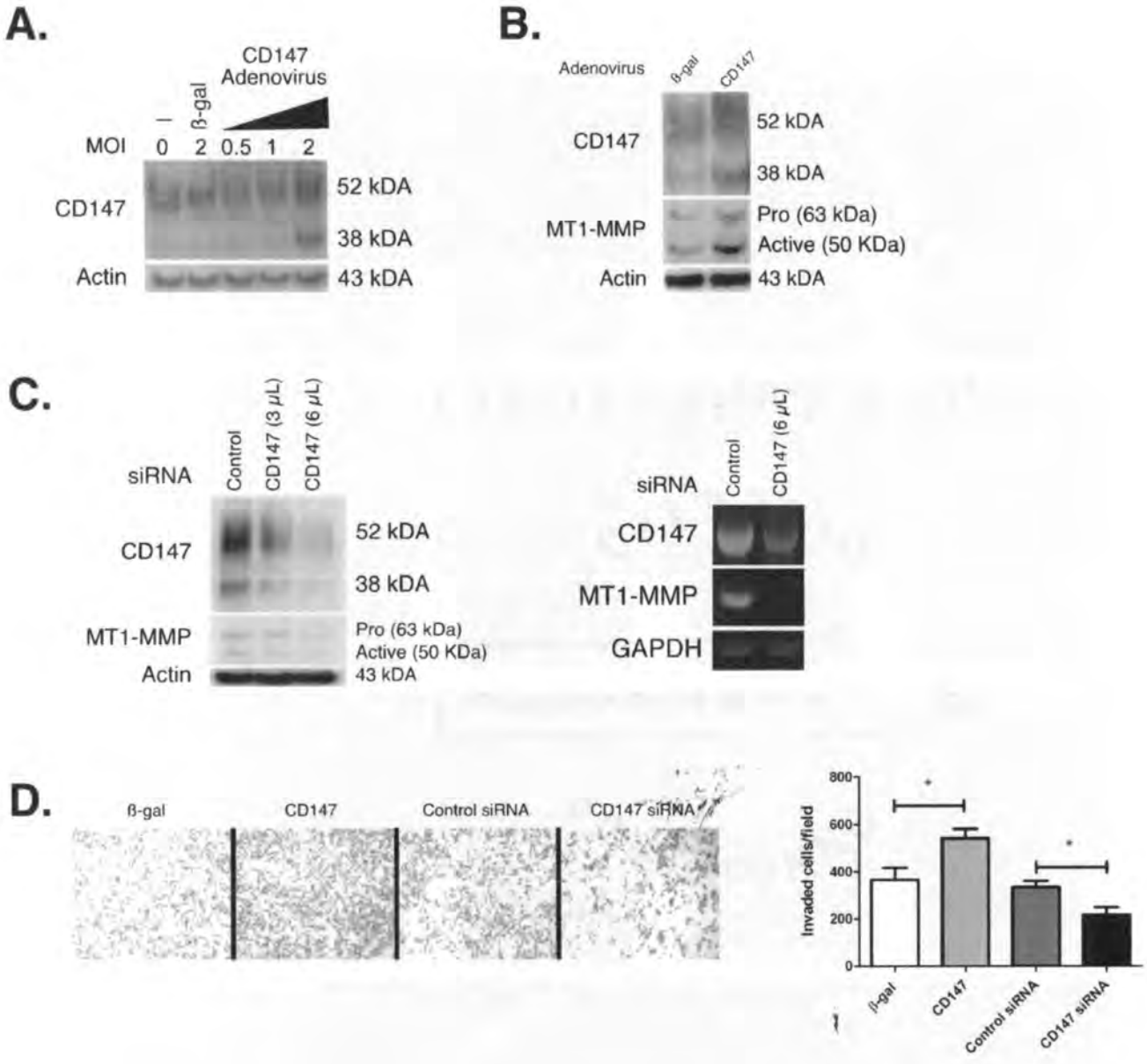

Figure 2-6. CD147 regulates MT1-MMP expression and Matrigel invasion in invasive breast cancer cells. (A) Western blot showing endogenous CD147 protein expression, CD147 expression following treatment with control adenovirus (β-gal), and CD147 expression following treatment with increasing amounts of recombinant CD147 adenovirus in MDA-MB-231 cells; n=2. An MOI of 2 was chosen for up-regulating CD147 in subsequent experiments. β-actin was used as the loading control. (B) Representative western blot of increased MT1-MMP levels following CD147 up-regulation in MDA-MB-231 cells; n=3. β-gal treatment was used as the control; β-actin demonstrates equal loading. C) Left panel: Western blot demonstrating that knockdown of CD147 with increasing concentrations (3 and 6μl) of pooled target-specific siRNA results in decreased MT1-MMP protein expression. Non-specific siRNA was used as a control and β-actin was used to demonstrate equal loading; n=3. Right panel: RT-PCR analysis of CD147 and MT1-MMP mRNA after treatment with control or CD147 siRNAs. D) Left panel: Representative images of Matrigel invasion assay with MDA-MB-231 cells treated with β-gal or CD147 adenovirus or with control or CD147-specific siRNA. Right panel: Quantification of invaded cells per field by evaluating four separate fields in 3 independent experiments. Columns represent means and bars are SEM. * p-value <0.05.

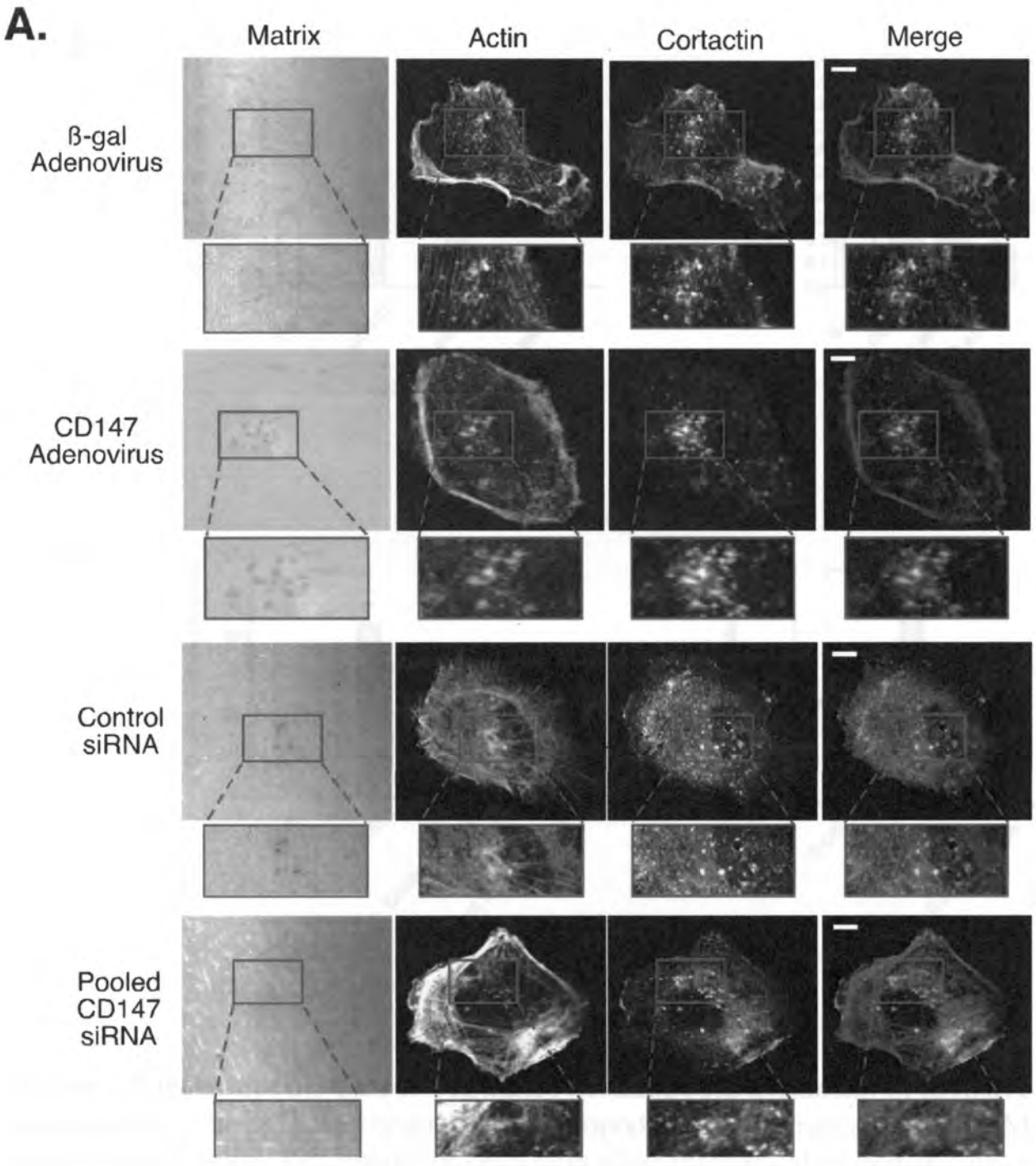

Figure 2-7. CD147 regulates invadopodia dynamics in invasive breast cancer cells. (A) Representative micrographs demonstrating MDA-MB-231 cells treated with β-gal or CD147 adenovirus or with control or CD147-targeted siRNA. Cells were cultured on Alexa Fluor 568-conjugated gelatin for 5 hours, fixed, and probed for actin (Alexa 647 phalloidin) and cortactin (primary 4F11 antibody followed by secondary Alex Fluor-488 antibody). Actin and the gelatin matrix were pseudo-colored to red and blue, respectively; this allows for easier visualization of colocalization (yellow) of actin (red) and cortactin (green). The left panels demonstrate invadopodia-mediated matrix degradation (dark holes). Boxed insets, higher magnifications of invadopodia. Bars, 10 μm. n=3.

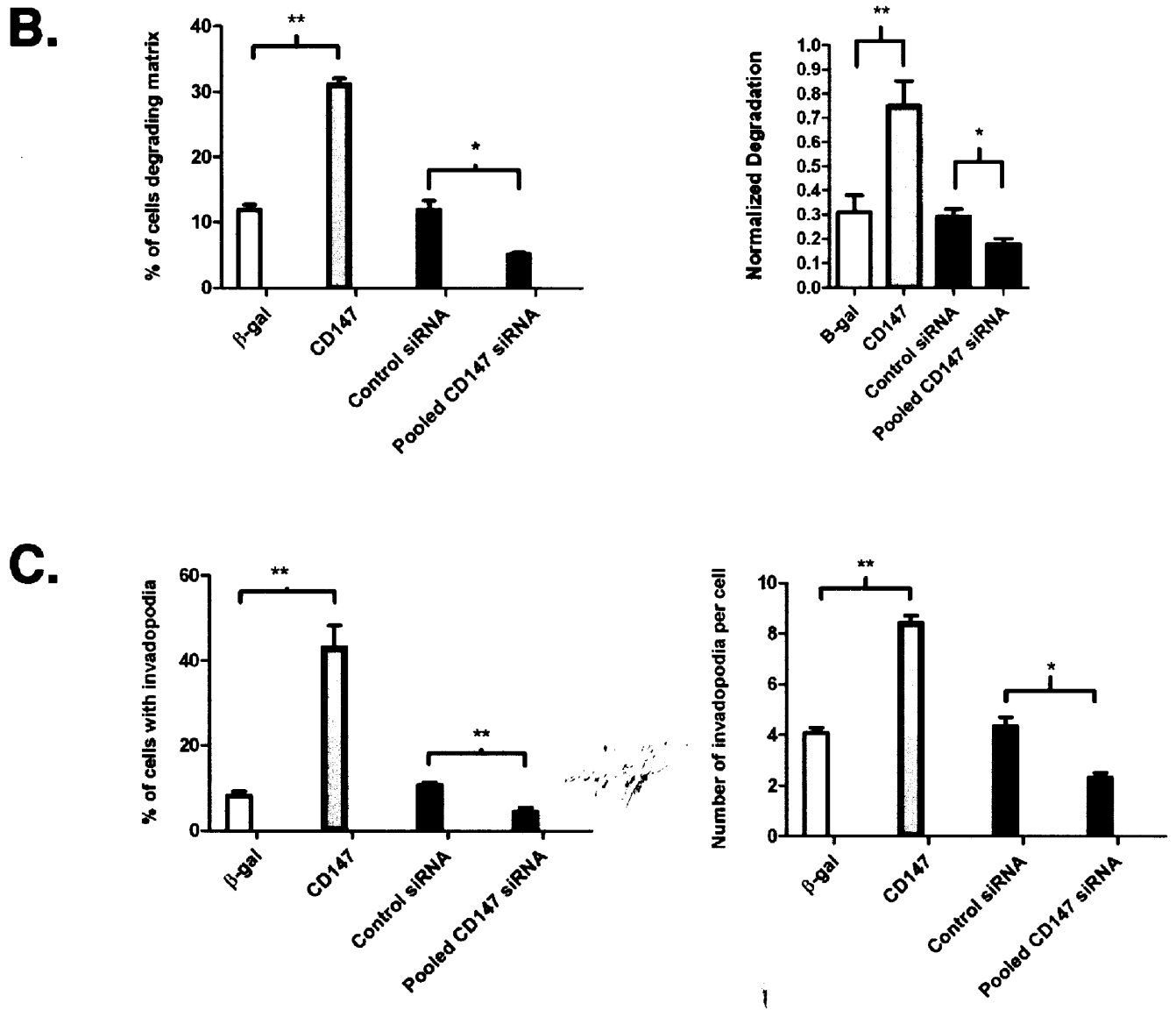

Figure 2-7 (continued). CD147 regulates invadopodia dynamics in invasive breast cancer cells. (B-C) Quantification of invadopodia characteristics for MDA-MB-231 cells: (B) Left panel: Percentage of cells degrading matrix; calculated as cells with at least one area of degradation underneath the cell or near cell border. Right panel: Normalized degradation, calculated as area of degradation/total cell area defined by actin channel. (C) Left panel: Percentage of cells with invadopodia, defined as actin-cortactin aggregates localized over degraded matrix. Right panel: Number of invadopodia/cell in cells exhibiting at least one invadopodium. Each parameter was calculated by evaluating 10 random fields containing at least 20 cells/field over 3 independent experiments. Columns, mean; Bars, SEM. * (p-value <0.05), ** (p-value <0.01).

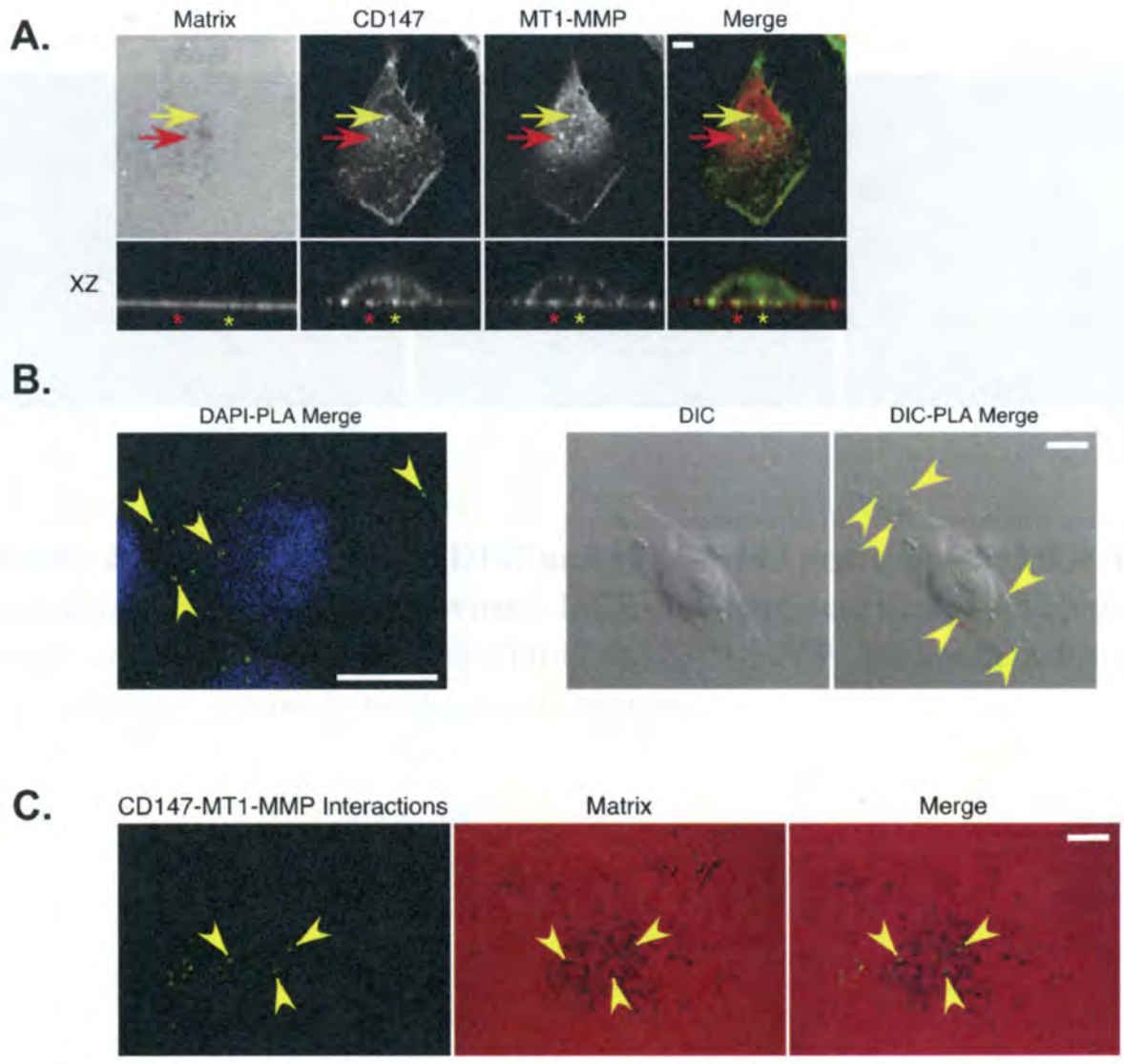

Figure 2-8. Co-localization of CD147 and MT1-MMP in invasive breast cancer cells. (A) Representative image demonstrating CD147 and MT1-MMP co-localization in MDA-MB-231 cells. Cells were cultured on Alexa Fluor 568-conjugated gelatin for 5 hours and probed with CD147-488 and MT1-MMP followed by an Alexa Fluor-647 secondary antibody. Polyclonal antibody against MT1-MMP (Millipore) was used for these images; monoclonal antibody against MT1-MMP (Epitomics) gave similar results (Supplemental Figure 2). MT1-MMP and the gelatin matrix were pseudo-colored to red and blue, respectively; this allows easier visualization of colocalization (yellow) of CD147 (green) and MT1-MMP (red). Yellow arrow depicts CD147-MT1-MMP co-localization over foci of degraded matrix; red arrow indicates colocalization of CD147 and MT1-MMP over an area not showing degraded matrix. XZ section: Yellow asterisk, CD147-MT1-MMP over a region of degraded matrix; red asterisk, CD147-MT1-MMP over an area not showing matrix degradation. n=3. (B-C) A proximity ligation assay (PLA) was employed to detect close protein-protein interactions (<40nm) of CD147 and MT1-MMP in MDA-MB-231 cells (see Materials and Methods for details). B) Left panel: interactions of CD147 and MT1-MMP (small green dots at arrowheads); cells were also stained with DAPI (blue). Right panel: DIC images of a single cell; arrowheads indicate sites of CD147-MT1-MMP interactions, which are restricted to areas over the cell. C) PLA combined with gelatin degradation assay, showing that CD147- MT1-MMP interactions occurred over areas of degradation (arrowheads), as well as over areas lacking degradation. Bars, 10 μm.

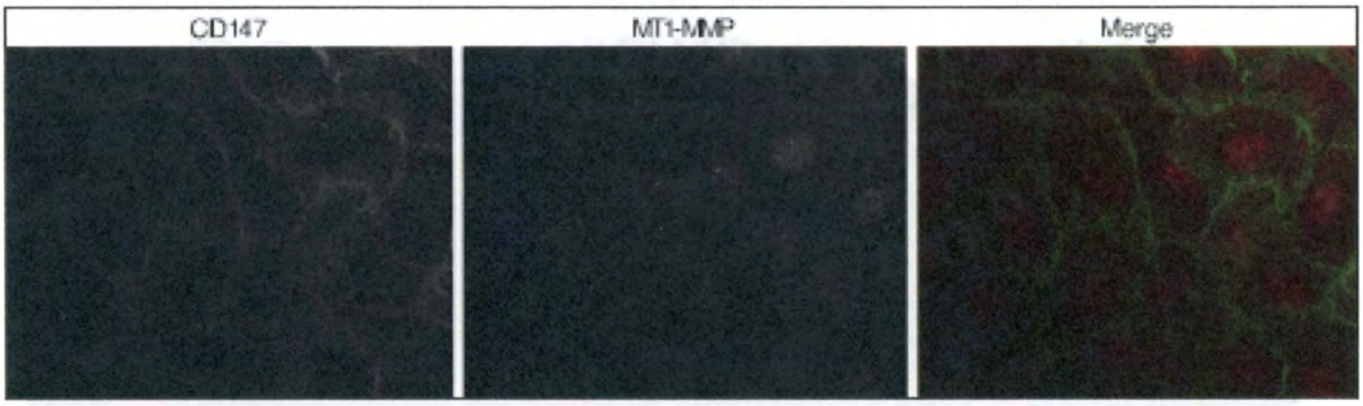

Figure 2. Supplemental 1. CD147 and MT1-MMP expression in MCF-10A cells treated with β-gal adenovirus. MCF-10A cells were treated with β-gal adenovirus, fixed and stained for CD147 and MT1-MMP. Images demonstrated that staining is relatively weak for both proteins.

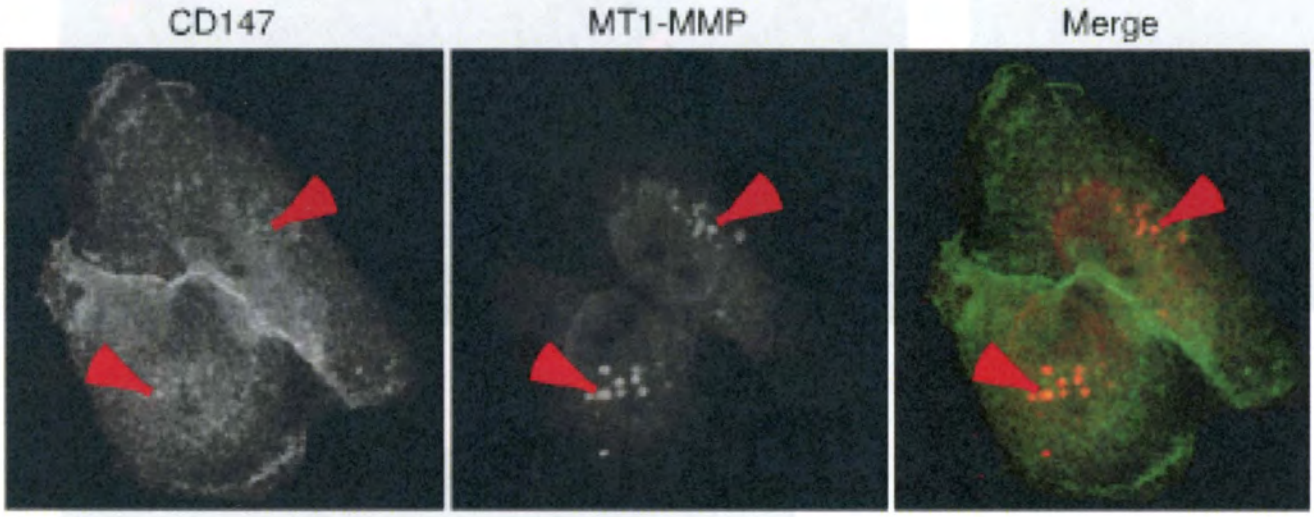

Figure 2. Supplemental 2. CD147 and MT1-MMP co-localize in MDA-MB-231 cells (alternative MT1-MMP antibody). Representative micrograph depicting MDA-MB-231 cells probed with CD147-488 conjugated antibody (Biolegend) and a monoclonal MT1-MMP antibody (Epitomics) followed by an Alexa Fluor-647 secondary antibody.

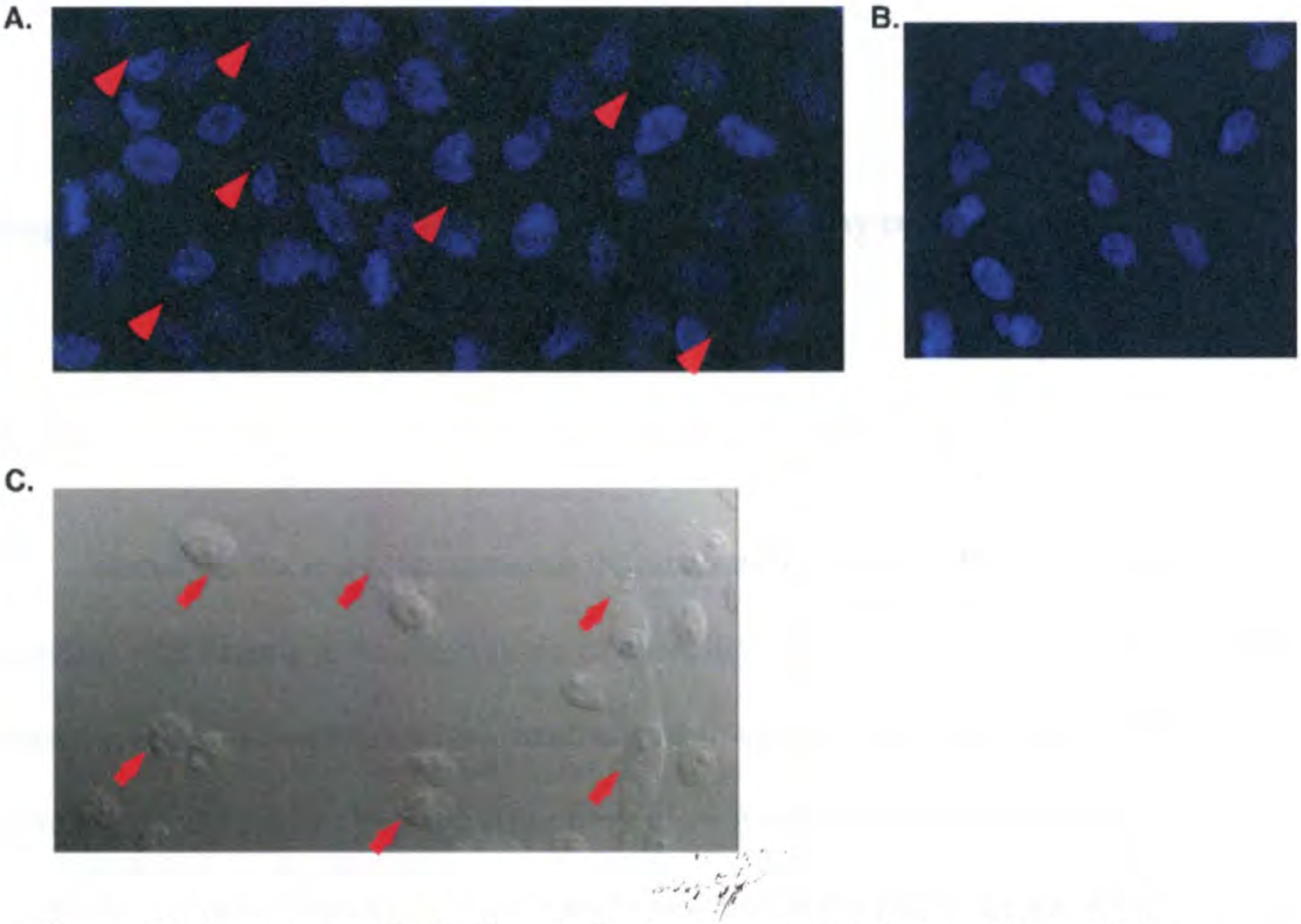

Figure 2. Supplemental 3. Proximity ligation assay demonstrates that endogenous CD147 and MT1-MMP are in close proximity in MDA-MB-231 cells. **A)** Cells were probed with CD147 (BD Pharmingen) and MT1-MMP (Millipore) primary antibodies using standard labeling methods. They were then probed with Duolink II secondary antibodies and detection kit reagents according manufacturers protocol. Protein-protein interactions appear as green dots. Red arrows depict examples of CD147-MT1-MMP interactions throughout the cell population. **B)** Using similar techniques as stated in **A)**, DIC microscopy demonstrates that CD147-MT1-MMP interactions are specific to cells and do not represent non-specific staining. Red arrows depict multiple interactions throughout the cell population. **C)** Control PLA experiment demonstrating specificity of Duolink reaction. Cells were initially probed with only CD147 (BD Pharmingen) primary antibody. This was then followed by reagents of the Duolink II kit. No signal (e.g. protein-protein interaction) was detected due to the lack of rolling circle amplification, which is dependent on the 2 primary antibodies localizing in close proximity.

Chapter 3: CD147 and the Ras-ERK signaling pathway co-regulate breast epithelial cell invasiveness

Abstract

Breast cancer is a heterogeneous disease, and similar to other cancers, metastases to distant vital organs is the main cause of mortality. It has become evident that invasive breast cancer cells employ various mechanisms to spread from their tissue of origin. One of the main mechanisms utilized is the formation of actin-rich membrane protrusions called invadopodia. Invadopodia are enriched with various signaling proteins, adhesion molecules and proteolytic enzymes and are thought to be a major superstructure at the leading edge of an invasive cell.

The IgSF protein, CD147 is associated with an invasive phenotype in various cancer types, including malignant breast cancer. CD147 was first identified as a major matrix metalloproteinase (MMP) inducer localized to the tumor cell surface. It has become clear, in addition to stimulation of soluble and membrane-type MMP synthesis, that CD147 has pleiotropic functions in various aspects of cancer progression, including cytoskeleton remodeling. Recent evidence suggested that up-regulation of CD147 alone in non-transformed and non-invasive breast epithelial cells induced an invasive phenotype characterized by MT1-MMP (MMP-14)-dependent invadopodia activity. Earlier evidence suggests that CD147 cooperates with various binding partners, including CD44 the main hyaluronan (HA) receptor, to promote a tumorigenic phenotype.

In this study we found that up-regulation of CD147 activates an EGFR-Ras-ERK signaling cascade that mediates invasiveness, and that these effects are partially dependent on HA-CD44 interactions. We also discovered that oncogenic Ras regulates CD147 expression and may elicit a positive feedback loop involving ERK signaling. We further found that enrichment of cells with differential CD147 surface levels afforded us the ability to isolate sub-populations of breast cancer cells with distinct phenotypes.

Introduction

CD147 (emmprin; basigin) is a highly and variably glycosylated transmembrane protein that is involved in both physiological and pathological cellular processes (Nabeshima et al., 2006; Yan et al., 2005; Yurchenko et al., 2010). CD147 expression is elevated in a wide range of cancer types, including breast cancer (Li et al., 2009; Riethdorf et al., 2006). Earlier studies employing *in situ* hybridization and immunohistochemistry techniques found that CD147 was expressed at pre-invasive and invasive areas, as well as proliferative regions in breast lesions; though CD147 was identified in normal breast tissue, it was expressed at much lower levels (Caudroy et al., 1999; Polette et al., 1997). CD147 expression gradually increases during progression from atypical ductal hyperplasia to invasive breast cancer and is correlated with hormone receptor negative and Erbb2 over-expressing breast cancers (Liu et al., 2010). Originally identified as a tumor-associated factor that induces stromal fibroblasts to synthesize and secrete matrix metalloproteinases (MMPs) (Biswas, 1984; Biswas et al., 1995; Ellis et al., 1989; Guo et al., 1997), CD147 has since been shown to have pleiotropic functions. In addition to

inducing MMP synthesis in stromal, tumor, and endothelial cells, CD147 contributes to therapy-resistance, angiogenesis, inflammatory signaling, cytoskeletal remodeling, and migration/invasion programs (Weidle et al., 2010). CD147 also participates in regulating the synthesis of the large extracellular polysaccharide, hyaluronan (HA), the main ligand for the cell surface receptor CD44 (Edward et al., 2011; Ghatak et al., 2005; Kato et al., 2011; Marieb et al., 2004; Qin et al., 2011). CD147-induced HA-CD44 interactions modulate various signaling pathways and potentiate tumorigenic properties in various cell types (Toole and Slomiany, 2008). CD147 also cooperates with cyclophilins to induce intracellular signaling pathways (Yurchenko et al., 2010), and with MCTs to influence tumor cell metabolism (Kennedy and Dewhirst, 2010), although in each case the exact mechanisms by which CD147 activates signaling cascades are not fully understood.

Dysregulated expression of Ras genes has been identified in many cancer types (Karnoub and Weinberg, 2008) and oncogenic Ras expression is associated with aggressive cancer phenotypes, such as proliferation, invasion/metastasis and therapy resistance (Pylayeva-Gupta et al., 2011). Though the common point mutations identified in oncogenic forms of Ras are a very rare occurrence in breast cancer, chronic Ras activity has been documented in breast cancer cell lines and patient tumor tissue in the absence of Ras mutations (Eckert et al., 2004; Lintig et al., 2000; Rochlitz et al., 1989). In the absence of oncogenic Ras signaling, up-regulation of normal Ras activity can facilitate similar transformed phenotypes (Zhang et al., 2009). Aberrant Ras signaling may be due to amplified expression and activation of cell surface receptor tyrosine kinases (RTKs), such as epidermal growth factor receptor (EGFR) family members,

mutations in modulators of the Ras activation state or effectors downstream of Ras (Campbell and Der, 2004; Stamatakos et al., 2010).

In this study we have identified novel signaling associations between CD147, HA-CD44 interactions, and EGFR, Ras and ERK signaling that regulate the invasive properties of breast epithelial cells.

Materials and Methods

Cell Culture

The human breast adenocarcinoma cell lines MDA-MB-231 and MCF-7 were obtained from American Type Culture Collection (ATCC) and were cultured in RPMI 1640 (R-8755) with 2.38 g/L HEPES, 2 g/L sodium bicarbonate, and 10% FBS (pH 7.4). The spontaneously immortalized human breast epithelial cell line MCF-10A was obtained from ATCC. MCF-10A cells stably expressing a lentivirus construct containing K-Ras^{V12} (10A-K-Ras^{V12}) or empty vector (10A-EV) were generously provided by Dr. Ben Ho Park (Konishi et al., 2007). Low passage MCF-10A cells and MCF-10A derivatives were maintained in Mammary Epithelial Cell Growth Medium (MEGM) with BulletKit supplements (Lonza) unless noted otherwise in legends. All cells were cultured in a humidified 95% air/5% CO_2 incubator at 37°C.

Antibodies and Reagents

The following primary antibodies were employed for these studies: CD147, CD147-FITC, IgG-FITC and caveolin-1 (BD Biosciences); Alexa-Fluor 647-conjugated

CD147, Alexa-Fluor 488-conjugated CD147 and PE-conjugated EGFR (Biolegend); cortactin (clone 4F11) and MT1-MMP/ hinge-region polyclonal (Millipore); phospho-ERK1/2 (Thr202/Tyr204), pan-ERK1/2, phospho-EGFR (Tyr1173), phospho-EGFR (Tyr1068), and EGFR (Cell Signaling Technology, Inc); CD44/HCAM (mouse) and Alexa-Fluor 647-conjugated CD44 (Santa Cruz Biotechnology, Santa Cruz, CA); PE-conjugated CD44 (Cedarlane Laboratories); CD44 (rabbit) (Epitomics); β-actin and β-tubulin (Sigma). Goat anti-mouse-HRP and Goat anti-rabbit-HRP (Chemicon) were used as secondary antibodies for immunoblotting. The inhibitors Tyrphostin (Calbiochem), U0126 and PD98059 (Cell Signaling Technology, Inc) were used at concentrations indicated in figure legends.

Recombinant adenovirus infections

Recombinant human CD147 adenovirus and control β-galactosidase (β-gal) adenovirus were constructed and used as described previously (Grass et al., 2012; Li et al., 2001).

Surface Biotinylation

Cell surface biotinylation was performed using a Cell Surface Protein Isolation Kit according to manufacturer's protocol (Pierce). Briefly, cells were treated with EZ-Link Sulfo-NHS-SS-Biotin for 45 minutes at 4°C, followed by quenching and harvesting of cell lysates. Equivalent amounts of protein from each experimental group was added to spin columns containing NeutrAvidin resin, incubated for several hours with rocking at 4°C, washed, eluted and followed by immunoblotting.

Ras Activity Assay

Ras activation status was evaluated by employing the Active Ras Pull-Down and Detection Kit according to manufacturer's protocol (Pierce). This assay is based on the observation that Ras-GTP (active), but not Ras-GDP (inactive), binds Raf-1 with high affinity. Briefly, fresh lysates from MCF-10A cells non-treated or treated with adenovirus were collected using standard procedures. GTPγS (0.1 mM) or GDP (1 mM) was added to control lysates for a positive and negative control, respectively. GST-Raf1-Ras-binding domain (GST-Raf1-RBD) fusion protein was added to the spin column containing a glutathione resin, followed by addition of 400-500 μg of protein from positive/negative controls and β-gal or CD147 treated cells. Lysates were incubated for 1 hour at 4°C with rocking, followed by elution and subsequent immunoblotting with a pan-Ras antibody.

Hyaluronan ELISA

Hyaluronan concentrations in the media were determined using an enzyme-linked immunosorbent-like assay described previously (Gordon et al., 2003).

Preparation of Hyaluronan Oligosaccharides

Hyaluronan oligosaccharides (oHAs) were prepared as described previously (Zeng et al., 1998). Briefly, oHAs used in this study were derived from degradation products of hyaluronan purified from rooster combs (Sigma). Hyaluronan was dissolved in sodium acetate buffer at a pH of 5.0 and treated with testicular hyaluronidase (Type I-S, Sigma) overnight. The digest was precipitated with TCA on ice, dialyzed for 48 hours using a 1000 dalton molecular weight cutoff (MWCO) and fractionated with 5000 MWCO spin-

dialysis tubes. Fractions mainly composed of 6-12 oligosaccharide units were further concentrated with lyophilization and concentration was determined using a Carbazole assay, which detects uronic acid. Oligomer size was assessed with the Morgan-Elson assay by determining the ratio between N-acetyl-D glucosamine D-glucuronic acid.

Matrigel invasion assay

Matrigel invasion inserts (8μm pores) for 24-well tissue culture plates were purchased from BD Biosciences. Briefly, the Matrigel inserts (upper and lower chambers) were rehydrated for 2 hours at 37°C with non-supplemented MEGM. $7.0x10^5$ MCF-10A-EV and MCF-10A K-Ras^{V12} or MCF10A-K-Ras^{V12} cells treated with siRNA (72 hours) or MEK inhibitors were detached and seeded in the upper chamber of the inserts and cultured for 24 hours at 37°C in non-supplemented MEGM, and medium in the lower chamber was replaced with MEGM containing 20 nM EGF. After incubation, the cells were fixed in 3.7% paraformaldehyde for 15 minutes at room temperature, rinsed with PBS and stained with 0.2% Crystal Violet for 10 minutes, followed by extensive washing. Cells were scraped from the top of the Matrigl membrane with a Q-tip and the cells that invaded through the 8μm pores in the membrane were imaged using a phase-contrast microscope (Leica DFC320). Cells were counted in four separate fields in three independent experiments.

Gelatin degradation assay for invadopodia

This assay was performed as described previously (Grass et al., 2012). Briefly, gelatin was conjugated with Alexa-Fluor-568 dye (Molecular Probes) using the manufacturer's protocol. 18 mm round glass coverslips were acid washed with 1 M HCl overnight

followed by extensive washing in water. Coverslips were sterilized with 70% ethanol and then coated with 50 μg/ml poly-L-lysine for 20 minutes at room temperature, washed with PBS, and fixed with ice-cold 0.5% glutaraldehyde for 15 minutes followed by extensive washing. The coverslips were then inverted on an 80 μl drop of fluorescent gelatin matrix (0.2% gelatin and Alexa-Fluor-gelatin at an 8:1 ratio) and incubated for 15 minutes at room temperature. The coverslips were washed with PBS and quenched in 5 mg/ml sodium borohydride in PBS for 10 minutes, followed by further washing in PBS. The coated coverslips were then placed in 12-well plates, sterilized in 70% ethanol for 10 minutes, washed in PBS and equilibrated in serum-free MEGM and switched to fully supplemented MEGM 30 minutes before the addition of cells. For invadopodia assays, 5.5×10^4 cells were plated on the coated coverslips and incubated at 37°C for 15-18 hours. Cells were fixed and permeabilized with 3.7% paraformaldehyde and 0.1% Triton X-100 for 10 minutes, washed with PBS, blocked in 3% BSA in PBS for 1 hour, and incubated with appropriate primary and secondary antibodies in 3% BSA in PBS. Actin filaments were visualized with Alexa-Fluor-647-phalloidin.

In situ proximity ligation assay

Protein-protein interactions were detected in situ, as described previously (Grass et al., 2012), using Duolink II secondary antibodies and detection kit (Olink Bioscience, Uppsala, Sweden) according to manufacturer's instructions. Briefly, primary antibodies targeting CD147 (mouse; BD Pharmingen), EGFR (rabbit; Cell Signaling), CD44 (mouse; Santa Cruz Biotechnology), CD44 (rabbit; Epitomics) were applied using standard procedures. Oligonucleotide-conjugated Duolink secondary antibodies were then added, followed by Duolink ligation solution. The oligonucleotides ligate together

in a closed circle only when the secondary antibodies are in close proximity (<40 nm) (Soderberg et al., 2006). Polymerase was added, which amplified any existing closed circles, and detection was achieved with complementary, fluorescently labeled oligonucleotides. Specificity of the reaction was determined by treating cells with a single primary antibody followed by Duolink secondary antibodies, which results in minimal to no signal amplification because of the absence of a second oligonucleotide needed for ligation and subsequent closed circle amplification.

Microscopy and image analysis

Images were acquired with a Leica Total Confocal System SP5 acoustic optical beam splitter confocal (TCS SP5 AOBS) microscope using a 63x, 1.4 NA oil objective at the Josh Spruill Molecular Morphology & Imaging Center in the Department of Regenerative Medicine and Cell Biology (MUSC, Charleston, SC). Images were captured at high confocality (pinhole =1 Airy unit) to achieve the thinnest possible optical slices at the cell-matrix interface. Potential overlaps in emission spectra were eliminated by sequential scanning and tuning of the AOBS. Differential interference contrast (DIC) microscopy was performed using the Leica SP5 Confocal System.

Assessment of invadopodia characteristics was performed as described previously (Grass et al., 2012). Briefly, at least 10 randomly chosen fields were imaged per experiment and evaluated for degraded matrix foci, which appear dark 'holes' in the fluorescent matrix field. A cell with at least one degradation foci underneath or near the cell edge was counted as a cell able to degrade matrix. Invadopodia, defined as actin puncta that colocalize with cortactin, were manually counted and analyzed for underlying matrix

degradation. Results were presented as percentage of cells degrading the matrix, number of invadopodia per cell or percentage of cells displaying cortactin-actin aggregates with or without degradation underneath.

qRT-PCR

For qRT-PCR experiments, total RNA was isolated using the RNeasy Mini kit according to the manufacturer's instructions (QIAGEN, Valencia, CA) and quality control and quantification was performed with the Agilent 2100 Bioanalyzer (Agilent Technologies, Inc., Santa Clara, CA) and Agilent RNA 6000 Pico LabChip kits. Complementary DNA (cDNA) was synthesized from equivalent concentrations of total RNA using the iScript cDNA Synthesis Kit (Bio-Rad) according to manufacturer's instructions. Coding sequences for *CD147* and *β-actin* (internal control) were amplified from synthesized cDNA using iQ SYBR Green Supermix (Bio-Rad, Hercules, CA). Custom primer sequences used for amplification were as follows: *CD147* sense 5'-*CAGAGTGAAGGCTGTGAAGTCG* -3'; *CD147* antisense 5'-*TGCGAGGAACTCACGAAGAA*-3'; *β-actin* sense 5'-*GGAAATCGTGCGTGACATT* -3'; *β-actin* antisense 5'-*GACTCGTCATACTCCTGCTTG* -3'. Amplification was performed using an iCycler IQ Real-Time PCR Detection System and cycle threshold (Ct) values were determined in duplicate for *CD147* and *β-actin* transcripts for each experiment. 'No template' (water) and 'no-RT' controls were used to ensure minimal background signal from DNA contamination. Using mean Ct values tabulated for different experiments and Ct values for *β-actin* as loading controls, fold changes for experimental groups relative to assigned controls were calculated using automated iQ5 2.0 software (Bio-Rad).

RNA interference

Control non-silencing siRNA and target-specific pooled siRNAs for CD147 and CD44 were purchased from Santa Cruz Biotechnology and used according to manufacturer's protocol. For all experiments, cells were transfected with siRNA 72 hours before each experiment.

Detergent-resistant membrane fractionation

Detergent-resistant membrane domains (e.g. lipid rafts) were isolated as described previously (Grass et al., 2012). Briefly, cells cultured in D150 plates were washed with ice-cold PBS three times. Cells were lysed in 500μL lysis buffer (25 mM Tris-HCl, pH 7.5, 150 mM NaCl, 1mM dithiothreitol, 10% sucrose, 1% Triton X-100 and protease inhibitors) on ice for 30 minutes. The cells were scraped and mechanically disrupted by passaging 20 times through a 3-inch 22-guage needle. The lysates were mixed directly with iodixanol stock solution (60% solution of Optiprep iodixanol) to yield a 40% (v/v) iodixanol-lysate solution, which was placed at the bottom of an ultracentrifuge tube. Equal volumes of 35%, 30%, 25%, 20% and 0% Optiprep in lysis buffer without Triton X-100 were carefully overlaid above the iodixanol-lysate solution. The samples were centrifuged at 160,000 x *g* for 8 hours at 4°C in a SW41-Ti rotor (Beckman Coulter). Equal fractions were collected from the top of the tube and equivalent aliquots of each fraction were subjected to immunoblotting using antibodies recognizing proteins of interest.

Labeling of live cells with Cholera toxin-B (Ctx-B) to identify lipid rafts

Lipid raft labeling was performed using the Vybrant Alexa-Fluor-488 Lipid Raft labeling kit using the manufacturer's protocol (Invitrogen Molecular Probes). Briefly, live cells were washed with ice cold PBS, labeled with Alexa-Fluor-488-conjugated Ctx-B, cross-linked with anti-CtxB antibody, followed by standard immunofluorescence staining and mounting techniques.

Cell surface analysis and fluorescent activated cell sorting of $CD147^{Lo}$ and $CD147^{Hi}$ Sub-populations

For cell surface analysis, $2.0x10^5$ cells were trypsinized to achieve single cell suspensions, counted and blocked with 3% BSA in PBS, and incubated with primary-conjugated antibodies for 30 minutes on ice. Unbound antibody as removed in subsequent washes and cells were analyzed no longer than 1 hour post-staining. Cell sorting of $CD147^{Lo}$ and $CD147^{Hi}$ sub-populations was achieved in the following manner: cells (10A-K-Ras^{V12}, MDA-MB-231, and MCF-7) were trypsinized into single cell suspensions, counted, blocked with 3% BSA in PBS, and treated with antibodies in culture medium. Cells were incubated with anti-CD147-FITC or IgG-FITC (negative control) for 30 minutes on ice. Unbound antibody was washed off and cells were resuspended in fresh media with DNase (Promega), filtered and sorted. Cells expressing the lowest surface levels of CD147 (bottom 20%) and the highest surface levels of CD147 (top 20%) were selected as $CD147^{Lo}$ and $CD147^{Hi}$ sub-populations, respectively. For subsequent invadopodia or immunoblotting analyses, cells were directly seeded on gelatin or lysed post-sort, respectively. All FACS analysis and cell sorting was

performed with a Beckman Coulter MoFlo Astrios instrument in the Department of Regenerative Medicine and Cell Biology Flow Cytometry Facility (MUSC, Charleston, SC).

Immunoblotting

Whole cell lysates were prepared for immunoblotting using a RIPA buffer modified to contain 1mM PMSF, 10 μg/ml aprotinin and leupeptin, 2 mM sodium orthovanadate and 10 mM sodium fluoride. Protein content was quantified using a BCA assay (Pierce), aliquots were solubilized in reducing sample buffer, resolved on Pierce 4-20% polyacrylamide gels, transferred to nitrocellulose (Osmonics, Westborough, MA) with a Pierce apparatus, and stained with antibody. Densitometric analysis of western blots was performed using Image J software (version 1.43s).

Results

Up-regulation of CD147 induces activation of EGFR-Ras-ERK signaling

In a recent study we showed that up-regulation of CD147 is sufficient to induce invasion and formation of active invadopodia in the non-transformed human breast epithelial line, MCF-10A (Grass et al., 2012). Here we have investigated the signaling pathways that might be involved in mediating the effects of CD147 on these processes. As shown in our previous study, an MOI of 2 of our CD147 adenovirus construct gives rise to levels of CD147 in MCF-10A cells that are commonly found in aggressive human breast cancer cells. In addition, we have now shown that the level of CD147 at the surface of MCF-

10A cells, resulting from treatment with an equivalent MOI of virus, is similar to that expressed on the surface of the malignant breast carcinoma cell line, MDA-MB-231, but as shown previously the adenovirus induces mainly the less glycosylated form of CD147 found endogenously in cancer cells (Fig. 3-1A). As in our previous study, we used cells infected with a β-galactosidase (β-gal) adenovirus construct as a control; this adenovirus did not cause significant changes in CD147 expression.

Prior evidence suggests that CD147 can activate ERK signaling (Cui et al., 2012; Marieb et al., 2004; Misra et al., 2003; Tang et al., 2006), though the upstream regulators of this pathway have not been fully characterized. First we evaluated the effect of increased CD147 on the activation status of Ras in MCF-10A cells, as Ras is frequently upstream of ERK activation (Bodart, 2010). We found that up-regulation of CD147 led to increased Ras activation, measured as an increased proportion of Ras-bound GTP, as well as a concomitant increase in phosphorylated ERK (Figure 3-1B). Next we investigated EGFR signaling since it is often dysregulated in breast cancer and is commonly upstream of Ras and ERK (Eccles, 2011). We found that subsequent treatment of CD147-upregulated MCF-10A cells with increasing concentrations of the specific EGFR kinase inhibitor, AG1478, resulted in attenuated p-ERK (Fig. 3-1C), suggesting that CD147 may be involved in EGFR activation. Since phosphorylation of tyrosine 1173 or 1068 on the cytoplasmic tail of EGFR has been associated with regulation of Ras-MAPK signaling (Rojas et al., 1996; Sakaguchi et al., 1998), we determined whether one or both of these tyrosine residues is activated in response to increased CD147 expression. We found that there was no difference in phosphorylation of the Tyr 1173 residue, but increased CD147 led to increased phosphorylation of the Tyr

1068 residue. This Tyr 1068 phosphorylation occurred whether or not EGF was present in the medium (Fig. 3-1D).

Hyaluronan-CD44 interaction mediates CD147-induced activation of EGFR signaling.

Previously we demonstrated that CD147 stimulates the synthesis of HA in breast carcinoma cells (Marieb et al., 2004). Here we found that up-regulation of CD147 in non-transformed, MCF-10A breast epithelial cells also leads to ~2-fold increase in HA production compared to control cells (Fig. 3-2A). Several studies have demonstrated that either endogenous or exogenous HA can elicit the activation of multiple signaling pathways, including those involving RTKs such as EGFR and downstream effectors such as Ras and ERK (Toole, 2009), which are frequently dysregulated in breast cancer. Consequently we determined whether the effects of CD147 on activation of EGFR and ERK were dependent on HA-receptor interactions. We first employed treatment with oligosaccharides of HA (oHA) that are 6-18 residues in length, which compete with multivalent, HA-receptor interactions, replacing them with monovalent, oHA-receptor interactions (Lesley et al., 2000; Underhill and Toole, 1979) and thus attenuating endogenous HA-receptor signaling (Ghatak et al., 2002; Ghatak et al., 2005). We found that treatment of CD147-upregulated MCF-10A cells with oHA resulted in attenuated phosphorylation of EGFR-Tyr 1068 and ERK (Fig. 3-2B). Interestingly, the levels of p-ERK reached near baseline activation levels before Tyr 1068 phosphorylation returned to baseline. To determine whether this perturbation of HA-receptor signaling may be dependent on CD44, the main HA receptor in breast cancer cells, we determined the effects of pooled siRNA-mediated knockdown of CD44 in CD147-upregulated MCF-

10A cells. This treatment resulted in a partial decrease in p-Tyr 1068 and p-ERK levels, whereas no significant difference was seen in membrane type-1 MMP (MT1-MMP; MMP-14) protein levels (Fig. 3-2C); this suggests that CD147-induced activation of the EGFR-ERK pathway was at least partially mediated by HA-CD44 interactions and that CD147-induced MT1-MMP expression may be separate from this pathway.

CD44 has been shown to interact with EGFR family members in a HA-dependent manner (Bourguignon et al., 2006; Ghatak et al., 2005; Wang and Bourguignon, 2006) and our above data suggests that up-regulation of CD147 results in increased HA-CD44-mediated activation of EGFR. To evaluate whether up-regulation of CD147 increases EGFR-CD44, CD147-CD44, or CD147-EGFR interactions, we employed a proximity ligation assay technique that detects associations of proteins occurring within 40 nm of each other (Soderberg et al., 2006). We found that there were significant differences between CD147-upregulated and control MCF-10A cells in regards to the percentage of the cell population demonstrating close protein-protein associations of EGFR with CD44, CD147 with CD44 and CD147 with EGFR (Fig. 3-2D, E). We and others have demonstrated that CD147, CD44, and EGFR partially localize in membrane fractions with properties of lipid rafts in malignant cancer cells (Ghatak et al., 2005; Grass et al., 2012; Irwin et al., 2010; Tang and Hemler, 2004; Toole, 2009). To determine whether this also occurs in MCF-10A cells with up-regulated CD147, we showed that CD147 colocalizes with cholera toxin-B (CtxB), a lipid raft marker, at the leading edge of cells and appears to arrange in a single-file fashion along CtxB-enriched filopodial projections (Fig. 3-3A). We also found that CD147, CD44 and EGFR are enriched in caveolin-rich raft domains after up-regulation of CD147, as compared to the control cells (Fig. 3-3B).

To evaluate whether enrichment in lipid rafts may be due to increased trafficking of CD44 and EGFR to the cell surface in cells with up-regulated CD147, we utilized FACS analysis to evaluate surface expression levels. We found that the MCF-10A cells with up-regulated CD147 demonstrated no significant differences in levels of CD44 or EGFR at the cell surface (Fig. 3-3C), suggesting that the major effect is on organization of these proteins into raft-like complexes.

Activated Ras and ERK regulate hyaluronan, CD147 and MT1-MMP expression, and invasiveness

We previously found that up-regulation of CD147 alone in MCF-10A cells is sufficient to induce an invasive program characterized by matrigel invasion and active invadopodia formation, the latter being dependent on MT1-MMP activity (Grass et al., 2012). Our data here indicate that up-regulation of CD147 increases activation of the Ras-MEK-ERK pathway via HA-CD44 interactions. However, other evidence indicates that the MEK-ERK pathway may also regulate CD147 expression (Pons et al., 2011; Ramos and Dang, 2011; Venkatesan et al., 2009), suggesting the possibility of a positive feedback loop. Therefore we evaluated if this was the case in our system. To evaluate whether the Ras-MEK-ERK signaling pathway influences CD147 expression we employed a MCF-10A cell line stably expressing the oncogenic K-Ras^{V12} mutant (10A-K-Ras^{V12}), since this cell line has been shown to activate ERK signaling to a greater extent than PI3K (Konishi et al., 2007). First, we found that the 10A-K-Ras^{V12} cells contain significantly higher levels of HA, CD147 and MT1-MMP than empty vector MCF-10A (10A-EV) cells (Fig. 3-4A,B). Interestingly, qPCR demonstrated only a slight increase in CD147 message compared to 10A-EV cells, suggesting that K-Ras^{V12} may

regulate CD147 expression post-transcriptionally (Fig. 3-4C). We also found that the 10A-K-Ras ^{V12} cells invaded matrigel (Fig. 3-4D) and formed active invadopodia (Fig.3-4E) to a greater extent than 10A-EV cells. In the invadopodia assay, ~60% of the cells degraded underlying fluorescent matrix compared to the 10A-EV (Fig. 3-4F). Of the 10A-K-Ras^{V12} cells with invadopodia, the majority of the population had a mean of 10-12 invadopodia/cell, with a range of 1-28 invadopodia/cell, whereas 10A-EV cells demonstrated essentially no invadopodia (Fig. 3-4G). Thus, this data indicates that the K-Ras^{V12} oncogene imparts an invasive phenotype in MCF-10A cells, similar to that demonstrated previously in pancreatic cells (Botta et al., 2011; Campbell and Der, 2004; Neel et al., 2012).

As we and others have shown previously that CD147 regulates MT1-MMP expression and HA synthesis (Marieb et al., 2004; Yan et al., 2005), we determined whether the increased expression of MT1-MMP or HA in 10A-K-Ras^{V12} cells was due to the increase in CD147. Knockdown of CD147 using siRNA demonstrated that MT1-MMP expression and HA production were partially dependent on CD147 (Fig. 3-5A,B). Since CD147 plays a prominent role in breast cancer cell invasion and invadopodia formation (Grass et al., 2012; Zucker et al., 2001), we also evaluated effects on matrigel invasion and invadopodia formation and activity. We found that knockdown of CD147 resulted in a partial, yet significant, decrease in matrigel invasion in the 10A-K-Ras^{V12} cells (Fig. 3-5C). Likewise, in the invadopodia assay, we found that CD147 knockdown decreased the percentage of cells degrading matrix (Fig. 3-5D,E) and that most of this inhibition was due to decreased activity of invadopodia rather than formation (Fig. 3-5F).

Next we determined whether increased CD147 expression in 10A-K-Ras^{V12} cells was dependent on ERK signaling. Treatment of 10A-K-Ras^{V12} cells with two different MEK inhibitors resulted in a decrease in CD147 and MT1-MMP protein levels as well p-ERK (Fig. 3-6A), though this effect did not appear to be at the transcriptional level for CD147 (Fig. 3-6B). We next evaluated whether ERK signaling mediates the invasive characteristics that we described above in 10A-K-Ras^{V12} cells. We found that MEK-ERK inhibition greatly decreased matrigel invasion (Fig. 3-6C), as well as invadopodia formation and activity (Fig. 3-6D,E,F). In contrast to CD147 depletion in 10A-K-Ras^{V12} cells, MEK inhibition greatly decreased invadopodia formation as well as activity.

Similar to our approach with CD147-upregulated MCF-10A cells, we evaluated endogenous protein-protein associations of CD44 with EGFR, CD147 with EGFR, and CD147 with CD44 in 10A-K-Ras^{V12} cells, using the PLA. We found that 10A-K-Ras^{V12} cells also exhibited these associations (Fig. 3-7A), but the incidence of these associations varied in the following manner: CD147-CD44 > CD147-EGFR > CD44-EGFR (Fig. 3-7 A,B). This data suggests a similar relationship to what we identified in CD147-upregulated MCF-10A cells (Fig. 3-2D,E). As with MCF-10A cells with up-regulated CD147, we showed that endogenous CD147 co-localizes with Ctx-B (Fig. 3-7C) and that CD147, CD44 and EGFR are enriched in caveolin-rich raft domains in 10A-K-Ras^{V12} cells as compared to the 10A-EV cells (Fig. 3-7D).

10A-K-Ras^{V12} cells with high constitutive levels of CD147 are more invasive than those with low constitutive levels of CD147

It has been clearly demonstrated that cancer cells exhibit heterogeneity in cell surface marker expression and contain sub-populations with different functional capacities (Ricardo et al., 2011). Therefore we extended our current findings further by evaluating whether sub-populations of 10A-K-Ras^{V12} cells with different levels of constitutive CD147 expression could be isolated from the parent cells. Immuno-staining of 10A-K-Ras^{V12} cells demonstrated a sub-population of cells with greater CD147 and CD44 staining intensity (Fig. 3-8A). Next, using FACS, we isolated cells with relatively low surface expression of CD147 (CD147^{Lo}) versus relatively high surface expression of CD147 (CD147^{Hi}). We separated the bottom 20% and top 20% with respect to CD147 cell surface expression and found that these two sub-populations exhibited distinct properties as indicated by scatter analysis (Fig. 3-8B). The CD147^{Hi} population also demonstrated 3-fold more CD44 and 2.5-fold more EGFR on the surface compared to the CD147^{Lo} population (Fig. 3-8C; left panel). Similar analysis of highly invasive MDA-MB-231 breast cancer cells, which possess an endogenous K-Ras^{G13D} mutation (Kozma et al., 1987), demonstrated a 1.8-fold increase in CD44 and 1.9-fold increase in EGFR in CD147^{Hi} vs. CD147^{Lo} cells (Fig. 3-8C; middle panel) while much less invasive MCF-7 cells demonstrated very little CD44 or EGFR surface staining, and sub-population analysis for differential CD147 expression revealed no significant differences (Fig. 3-8C; right panel). We also measured levels of various proteins in the two sub-populations by immuno-blotting and found that CD147^{Hi} cells demonstrated increased p-ERK and p-EGFR compared to CD147^{Lo} cells, whereas the total levels of CD44 and EGFR were

similar (Fig. 3-8D). Finally, we evaluated the invasive characteristics of the $CD147^{Hi}$ vs. $CD147^{Lo}$ cells and similar to our above results in CD147-depleted 10A-K-Ras^{V12} cells (Fig. 3-5F), we found that $CD147^{Hi}$ cells had a much greater percentage of cells with actively degrading invadopodia than $CD147^{Lo}$ cells, whereas no significant difference was observed between $CD147^{Hi}$ vs. $CD147^{Lo}$ cells in regards to invadopodia formation (Fig. 3-8E).

Discussion

Breast cancer is a heterogeneous disease and, as with other cancers, metastases to distant organs remains the primary cause of mortality (Chaffer and Weinberg, 2011). Currently the evaluation of hormone receptor expression, ErbB2 amplification and the presence of cytokeratin forms represent the mainstay utilized clinically for treatment stratification, though much effort has also been placed on characterizing distinct sub-populations isolated from the tumor bulk with differing cell surface expression profiles. One of the main surface markers that has emerged in identifying invasive and therapy-resistant cancer cells is CD44 (Alexander and Friedl, 2012). Hyaluronan (HA), a primary CD44 ligand, facilitates construction of pericellular matrix scaffolds which stabilize signaling and transporter complexes (Slomiany et al., 2009a; Slomiany et al., 2009b). Multiple studies have shown that HA-CD44 interactions are intimately involved in the integration of signaling pathways leading to RTK activation, therapy resistance and invasion (Toole, 2009).

Accumulating evidence suggests that the IgSF glycoprotein CD147 regulates HA synthesis in various cell types (Edward et al., 2011; Ghatak et al., 2005; Kato et al., 2011; Marieb et al., 2004; Qin et al., 2011), though the mechanism of this regulation is not fully understood. In addition, CD147 has an essential role in regulating MMP production, and our recent study found that CD147 plays a role in invadopodia activity (Grass et al., 2012). In this study we have begun to evaluate the functional relationship between CD147, HA, CD44 and MMP production in regards to breast cancer invasion.

We and others have previously demonstrated that CD147 influences migration and invasion via protease induction and cytoskeletal remodeling (Grass et al., 2012; Weidle et al., 2010; Zhao et al., 2011), though the exact signaling mechanisms regulating these processes have not been fully elucidated. Here we have shown that up-regulation of CD147 in non-transformed breast epithelial cells leads to increased EGFR, Ras and ERK activation. Moreover, we show that the activation of EGFR and ERK by CD147 is mediated in large part by increased HA-CD44 signaling and is accompanied by enhanced interactions between CD147, CD44 and EGFR. These interactions most likely take place within lipid raft-like regions of the plasma membrane, which are known to participate in cell signaling complex formation (Staubach and Hanisch, 2011). Of interest, our microscopic evaluation of CD147 and lipid rafts revealed that CD147 co-localizes with Ctx-B at the leading edge of the cells and appears to arrange in a single-file fashion along Ctx-B-enriched filopodial projections (Fig. 3-3A). Our evidence suggests that enrichment of CD44 and EGFR in lipid rafts is not due to increased trafficking to the cell surface, since our cell surface analysis revealed no significant differences in either CD44 or EGFR expression (Fig. 3-3C). Rather, we hypothesize that this may be due to

increased assembly of signaling complexes in lipid rafts on the cell surface, which are vital for invadopodia formation and activity (Caldieri et al., 2009; Yamaguchi et al., 2009).

Oncogenic Ras signaling has a less appreciated role in breast cancer pathology since Ras mutations are infrequent (Pylayeva-Gupta et al., 2011). However, chronic Ras activity has been found in multiple breast cancer cell lines and patient tumor tissues without any apparent Ras mutations (Eckert et al., 2004; Lintig et al., 2000). A recent study suggests that increased activity of wild type Ras can result in a similar phenotype induced by oncogenic Ras (Zhang et al., 2009). The present study suggests that CD147 can stimulate wild type Ras activity, as MCF-10A cells have not been found to contain any mutant Ras forms (Soule et al., 1990). To evaluate this relationship between CD147 and Ras further, we utilized 10A-K-Ras^{V12} cells, as K-Ras mutations are the most frequent of those that do occur in breast cancer (Karnoub and Weinberg, 2008). We found that oncogenic Ras increases HA synthesis (Fig. 3-4A), as found previously (Hamilton et al., 2007), and also stimulates expression of CD147 and MT1-MMP protein (Fig. 3-4B). Interestingly, qPCR analysis revealed only minor differences in CD147 message between empty vector and 10A-K-Ras^{V12} cells (Fig. 3-4C), suggesting that Ras may influence CD147 expression predominantly at the post-transcriptional level.

We also showed that 10A-K-Ras^{V12} cells are highly invasive in matrigel and formed highly active invadopodia (Fig. 3-4D,E,F), which is similar to earlier studies in pancreatic cancer cells (Neel et al., 2012). The invasiveness of these cells was found to be dependent on MEK-ERK signaling. Also, in agreement with our previous study demonstrating that CD147 is involved in invadopodia activity (Grass et al., 2012), we

showed that CD147, at least in part, mediates the invasive phenotype seen in 10A-K-Ras^{V12} cells. We found that CD147 expression in these cells is also dependent on MEK-ERK signaling and that endogenous CD44, EGFR, and CD147 associate and co-localize in lipid raft fractions in these cells in similar fashion to cells with upregulated CD147. Again, CD147 message levels were not significantly affected by the MEK-ERK signaling pathway, suggesting that regulation of CD147 expression by this pathway is also predominantly post-transcriptional. A striking finding was that, although HA-CD44 interactions clearly mediate most CD147-induced EGFR and ERK activation, disruption of HA-CD44 interactions with oHA or CD44 siRNA did not significantly affect CD147-induced MT1-MMP protein levels, as shown herein, or invasiveness (data not shown). This may be due to a divergence in CD147-induced signaling, where one effect of CD147 is mediated by HA extrusion and subsequent CD44 binding, and the other is mediated by other CD147-binding interactions independent of CD44.

We also found that CD147^{Hi} and CD147^{Lo} cell sub-populations isolated from 10A-K-Ras^{V12} cells, and from the metastatic breast cancer cell line MDA-MB-231, have distinct properties. The CD147^{Hi} cells have significantly more CD44 and EGFR on the cell surface than their CD147^{Lo} counterparts. Additionally, CD147^{Hi} 10A-K-Ras^{V12} cells had increased pEGFR and pERK levels as well as more active invadopodia compared to CD147^{Lo} cells. Interestingly, densitometric analysis of CD147 in the CD147^{Hi} and CD147^{Lo} western blots demonstrated small changes in total CD147 protein (data not shown). This suggests that increased CD147 on the cell surface may be due to increased retention at the cell surface and/or rapid recycling rather than increased protein synthesis.

Finally, our data shows that up-regulation of CD147 in non-transformed and non-invasive breast epithelial cells leads to activation of the EGFR-Ras-MEK-ERK signaling cascade. Ras mutations in breast cancer are a rare event (Pylayeva-Gupta et al., 2011), though chronic Ras activation is evident in patient-derived breast cancer tissue and cell lines without Ras mutations (Eckert et al., 2004; Lintig et al., 2000). Our data suggests that wild-type Ras activity is increased in CD147-upregulated MCF-10A cells and this may be a potential mechanism that CD147 employs to elicit the previous invasive phenotype we identified in CD147-upregulated MCF-10A cells (Grass et al., 2012). To our knowledge, no mutations or intrinsic signaling motifs have been identified in CD147, thus it is probable that CD147 mediates breast cancer progression by facilitating the assembly of pro-tumorigenic multi-protein complexes on the cell surface. Also, though we saw differences in protein levels of CD147 with MEK inhibition or comparison of 10A-EV to 10A-K-Ras^{V12} cells, negligible changes in the mRNA level of CD147 were observed in both cases. This may suggest that the influence of Ras-MAPK signaling on CD147 expression occurs more at a post-transcriptional level; similar post-transcriptional regulation of CD147 has been observed in previous studies (Chen et al., 2010; Deora et al., 2005; Fanelli et al., 2003; Gallagher et al., 2007; Noguchi et al., 2003). Thus, even though CD147 expression is clearly increased in most aggressive cancers, identification of CD147 as a differentially expressed message in microarray analyses may not always be apparent. CD147 may act as an independent prognostic factor in some breast cancer types (Liu et al., 2010; Reimers et al., 2004) and further studies should evaluate the utility of CD147 surface expression in stratifying sub-populations in breast cancer.

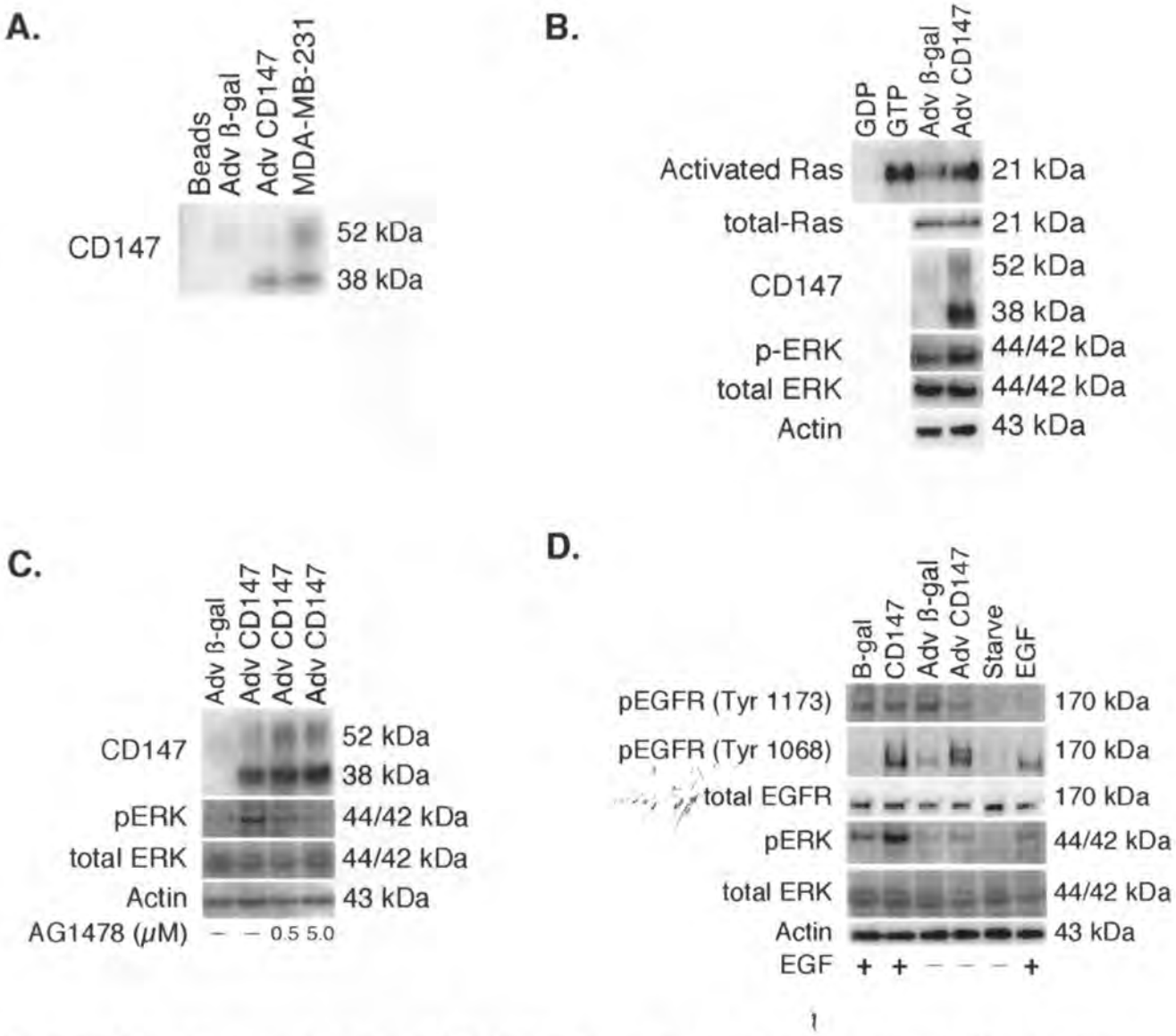

Figure 3-1. Up-regulation of CD147 induces activation of EGFR-Ras-ERK signaling. (A) Western blot depicting surface biotinylation of MCF-10A cells, treated with an MOI of 2 of β-gal or CD147 adenovirus, and parental MDA-MB-231 cells. An MOI of 2 was used in all subsequent adenovirus experiments. A lane with beads only was used as a negative control; n=3. (B) Evaluation of Ras activity in MCF-10A cells treated with β-gal or CD147 adenovirus. Lanes with GDP and GTP were used as negative and positive controls, respectively. Activated Ras was identified by probing with a pan-Ras antibody. β-actin was used as a loading control; n=4. (C) MCF-10A cells were treated with β-gal or CD147 adenovirus, starved and subsequently treated with vehicle (DMSO) or 0.5 μM and 5.0 μM tyrphostin (AG1478) overnight. β-actin was used as a loading control; n=3. (D) MCF-10A cells were treated with β-gal or CD147 adenovirus, starved and evaluated for EGFR activation by probing for phosphorylation at the Tyrosine 1173 or 1068 residues in the presence or absence of EGF in the medium. For controls, MCF-10A cells were starved or starved and treated with EGF (10 ng/ml). β-actin was used as a loading control; n=3.

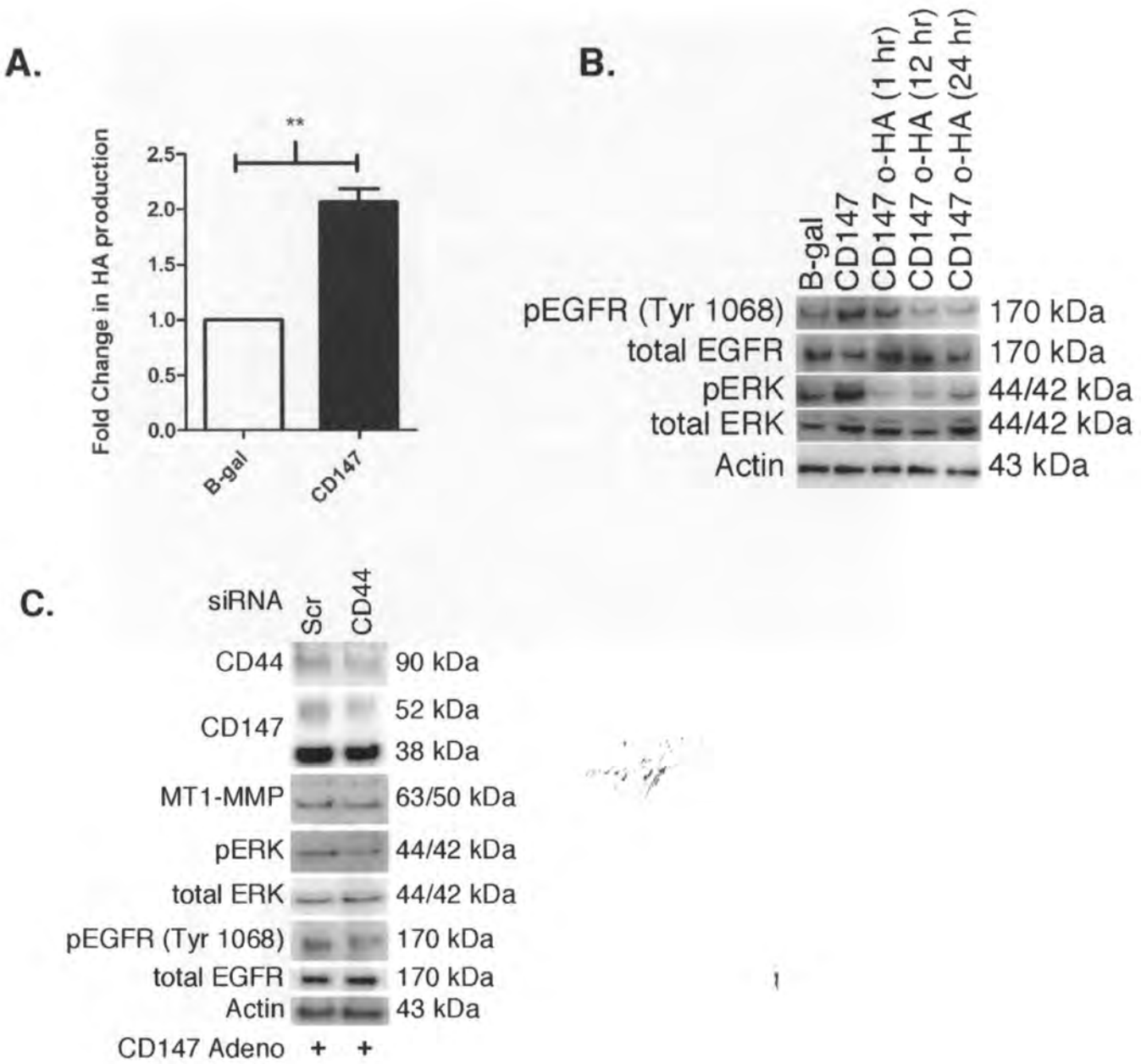

Figure 3-2. Hyaluronan-CD44 interaction mediates CD147-induced activation of EGFR signaling. (A) MCF-10A cells treated with β-gal or CD147 adenovirus were seeded into 24 well plates. The media was replaced with fresh media and after 24 hours it was collected and analyzed for hyaluronan concentration using an ELISA-like assay. Hyaluronan in the media was normalized to cell number and depicted as mean fold change; each column represents triplicate wells in three independent experiments. (B) MCF-10A cells treated with β-gal or CD147 adenovirus were subsequently treated with 100 μg/ml of o-HA for 1, 12 and 24 hours and probed for p-EGFR (Tyr^{1068}) and p-ERK. β -actin was used as a loading control; n=3. (C) MCF-10A cells treated with CD147 adenovirus were treated with non-specific control siRNA or pooled CD44-specific siRNA as described in *Materials and Methods* and probed for indicated proteins. β-actin was used as a loading control; n=3.

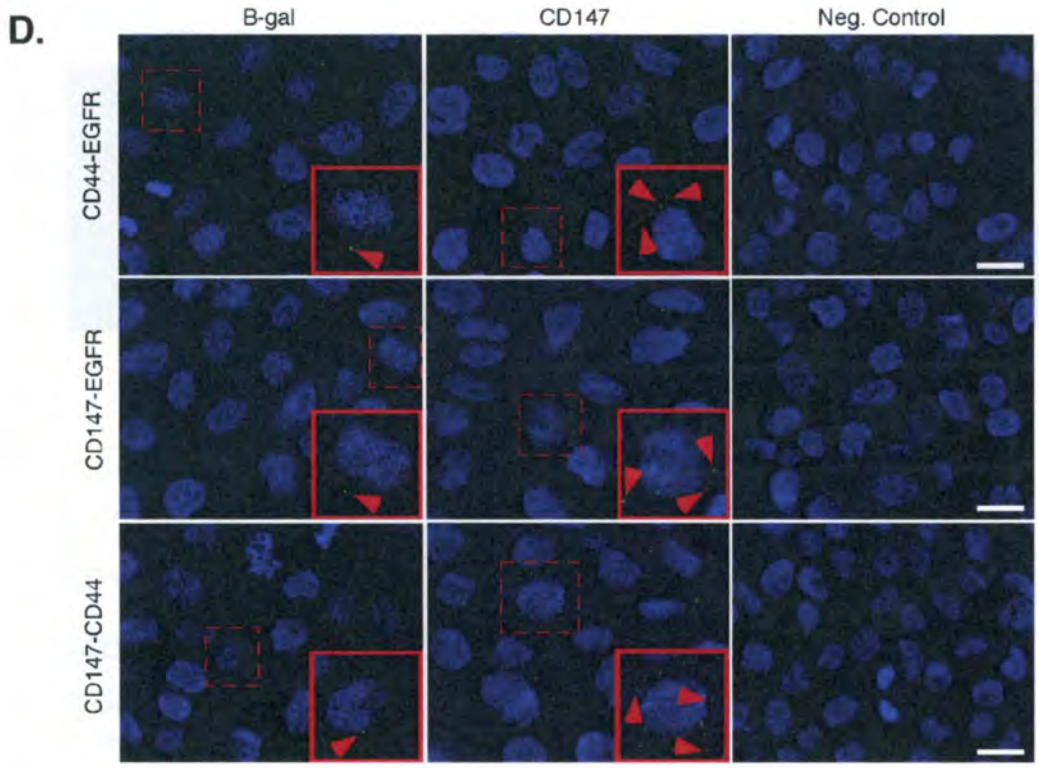

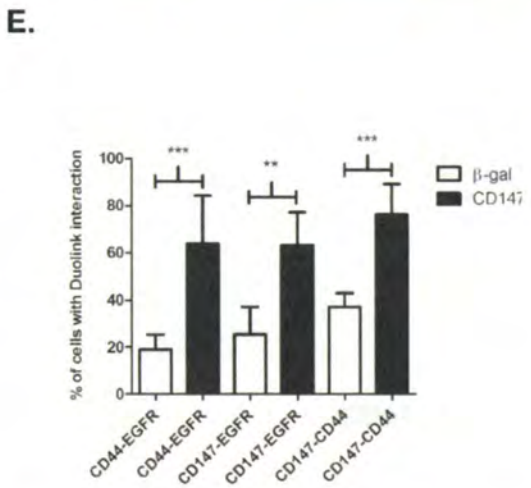

Figure 3-2 (continued). Hyaluronan-CD44 interaction mediates CD147-induced activation of EGFR signaling. (D) Representative images demonstrating protein-protein interactions (< 40 nm) using a proximity ligation assay (see *Materials and Methods* for details). CD147-treated MCF-10A cells were probed with primary antibodies in the following combinations: CD44 (mouse) and EGFR (rabbit) (top row); CD147 (mouse) and EGFR (rabbit) (middle row); and CD147 (mouse) and CD44 (rabbit) (bottom row) to detect protein-protein interactions in the cell population. Protein-protein interactions appear as small punctate green signals (i.e. dots) and cell nuclei were identified by co-staining with DAPI. Treatment of cells with a single primary antibody only was used as a negative control and indicates the specificity of the reaction (right panels in each row). (D) Quantification of indicated protein-protein interactions in the cell population over 5 random fields with at least 50 cells per field; column values are means ± s.e.m. over three independent experiments. $^{**}P<0.01$; $^{***}P<0.001$.

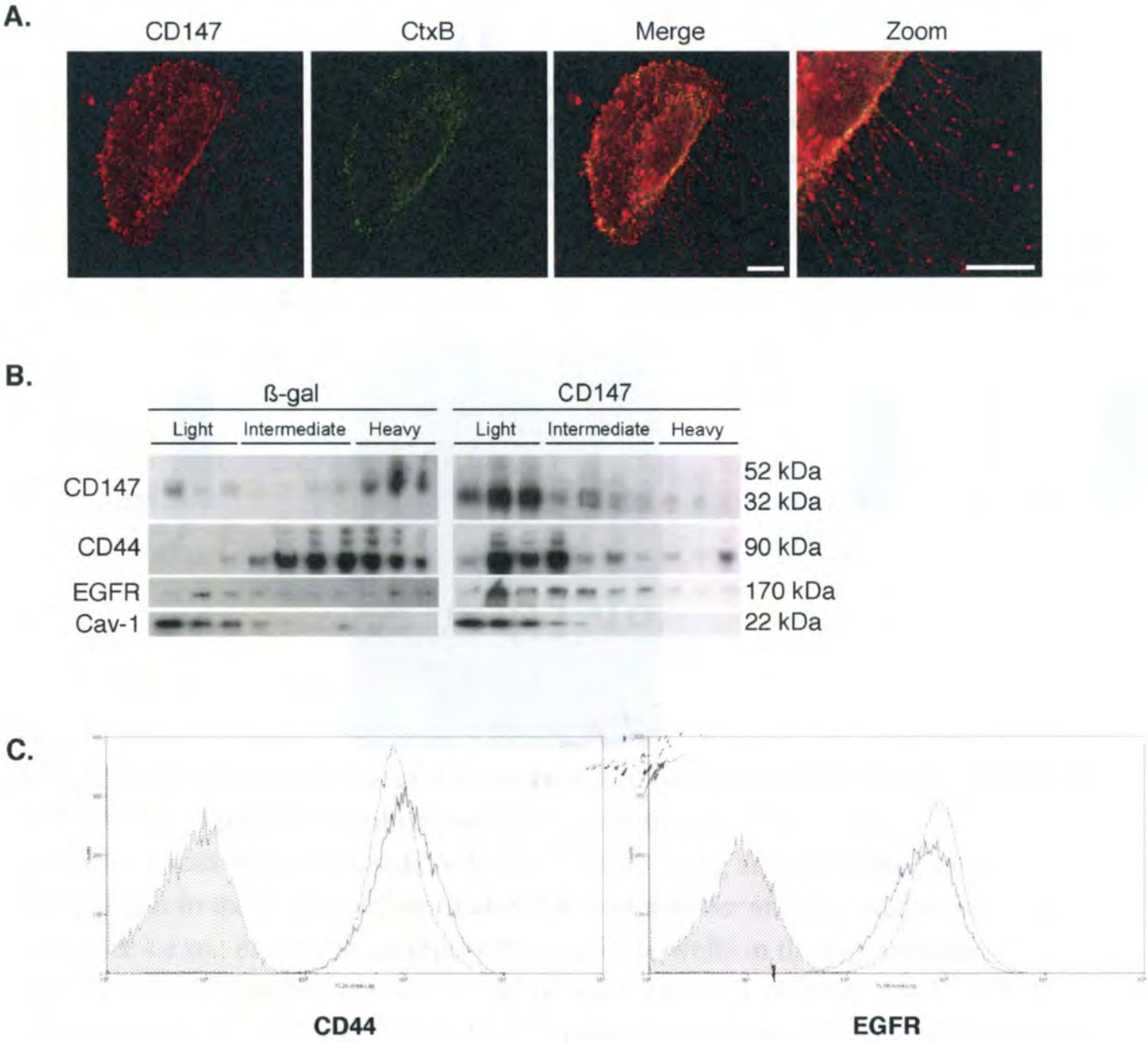

Figure 3-3. Up-regulation of CD147 promotes CD44 and EGFR enrichment in lipid rafts. (A) Representative image of MCF-10A cells treated with CD147 adenovirus and evaluated for CD147 (red) and cholera toxin-B (green) colocalization (yellow). Scale bar: 10 μm. (B) MCF-10A cells treated with β-gal or CD147 adenovirus were subjected to detergent-resistant membrane isolation and probed for indicated proteins. Light fractions are from the gradient interface (0-20%) where detergent-resistant membrane domains such as lipid rafts localize; n=3. (C) CD44 and EGFR surface expression was analyzed by FACS in CD147-treated MCF-10A cells. Distributions with dark gray shading, solid black lines with no shading and dotted black lines with light gray shading represent IgG-isotype control, β-gal and CD147 treated cells, respectively; n=3.

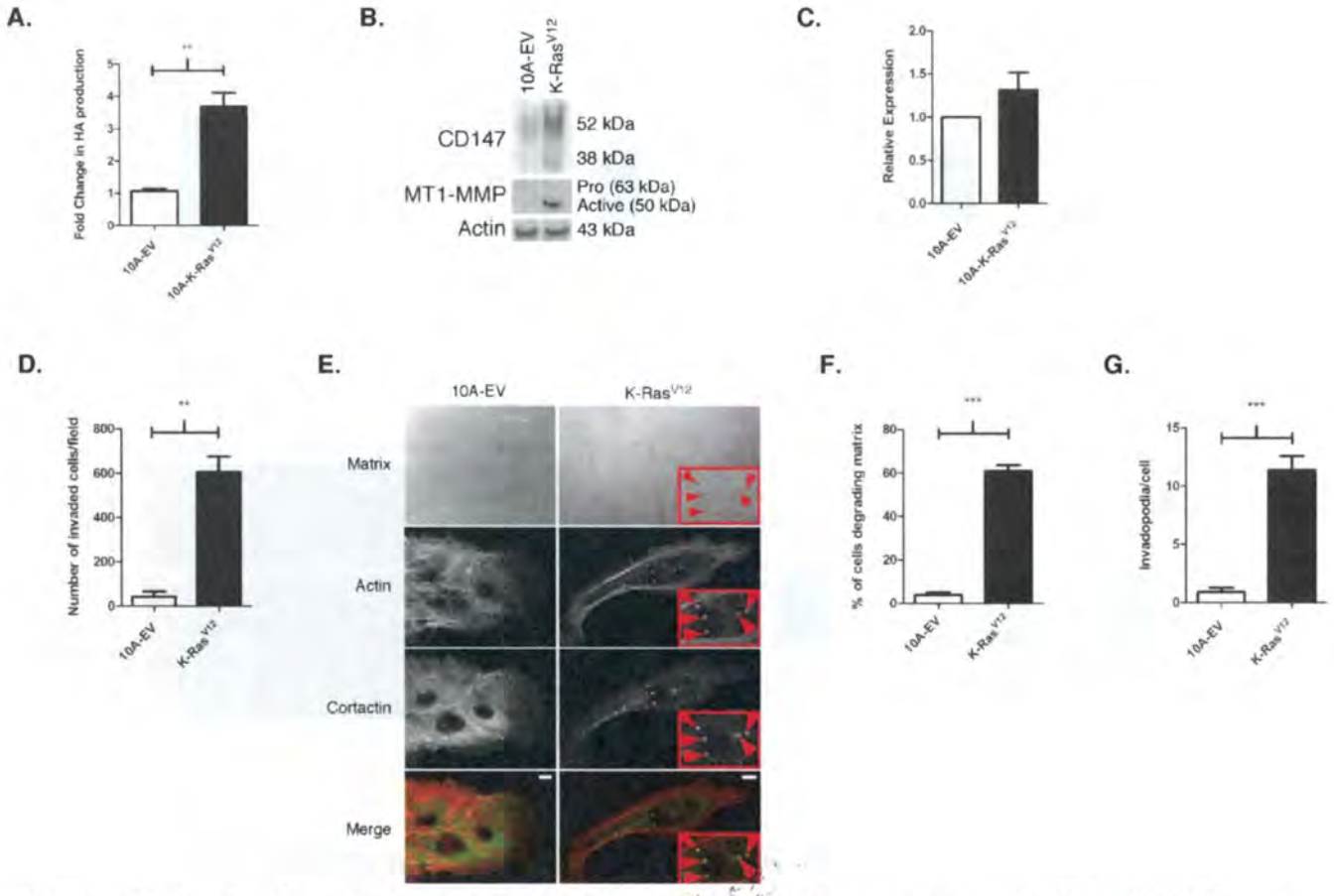

Figure 3- 4. Activated Ras and ERK regulate hyaluronan synthesis, CD147 and MT1-MMP expression and cancer invasiveness. (A) Hyaluronan synthesis was quantified from 10A-EV and 10A-K-Ras^{V12} cells using an ELISA-like assay. Hyaluronan in the media was normalized to cell number and depicted as mean fold change ± s.e.m.; each column represents triplicate wells in three independent experiments. (B) Representative western blot depicting CD147 and MT1-MMP expression in 10A-EV and 10A-K-Ras^{V12} cells. β-actin was used a loading control; n=4. (C) Comparison of CD147 mRNA levels in 10A-EV and 10A-K-Ras^{V12} cells, as measured by qPCR; normalized to β-actin; n=3. (D) Quantification of invasion through Matrigel by 10A-EV and 10A-K-Ras^{V12} cells. Columns represent the mean number of cells invaded (± s.e.m.) per field; n=3. (E) Representative micrograph demonstrating 10A-EV and 10A-K-Ras^{V12} cells cultured on fluorescent matrix. After fixation, cells were immunolabeled for cortactin followed by secondary Alexa-Fluor-488 antibody and Alexa-Fluor-647 phalloidin. Actin and gelatin matrix were pseudo-colored red and blue, respectively to allow easier visualization of colocalization (yellow) of actin (red) and cortactin (green). Invadopodia-mediated matrix degradation appears as dark black foci in the bright fluorescent matrix field. The boxed regions with red arrow heads depict actively degrading invadopodia. Scale bar: 10 μm. (F) Percentage of cells degrading the matrix; defined as a cell with at least one degradation spot underneath the cell or near the cell edge. (G) Quantification of invadopodia/cell; defined as actin-cortactin aggregate over degraded matrix. Each invadopodia parameter was calculated by evaluating random fields containing at least 15 cells per field over three independent experiments. Column values are means ± s.e.m. $^{**}P<0.01$; $^{***}P<0.001$.

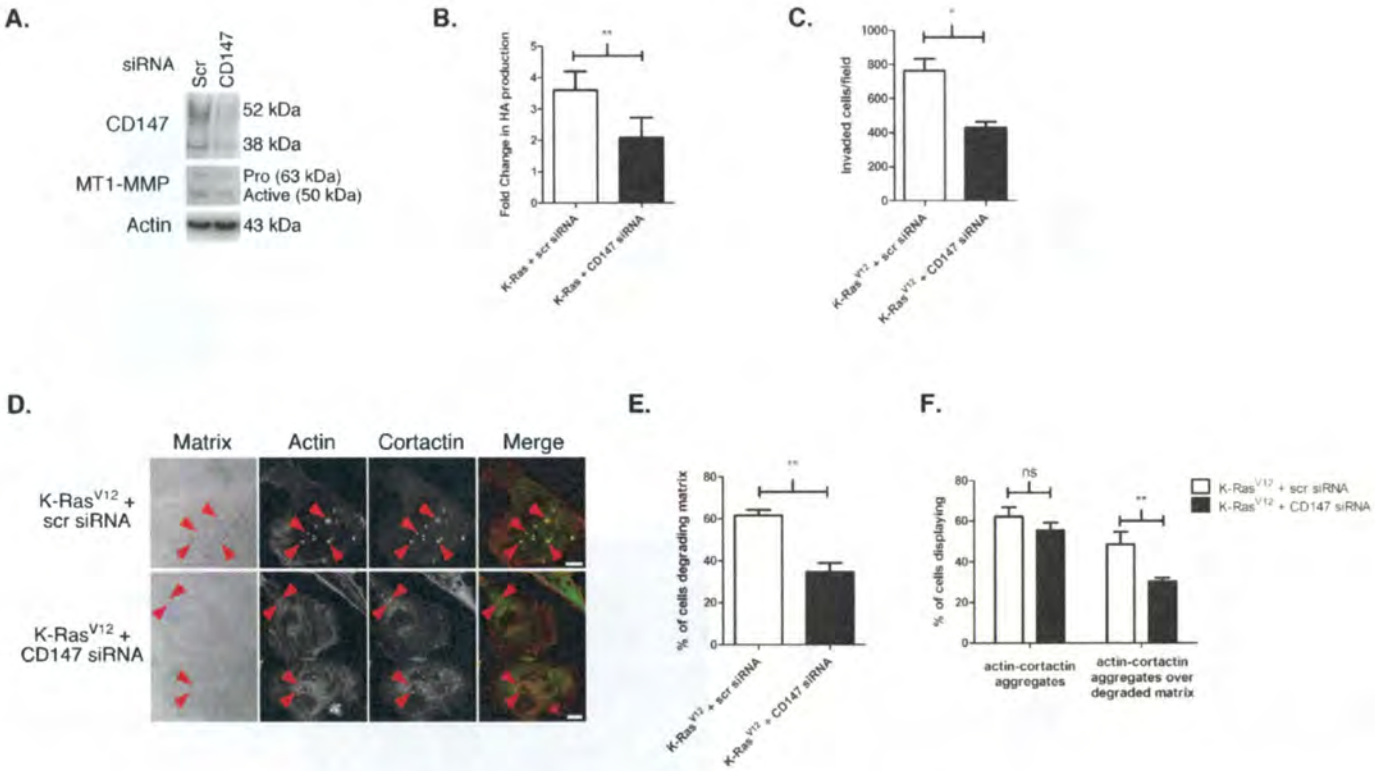

Figure 3-5. Knockdown of CD147 in MCF-10 K-Ras^{V12} cells results in decreased hyaluronan synthesis, MT1-MMP expression and invasiveness. (A) Western blot depicting CD147 and MT1-MMP protein levels in 10A-K-Ras^{V12} cells depleted of CD147 by treatment with pooled siRNAs. Scrambled (scr) siRNA was used as a control and β-actin was used as a loading control; n=3. (B) Comparison of HA production in 10A-K-Ras^{V12} cell treated with scrambled or pooled CD147-specific siRNA. Hyaluronan in the media was normalized to cell number and depicted as mean fold change ± s.e.m.; each column represents triplicate wells in three independent experiments. (C) Quantification of invasion through Matrigel by 10A-K-Ras^{V12} cells treated with scrambled or pooled CD147-specific siRNA. Columns represent the mean number of cells invaded (± s.e.m.) per field; n=3. (D) Representative micrograph demonstrating 10-K-Ras^{V12} cells treated with scrambled or pooled CD147-specific siRNA cultured on fluorescent matrix. Red arrow heads indicate actin-cortactin aggregates. Scale bar: 10 μm. (E) Percentage of cells degrading underlying matrix or (F) percentage of cells with actin-cortactin aggregates with or without underlying degraded matrix in 10A-K-Ras^{V12} cells treated with scrambled or pooled CD147-specific siRNA. Each invadopodia parameter was calculated by evaluating random fields containing at least 15 cells per field over three independent experiments. Column values are means ± s.e.m. *P<0.05; **P<0.01.

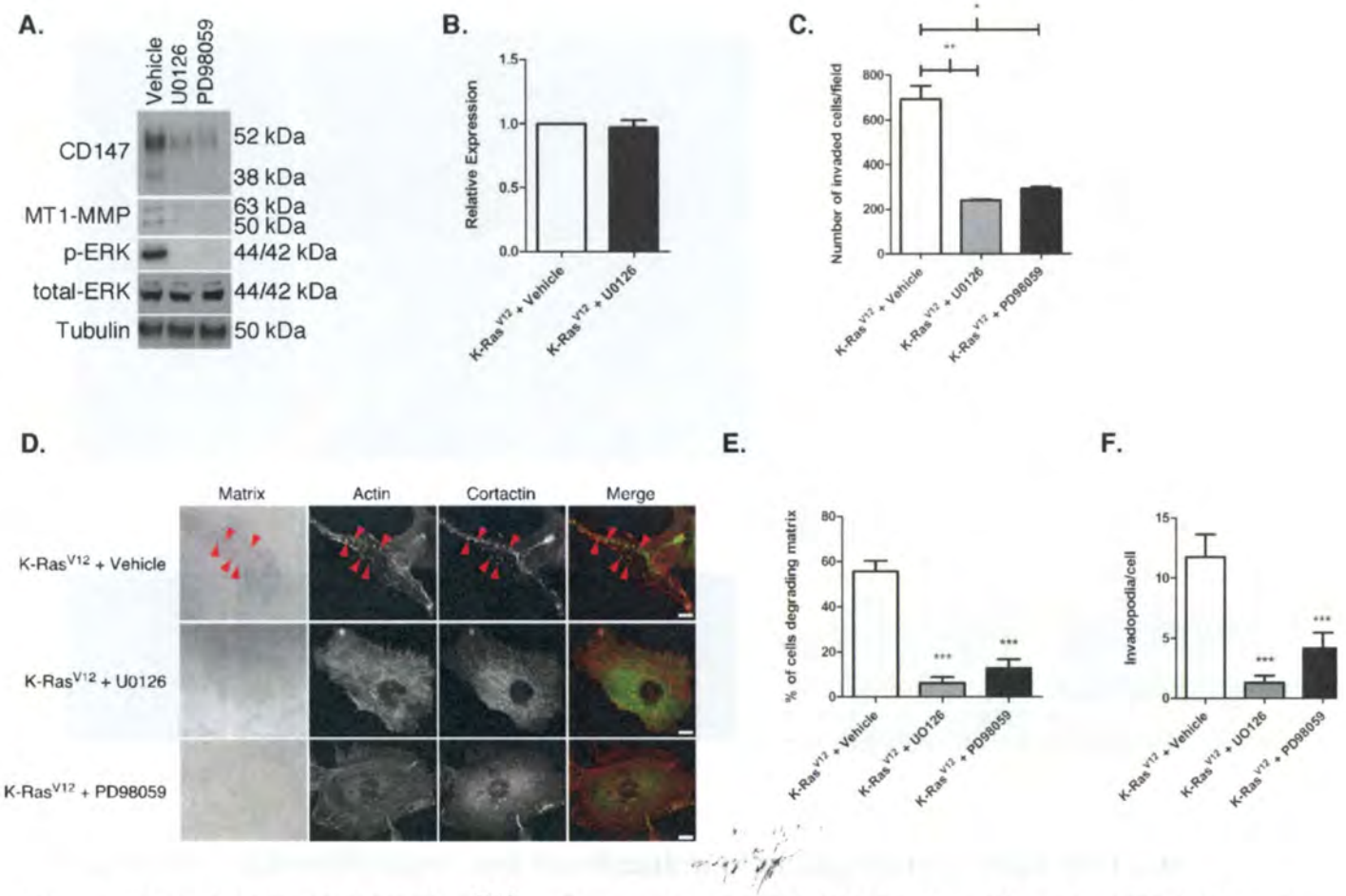

Figure 3-6. MCF-10A-K-Ras^{V12} cells employ MEK-ERK signaling for CD147 and MT1-MMP expression and invasiveness. (A) Western blot depicting 10A-K-Ras^{V12} cells treated with vehicle, U0126 (10 μM), or PD98059 (25 μM). β-tubulin was used as a loading control; n=3. (B) mRNA levels of 10A-K-Ras^{V12} cells treated with vehicle or UO126 (10 μM); normalized to β-actin; n=3. (C) Quantification of invasion through Matrigel by 10A-K-Ras^{V12} cells treated with vehicle, U0126 (10 μM) or PD98059 (25 μM). Columns represent the mean number of cells invaded (± s.e.m.) per field; n=3. (D) Representative micrograph of 10A-K-Ras^{V12} cells seeded on fluorescent matrix and treated with vehicle, U0126 (10 μM) or PD98059 (25 μM). Red arrow heads depict examples of invadopodia. Scale bar: 10 μm. (E) Percentage of cells degrading underlying matrix and (F) quantification of invadopodia/cell in 10A-K-Ras^{V12} cells treated with vehicle, U0126 (10 μM) or PD980539 (25 μM). Each invadopodia parameter was calculated by evaluating random fields containing at least 15 cells per field over three independent experiments. Column values are means ± s.e.m. *P<0.05; **P<0.01; *** P<0.001.

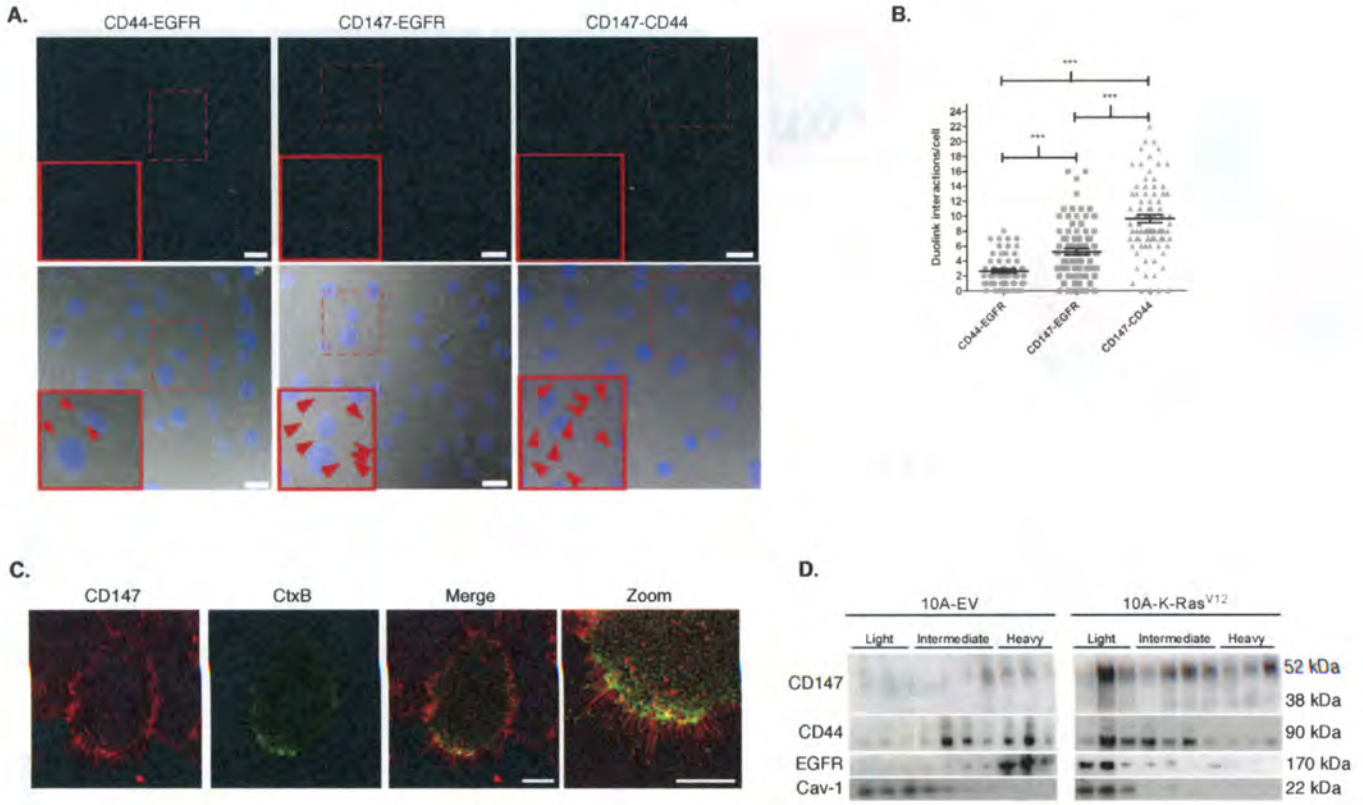

Figure 3-7. Identification and localization of endogenous proten-protein interactions in MCF-10A-K-Ras^{V12} cells. (A) Representative DIC-fluorescent merge images demonstrating endogenous protein-protein interactions (< 40 nm) using a proximity ligation assay (see *Materials and Methods* for details). 10A-K-Ras^{V12} cells were probed with primary antibodies in the following combinations: CD44 (mouse) and EGFR (rabbit) (left column); CD147 (mouse) and EGFR (rabbit) (middle column); and CD147 (mouse) and CD44 (rabbit) (right column) to detect protein-protein interactions in the cell population. Protein-protein interactions appear as punctate green signals (i.e. dots) and cell nuclei were identified by co-staining with DAPI (bottom row). The boxed regions are shown as higher magnification insets. Examples of protein-protein interactions are highlighted by arrow heads. Top row depicts automatic threshold images of the protein-protein interaction channel for easier visualization. Scale Bar: 25 µm. (B) Quantification of indicated protein-protein interactions per cell; Scatter plot with mean ± s.e.m.; n=3. (C) Representative image demonstrating colocalization (yellow) of endogenous CD147 (red) and cholera toxin-B (green) in 10A-K-Ras^{V12} cells. Scale bar: 10 µm. (D) Western blot comparing endogenous protein distribution between 10A-EV and 10A-K-Ras^{V12} cells subjected to detergent-resistant membrane isolation and probed for indicated proteins. Light fractions are from the gradient interface (0-20%) where detergent-resistant membrane domains such as lipid rafts localize; n=2. ***P<0.001.

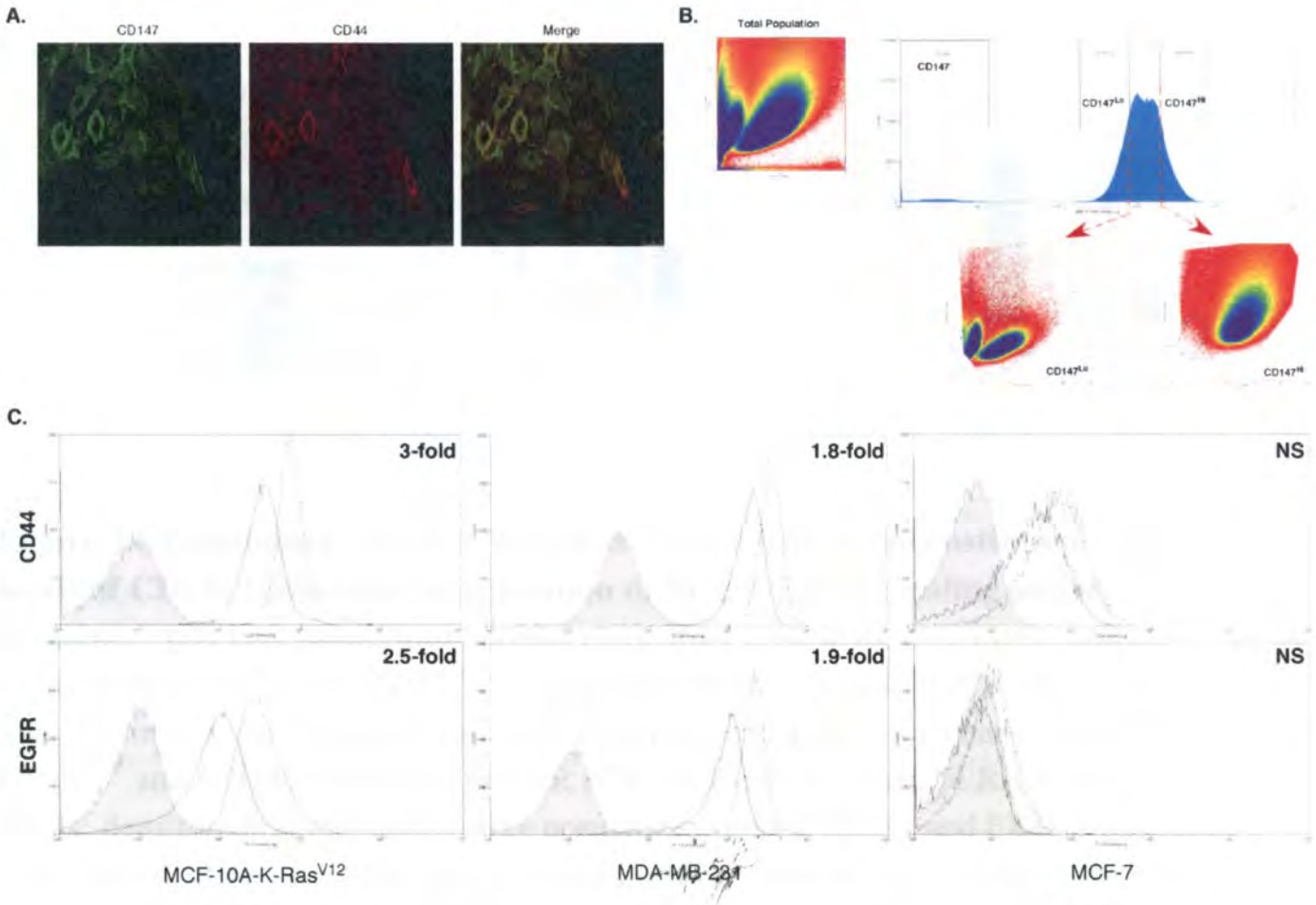

Figure 3-8. MCF-10A-K-Ras^{V12} cells with high constitutive surface levels of CD147 have elevated activation of EGFR-ERK signaling and are more invasive. (A) Representative micrograph demonstrating heterogeneity in CD147 and CD44 staining intensity across the 10A-K-Ras^{V12} cell population. Scale bar: 25 μm. (B) FACS scatter distribution of total 10A-K-Ras^{V12} cell population (left panel). Identification of CD147^{Lo} and CD147^{Hi} cells, bottom and top 20%, respectively, in the distribution of CD147-expressing cells (right top panel) with corresponding scatter characteristics (bottom right panels). Note that this cell sorting scheme identifies two distinct cell populations. (C) FACS analysis of cell surface expression of CD44 and EGFR in CD147^{Lo} and CD147^{Hi} cells in 10A-K-Ras^{V12} (left column; n=3), MDA-MB-231 (middle column; n=3), and MCF-7 (right column; n=2) cells. Distributions with dark gray shading, solid black lines with no shading and dotted black lines with light gray shading represent IgG-isotype control, CD147^{Lo} and CD147^{Hi} cell, respectively.

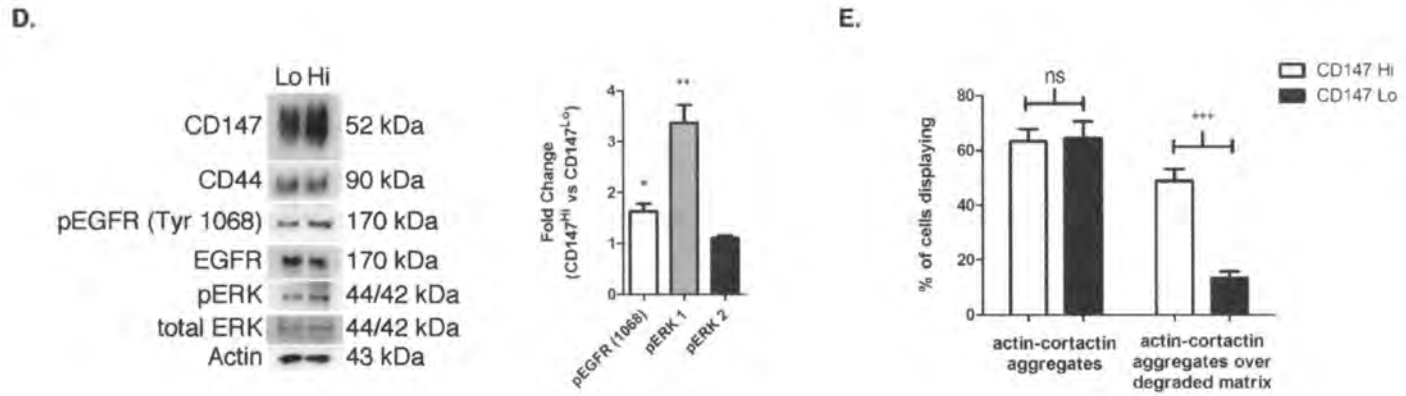

Figure 3-8 (continued). MCF-10A-K-Ras^{V12} cells with high constitutive surface levels of CD147 have elevated activation of EGFR-ERK signaling and are more invasive. (D) Left panel: Immunoblot comparing protein expression of indicated proteins in CD147^{Lo} and CD147^{Hi} 10A-K-Ras^{V12} cells. β-actin was used as a loading control; n=2. Right panel: Histogram demonstrates fold change between CD147^{Hi} and CD147^{Lo} cells for pEGFR (Tyr 1068), pERK1 and pERK2 protein levels; densitometric intensities were normalized to total EGFR and ERK1/2 protein. (E) Quantification of percentage of cells with actin-cortactin aggregates with or without underlying degraded matrix in CD147^{Lo} and CD147^{Hi} 10A-K-Ras^{V12} cells was calculated by evaluating random fields containing at least 15 cells per field over three independent experiments. Column values are means ± s.e.m. *$P<0.05$; **$P<0.01$; ****$P<0.001$.

Chapter 4: Overview, Novel Contributions and Future Work

As described above, CD147 participates in a variety of biological functions. CD147 expression is associated with an invasive phenotype in a wide array of cancer types, including breast cancer. One of the most significant findings supporting a role for CD147 in breast cancer invasion was a study discovering that weakly malignant breast cancer cells overexpressing CD147, which were injected into mouse mammary fat pads, demonstrated increased local invasion and extensive metastases to the liver, mediastinum, pleura, spleen, lymph nodes and mesentery (Zucker et al., 2001). CD147 is a predominant marker (~90%) in bone micrometastases (Klein et al., 2002; Reimers et al., 2004) isolated from breast cancer patients, is enriched in malignant pleural effusions (Davidson et al., 2004) and is expressed on circulating tumor cells (Pituch-Noworolska et al., 2007), suggesting a prominent role for CD147 in cancer progression. CD147 expression may also be an independent prognostic factor in some breast cancer types (Liu et al., 2010; Reimers et al., 2004).

CD147-induced MT1-MMP Induction Mechanism

The mechanism mostly attributed to CD147-induced invasion is the induction of proteases, including soluble and membrane-type MMPs (Yan et al., 2005). In support of this, CD147 has been identified at the invasive edge of breast carcinomas

(Polette et al., 1997) and in some invasive breast and lung cancers it colocalizes on the cell surface with MT1-MMP and MMP-1, respectively (Dalberg et al., 2000; Guo et al., 2000). CD147 regulates MT1-MMP synthesis and cell surface expression in various cell models (Sameshima et al., 2000; Schmidt et al., 2006; Seizer et al., 2010). MT1-MMP regulation is very stringent, as the increased presence of a highly proteolytic enzyme on the cell surface could be detrimental to cells not needing to cleave matrix substrates or cell surface factors that facilitate invasion. Similar to other MMPs, MT1-MMP is synthesized as a zymogen that needs processing to the active form. In the case of MT1-MMP, processing occurs via a furin-mediated cleavage event in the Trans-Golgi network during protein trafficking to the cell surface. MT1-MMP is then endocytosed and recycled back to the cell surface or sent for degradation, thus active MT1-MMP is the predominant form localized on the cell surface (Frittoli et al., 2011). Our recent publication suggests that CD147 may regulate the trafficking of MT1-MMP into cell surface localized lipid rafts within invadopodia (Grass et al., 2012). Support for CD147 having a role in MT1-MMP trafficking is found in a study identifying that CD147 associates with both pro and active forms of MT1-MMP (Niiya et al., 2009), though further work with live-cell imaging will be needed to fully prove this hypothesis. Alternatively, CD147 may be associated in a complex that regulates pro-MT1-MMP processing in the golgi.

CD147-induced EGFR-Ras-ERK Signaling

It has been recognized that xenografts of CD147-overexpressing breast cancer cells contain increased ERK activation at the advancing margin of the tumor (Tang et al., 2006). The current mechanisms explaining CD147-mediated ERK activation are *cis* homodimerization of CD147 (Cui et al., 2012), cooperation with cyclophilins (Yurchenko et al., 2010), syndecan-1 (Pakula et al., 2007) or HA-CD44 interactions (Marieb et al., 2004). Our studies provide further evidence of an involvement of CD147 cooperating with HA-CD44 signaling. In this respect, we found that up-regulation of CD147 increases HA synthesis, which in turn led to EGFR activation and subsequent activation of ERK. Abrogation of HA-receptor interactions with oHAs attenuated CD147-induced EGFR and ERK phosphorylation; CD44 depletion also reduced EGFR and ERK activation, but to a lesser extent. Our earlier findings identified that up-regulation of CD147 in MCF-10A cells led to increased MT1-MMP protein levels (Grass et al., 2012), though when CD44 was knocked down in CD147-overexpressing MCF-10A cells no difference in MT1-MMP protein was noticed. Similar results were obtained in a previous study where it was shown that increased HA stimulates invasiveness and MMP expression, but subsequent treatment with oHAs had no effect on MMP expression and only moderate inhibitory effect on invasion (Zoltan-Jones et al., 2003). Thus, there may be diverging pathways elicited by CD147: one that is mediated via HA-CD44 interactions and others that may utilize other molecular partners. In conjunction with our earlier findings, this data suggests that up-regulation of CD147 may lead to an invasive phenotype by facilitating assembly of CD44-EGFR-CD147 signaling complexes that activate ERK and result in increased MT1-MMP protein levels.

When initially evaluating upstream regulators of CD147-induced Ras activation, we found that the specific EGFR inhibitor AG1478 attenuated CD147-mediated ERK activation. The cytoplasmic tail of EGFR contains six tyrosine residues, which can be trans-autophosphorylated via the intrinsic tyrosine kinase activity of EGFR (Eccles, 2011). Earlier studies have identified that the Tyrosine 1173 (Sakaguchi et al., 1998) and 1068 (Rojas et al., 1996) residues are important for EGFR-mediated Ras-MAPK signaling by acting as docking sites for the scaffold proteins Shc and Grb2, respectively. Further evaluation of CD147-induced EGFR activation revealed that EGFR was specifically phosphorylated on the Tyrosine 1068 residue. Why CD147 induced only Tyrosine 1068 phosphorylation and not 1173 is currently not known, but may depend on the spatio-temporal interactions between the phosphorylated tyrosine residues and associated scaffold proteins. Such a relationship was identified between Tyrosine 1173 and SHP-1, a protein-tyrosine phosphatase, where binding attenuated EGFR-mediated signaling (Keilhack et al., 1998) and later studies suggested that the main role of Tyrosine 1173 phosphorylation was to recruit SHP-1 and inactivate ERK signaling (Hsu et al., 2011). Individual phosphosite activation may correlate with bias toward specific cellular phenotypes. For instance, a recent study identified that specific EGFR tyrosine residue activation resulted in differential abilities of cells to undergo chemotaxis and wound healing (Yamaoka et al., 2011). Furthermore, a study evaluating non-small cell lung cancer tissues identified that specific EGFR tyrosine residues are biased in their activation state (VanMeter et al., 2008). Even though CD147 increases Tyrosine 1068 phosphorylation, the specific function of this phosphosite activation is not known. Additionally, this may be due to a cell- or tissue-specific context, since EGFR is known

to promiscuously dimerize with other ErbB family members; thus EGFR activation bias may depend on which isoforms of Erb receptors a cell expresses (Eccles, 2011). In line with this, we found that treatment of MCF-10A cells with EGF resulted in a greater activation of Tyrosine 1068 than 1173; as mentioned above this may be due to certain cellular contexts, as MCF-10A cells express very low levels of ErbB2, a potential heterodimeric binding partner for EGFR.

CD147 and Ras in Breast Cancer

Oncogenic Ras forms are rarely identified in breast cancer (Pylayeva-Gupta et al., 2011), yet chronic Ras activation has been observed in several breast cancer cell lines and patient-derived tumor tissues with no evident Ras mutations (Eckert et al., 2004; Lintig et al., 2000). A recent study identified that up-regulation of wild type Ras resulted in an oncogenic phenotype in non-transformed breast epithelial cells (Zhang et al., 2009). CD147 expression intensity seems to progressively increase as breast cancer transitions from a benign proliferation to an invasive carcinoma (Liu et al., 2010), but whether CD147 alone is a driver or just a passenger oncogene is not known. We have identified that up-regulation of CD147 alone in non-transformed breast epithelial cells initiates an invasive program, increases HA synthesis and activates an EGFR-Ras-MEK-ERK signaling cascade, supporting its possible role as a driver of oncogenesis, especially with respect to invasiveness.

Complex signaling networks have been suggested between HA and Ras and descriptions of these relationships follow. Some of the strongest evidence comes from

studies employing HA synthase 2 (*Has2)* null mice, which are embryonic lethal, are defective in EGFR family signaling, and demonstrate Ras dependence in cellular invasion and the ability to undergo an EMT (Camenisch et al., 2002; Camenisch et al., 2000). Additionally, HA has been shown to increase Ras activity *in vitro* (Fitzgerald et al., 2000; Serbulea et al., 1999) and oncogenic Ras has been shown to increase HA synthesis (Hamilton et al., 2007), thus forming a potential positive feedback loop. CD44, the main HA receptor, also cooperates with Ras activation (Sohara et al., 2001) and HA-CD44 interactions have been demonstrated to activate various RTKs upstream of Ras (Bourguignon et al., 2006; Misra et al., 2006; Wang and Bourguignon, 2006) as well as downstream effectors of Ras (Bourguignon et al., 2005; Hamilton et al., 2007). An additional feedback loop was identified between Ras and CD44, where Ras induced CD44 alternative splicing, which in turn facilitated further Ras activation (Cheng et al., 2006). Later studies found that CD44 splice isoform switching was important in initiating an EMT program in breast epithelial cells (Brown et al., 2011) and different CD44 splice isoforms may correlate with different breast cancer subtypes (Olsson et al., 2011). Our finding that CD147 increases HA synthesis and EGFR-Ras-ERK activation suggests that CD147 integrates into this HA-CD44-Ras signaling module. Previous evidence indicates that HA is involved in assembling signaling complexes in lipid rafts (Ghatak et al., 2005), thus CD147-induced HA signaling may also lead to a similar phenomenon. We have found that increased CD147 expression leads to enrichment of MT1-MMP, CD44 and EGFR in lipid raft domains, suggesting that CD147-induced HA-CD44 interactions, higher order oligomerization of CD147 or heterophilic protein interactions between CD147 and other binding partners results in multi-protein complex

assembly. It will be interesting to see if the integration of CD147 with HA-CD44-Ras-ERK signaling plays a role in different aspects of tumor progression. A previous study suggested that initiation of tumor growth is dependent on Ras-mediated effector pathways, but a reduction in the requirement of Ras occurs during tumor maintenance, even though Ras effector pathways still remain active (Lim and Counter, 2005). It is clear that the tumor microenvironment changes during cancer progression, hence it will be important to evaluate whether CD147-induced signaling pathways can potentiate Ras effector pathways independent of Ras. This may be the case because increases in HA synthesis confer an anchorage-independent growth advantage to cells (Zoltan-Jones et al., 2003). Since CD147 induces HA-CD44-dependent anchorage-independent growth (Marieb et al., 2004), it is likely that CD147-mediated resistance to anoikis (Yang et al., 2006) is dependent on HA-CD44 interactions, which supply the cell with supplemental pro-survival ECM signals in the absence of integrin-based adhesion.

Glycosylation and CD147 Function and Stability

As mentioned previously, the core protein of CD147 may contain diverse combinations of carbohydrate attachments. Several authors have observed that CD147 migrates on SDS-PAGE between 31-65 kDa, a characteristic attributed to heterogeneous glycosylations, composed of branched polylactosamine, fucosylation, sialylation and Lewis^x glycan attachments. CD147 glycoforms were previously characterized as mannose-rich LG-CD147 and branched polylactosamine HG-CD147 (Tang et al., 2004a). Currently, HG-CD147 is the only glycoform that has been attributed with a specific

function; in this case HG-CD147 is associated with MMP induction. In contrast, accumulating evidence suggests that the high-glycosylated form is not necessary to induce MMPs (Attia et al., 2011; Belton et al., 2008; Kawakami et al., 2011).

Protein N-glycosylation begins in the endoplasmic reticulum and is followed by sequential addition or removal of sugar residues by various enzymes as the protein transits through the golgi apparatus (Lau and Dennis, 2009). An elegant study demonstrated that the protein glycoform synthesized by the cell is highly dependent upon cooperation between the expression profile of golgi transferases and metabolic flux through the hexosamine pathway (Lau et al., 2007). This cooperativity between cell environment (e.g. metabolic substrates) and cell-type specific expression of tranferases may explain the variation in CD147 glycoforms identified from cell lines derived from the same tissue of origin (Riethdorf et al., 2006).

The HG-CD147 form contains β1,6-branched, polylactosamine-type sugars attachments initiated by the activity of N-acetlyglucosaminyltransferase V, which is encoded by the gene *Mgat5* (Lau and Dennis, 2009). Interestingly, *Mgat5* transcription is increased by Ras signaling (Chen et al., 1998) and Ras has been shown to lead to differential sialylation of integrins (Seales et al., 2003). Whether Ras regulates CD147 glycosylation by initiating branching of polylactosamines or addition of sialic acid residues is unknown, but our current evidence suggests that this may be plausible as Ras does not appear to increase CD147 transcription dramatically and our immunoblots demonstrate differential CD147 glycoforms between cells with or without oncogenic Ras.

The LG-CD147 form was characterized to contain high-mannose type carbohydrates, possibly via caveolin-1-mediated inhibition of further branching by *Mgat5* in the golgi (Tang et al., 2004a). Earlier studies proposed that the LG-CD147 form is immature and remains confined to the endoplasmic reticulum (Gallagher et al., 2007), yet our surface biotinylation results as well as others demonstrate that the LG-CD147 form is present on the cell surface (Tang et al., 2004a; Tang and Hemler, 2004). As discussed previously, LG-CD147 preferentially associates with caveolin-1, but may also associate with $\alpha^3\beta_1$ or $\alpha^6\beta_1$ integrins (Berditchevski et al., 1997). Pulse-chase analysis discovered that LG-CD147 was converted to HG-CD147 or degraded in less than two hours (Tang and Hemler, 2004), suggesting that the kinetics of LG-CD147 may be different than HG-CD147.

Whether LG-CD147 participates in different functions than HG-CD147 is unknown. It is possible that LG-CD147 preferentially localizes in the rapid recycling compartments previously identified (Eyster et al., 2009) and takes part in dynamic cellular processes such as matrix remodeling and metabolic substrate transport, whereas HG-CD147 is more confined to the cell surface and aids in cell adhesion events (Sun and Hemler, 2001). Possibilities for the differences in membrane retention may be depend upon HG-CD147 N-glycan interactions with extracellular matrix protein scaffolds such as galectins (Liu and Rabinovich, 2005). For instance, branched glycans in HG-CD147 would be expected to have stronger avidity for galectins compared to high-mannose LG-CD147 forms (Lau et al., 2007), which could lead to retention of HG-CD147 on the cell surface and allow dynamic trafficking of the LG-CD147 form. Additionally, decreased glycosylation has been shown to promote ubiquitination and subsequent degradation of

CD147 (Wang et al., 2008), yet further work is needed to elucidate how recycling and protein turnover cooperate in regulating CD147 function. Whether specific glycosylations on CD147 dictate function is unknown and future studies should determine localization patterns of different glycoforms using various lectin approaches coupled with subcellular organelle characterization techniques.

Utility of CD147 as a Cell Surface Marker for Breast Cancer Cell Sub-population Analysis

Breast cancer is a heterogeneous disease that has been separated into several clinical subsets (Voduc et al., 2010). Profiling of breast cancer specimens using genetic profiling and immunohistochemistry demonstrates that breast cancer is divided into distinct subtypes: Luminal A, Luminal B, Luminal-ErbB2 positive, ErbB2-amplified, basal-like and triple negative. The latter two are considered similar by some investigators, though much debate currently exists with respect to this classification (Foulkes et al., 2010). A recent study found that six additional subtypes can be clustered into triple negative breast cancer, making the classification scheme even more complex (Lehmann et al., 2011). Currently, evaluation of hormone receptor status, cytokeratin expression and ErbB2 amplification represent the mainstay utilized clinically for treatment stratification, but higher resolution characterization of breast cancers is needed to identify responders and non-responders to our current treatment modalities.

Complementary to these analytical approaches, evaluation of cell surface expression profiles on individual cancer cells has also demonstrated utility (Ricardo et al.,

2011). In this respect, differential surface expression of CD44, CD24 and others markers have aided in identifying cells with stem-like properties that are invasive and resistant to current therapies (Visvader and Lindeman, 2008). CD147 associates with CD44 (Slomiany et al., 2009b) and EpCAM (Xu and Hemler, 2005), two proteins that were employed in the initial isolation of highly tumorigenic breast cancer cells (Al-Hajj et al., 2003) and cells from breast cancer cell lines with stem-like qualities and intrinsic resistance to chemotherapy (Fillmore and Kuperwasser, 2008). We have shown that enrichment of cells with differing CD147 surface expression patterns affords us the ability to isolate cells with different capacities to invade and activate EGFR-ERK signaling pathways. Additionally, cells with high constitutive surface expression of CD147 have increased CD44 and EGFR surface levels. Future studies should address whether enriching for cells with differential surface levels of CD147 may be an alternative approach to isolate cells with diverse functional phenotypes in breast cancer or aid in classifying certain breast cancer subtypes.

Translating CD147 to the Clinic

The presence of CD147 on the cell surface makes it a plausible molecular target for various targeted therapies, including monoclonal antibody therapy. In this regard, a dose-escalation study with a murine IgM monoclonal antibody targeting CD147 was evaluated in the context of steroid-refractory acute graft-versus-host disease. In this study, the dose-limiting factor was severe myalgias at 0.3 mg/kg, which could be controlled by narcotics. Additionally, no significant differences were seen in T cell or B cell numbers,

though the treatment demonstrated efficacy in this setting (Deeg et al., 2001). Neutrophil or erythrocyte counts were not evaluated in this study.

The first cancer-related study targeting CD147 in patients was performed in Phase I/II trials in China using a CD147-specific $F(ab')_2$ fragment conjugated to $iodine^{131}$, which is called metuximab (Licartin). In this study metuximab was infused into the hepatic artery and the safety and efficacy of this therapy was evaluated in hepatocellular carcinoma (HCC) patients. No life-threatening toxic side effects were identified, though Grade 3 hematologic and hepatic toxicity was identified in some patients. The CD147-targeting antibody fragment was found to concentrate primarily in the tumor tissue and resulted in an improved survival rate, with a median survival time of 19 months; normally patients with HCC progress rapidly and have a survival time of 3.2 months. Interestingly, unconjugated metuximab demonstrated low clinical efficacy alone and was not tested in these trials (Chen et al., 2006b).

Preclinical studies in HNSCC are also underway. In tumor xenografts in mice, administration of CNTO3899, a chimerized monoclonal human IgG1 antibody targeting CD147, resulted in decreased cell proliferation and in combination with irradiation resulted in additive toxic effects to the tumor (Dean et al., 2009). Additional studies found that this antibody also induced apoptosis (Dean et al., 2010) and partially slowed down glucose uptake in pancreatic cancer xenografts (Shah et al., 2011).

Though CD147-targeting monoclonal antibody therapy appears to have clinical benefit, the epitope targeted by the antibody should be closely examined. Antibodies directed against different epitopes of the extracellular domain of CD147 have resulted in

opposing effects. For example, a study characterizing antibodies generated toward CD147 found that some inhibited invasion and MMP synthesis, whereas others increased both invasion and MMP synthesis (Wang et al., 2006). Furthermore, studies in immune cells identified that CD147 may contain two separate bioactive domains, one involved in cell aggregation and the other in T cell activation (Chiampanichayakul et al., 2006), thus binding of natural ligands or targeted antibodies may elicit differing cellular responses. Alternatively, antibodies targeting CD147 may alter CD147 homo- or hetero-philic protein interactions leading to reorganization of lipid raft domains (Staffler et al., 2003). Thus before CD147-targeted antibody therapy makes a stride towards the clinic, stringent evaluation of epitope-associated CD147 function needs to be clarified. A better suited use of CD147-targeted antibodies may be in the utility of *in vivo* detection of tumor cells by employing fluorescently-conjugated CD147 antibodies (Newman et al., 2008b).

Due to the pleiotropic nature of CD147 function, consideration should be taken into account when evaluating therapies to down-regulate CD147. Various physiological processes, such as fertilization, immune cell differentiation, transport of metabolic intermediates, wound healing and blood-brain barrier maintenance have all been attributed to CD147 function. It is of interest, that in the above clinical studies, no mention of deleterious side effects was noted. This may be due to the highly targeted administration of metuximab through the hepatic artery and subsequent concentration primarily in liver tissue or the masking of side effects seen in the graft-versus-host disease cohort, which had poor baseline function of various organs. Further prospective randomized controlled studies are needed for evaluating CD147 efficacy in patients, since the CD147-targeting cancer trial did not compare results to any standard of care.

Various studies have evaluated tumor biology by examining patient tumor samples before, during or after therapy regimens. Many of these studies focus primarily on the mRNA levels of proteins and rate whether differences are significant by setting a threshold ratio. Our data presented in this thesis, as well as data from other groups, have found that CD147 expression may be regulated more at a post-transcriptional level (Chen et al., 2010; Deora et al., 2005; Fanelli et al., 2003; Gallagher et al., 2007; Noguchi et al., 2003). Thus, in some experimental contexts underestimation of differences in CD147 expression may occur when evaluating tumor samples. Additionally, CD147 is extensively modified by post-translational carbohydrate additions and interacts in diverse cellular compartments with various binding partners, all features that are missed in broad microarray analyses. Future studies should be directed to elucidating the mechanisms that regulate CD147 post-transcriptionally, including: message stability, translation regulators, and glycosylation modulators.

Closing Remarks

It is becoming evident that the name Extracellular Matrix MetalloPRoteinase INducer (EMMPRIN) does not suffice to describe the role of CD147 in cell biology. Though CD147 has a prominent role in MMP induction in various cell models, it also appears to have a distinct role in organizing multi-protein complexes consisting of RTKs, metabolic transporters, drug efflux pumps and cell adhesion molecules. Additionally,

CD147 is emerging as a regulator of the cytoskeleton and participates in the migration/invasion phenotype of various cancer cells, both *in vitro* and *in vivo*.

In this thesis, we have identified several novel roles of CD147 in breast cancer invasion. We have demonstrated that CD147 can regulate invadopodial dynamics, membrane reorganization events and the assembly of signaling complexes. Specifically, we found that interweaved relationships are present between MT1-MMP, HA-CD44 interactions and EGFR-Ras-ERK signaling in breast cancer biology (Figure 4-1). Further studies should investigate whether similar relationships exist in other cancer types, especially those that have been identified to rely strongly on EGFR and Ras signaling for their progression.

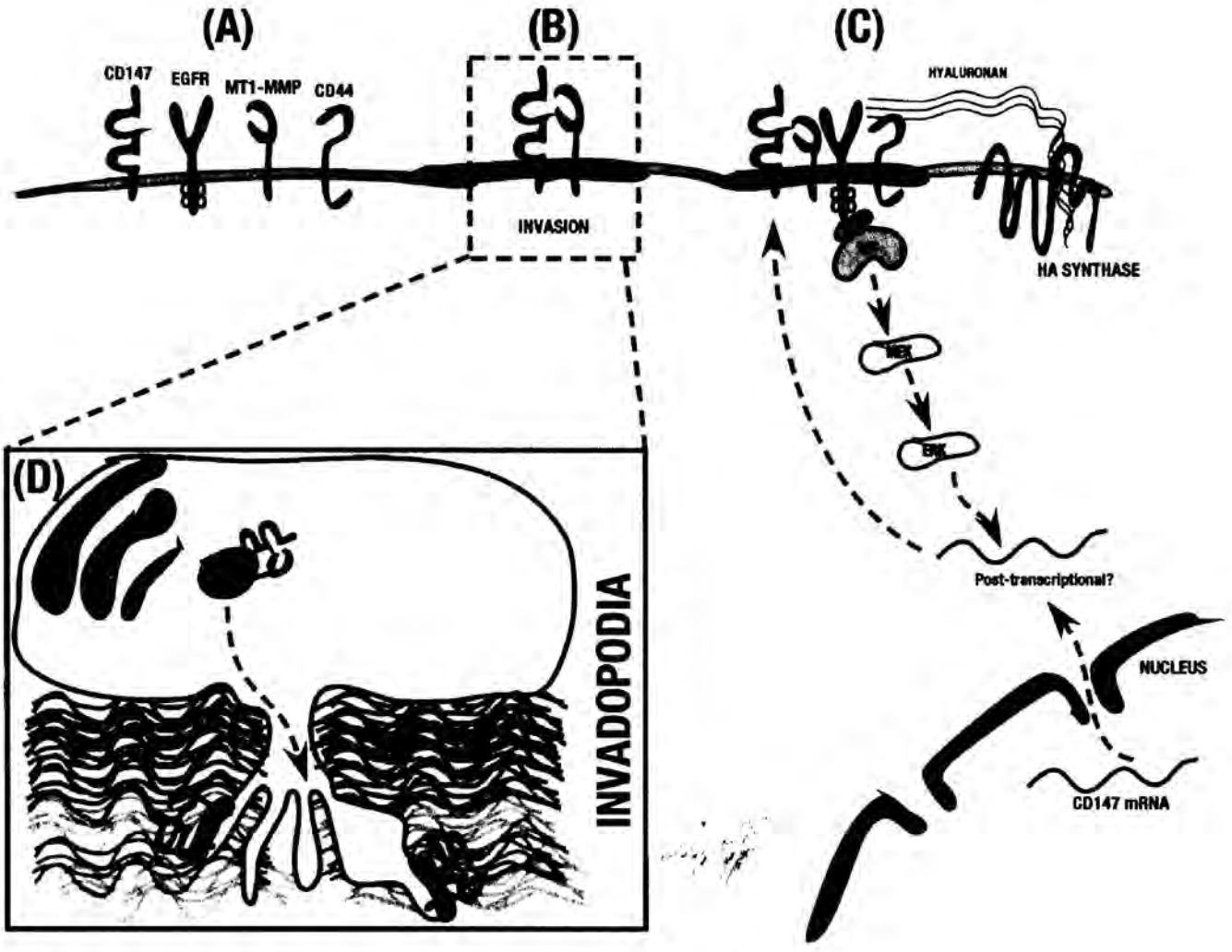

Figure 4-1. Working model: CD147 regulates invadopodia dynamics by facilitating the assembly of multi-protein signaling complexes in lipid rafts. A) Distribution of endogenous CD147, EGFR, MT1-MMP and CD44 in the absence of CD147 up-regulation. Thin yellow membrane indicates non-raft membrane. See Figures 2-5C and 3-3B for supporting data. B,D) Up-regulation of CD147 leads to MT1-MMP accumulation in lipid raft domains (dark brown membrane) possibly enriched in invadopodia. C) Up-regulation of CD147 leads to assembly of multi-protein complexes containing CD147, MT1-MMP, EGFR and CD44, which facilitate invasion. Also, these complexes activate EGFR-Ras-MEK-ERK signaling cascades that are dependent on HA-CD44 interactions. Of note, the Ras-MEK-ERK pathway may regulate CD147 via post-transcriptional modulation.

LIST OF REFERENCES

Abe, N., T. Osanai, T. Fujiwara, K. Kameda, T. Matsunaga, and K. Okumura. 2006. C-reactive protein-induced upregulation of extracellular matrix metalloproteinase inducer in macrophages: Inhibitory effect of fluvastatin. *Life Sciences*. 78.

Al-Hajj, M., M.S. Wicha, A. Benito-Hernandez, S.J. Morrison, and M.F. Clarke. 2003. Prospective identification of tumorigenic breast cancer cells. *PNAS*. 100:3983-3988.

Albiges-Rizo, C., O. Destaing, B. Fourcade, E. Planus, and M.R. Block. 2009. Actin machinery and mechanosensitivity in invadopodia, podosomes and focal adhesions. *Journal of Cell Science*. 122:3037-3049.

Alexander, N.R., K.M. Branch, A. Parekh, E.S. Clark, I.C. Iwueke, S.A. Guelcher, and A.M. Weaver. 2008. Extracellular Matrix Rigidity Promotes Invadopodia Activity. *Current Biology*. 18:1295-1299.

Alexander, S., and P. Friedl. 2012. Cancer invasion and resistance: interconnected processes of disease progression and therapy failure. *Trends in Molecular Medicine*. 18:13-26.

Als, A.B., L. Dyrskjot, H.v.d. Maase, K. Koed, F. Mansilla, H.E. Toldbod, J.L. Jensen, B.P. Ulhoi, L. Sengelov, K.M.E. Jensen, and T.F. Orntoft. 2007. Emmprin and Survivin Predict Response and Survival following Cisplatin-Containing Chemotherapy in Patients with Advanced Bladder Cancer. *Clinical Cancer Research*. 13:4407-4414.

Altruda, F., P. Cervella, M.L. Gaeta, A. Daniele, F. Giancotti, G. Tarone, G. Stefanuto, and L. Silengo. 1989. Cloning of cDNA for a novel mouse membrane glycoprotein (gp42): shared identity to histocompatability antigens, immunoglobulins and neural-cell adhesion molecules. *Gene*. 85:445-452.

Arjonen, A., R. Kaukonen, and J. Ivaska. 2011. Filopodia and adhesion in cancer cell motility. *Cell Adhesion & Migration*. 5:421-430.

Artym, V.V., K. Matsumoto, S.C. Mueller, and K.M. Yamada. 2010. Dynamic membrane remodeling at invadopodia differentiates invadopodia from podosomes. *European Journal of Cell Biology*. 90:172-180.

Attia, M., E. Huet, J. Delbe, D. Ledoux, S. Menashi, and I. Martelly. 2010. Extracellular Matrix Metalloproteinase Inducer (EMMPRIN/CD147) as a Novel Regulator of Myogenic Cell Differentiation. *Journal of Cellular Physiology*. 226:141-149.

Attia, M., E. Huet, J. Delbe, D. Ledoux, S. Menashi, and I. Martelly. 2011. Extracellular matrix metalloproteinase inducer (EMMPRIN/CD147) as a novel regulator of myogenic cell differentiation. *Journal of Cellular Physiology*. 226:141-149.

Ayala, I., M. Baldassarre, G. Giacchetti, G. Caldieri, S. Tete, A. Luini, and R. Buccione. 2007. Multiple regulatory inputs converge on cortactin to control invadopodia biogenesis and extracellular matrix degradation. *Journal of Cell Science*. 121:369-378.

Baba, M., M. Inoue, K. Itoh, and Y. Nishizawa. 2008. Blocking CD147 induces cell death in cancer cells through impairment of glycolytic energy. *Biochemical and Biophysical Research Communications*. 374:111-116.

Baldassarre, M., A. Pompeo, G. Beznoussenko, C. Castaldi, S. Cortellino, M.A. McNiven, A. Luini, and R. Buccione. 2003. Dynamin Participates in Focal Extracellular Matrix Degradation by Invasive Cells. *Molecular Biology of the Cell*. 14:1074-1084.

Bao, W., D. Min, S.M. Twigg, N.A. Shackel, F.J. Warner, D.K. Yue, and S.V. McLennan. 2010. Monocyte CD147 is induced by advanced glycation end products and high glucose

concentration: possible role in diabetic complications. *American Journal of Physiology Cell Physiology*. 299:C1212-C1219.

Barth, K., R. Blasche, and M. Kasper. 2006. Lack of evidence for caveolin-1 and CD147 interactions before and after bleomycin-induced lung injury. *Histochemistry and Cell Biology*. 126:563-573.

Beesley, A.H., A.J. Cummings, J.R. Freitas, K. Hoffmann, M.J. Firth, J. Ford, N.H.d. Klerk, and U.R. Kees. 2005. The gene expression signature of relapse in paediatric acute lymphoblastic leukemia: implications for mechanisms of therapy failure. *British Journal of Haematology*. 131:447-456.

Belton, R.J., L. Chen, F.S. Mesquita, and R.A. Nowak. 2008. Basigin-2 Is a Cell Surface Receptor for Soluble Basigin Ligand. *Journal of Biological Chemistry*. 283:17805-17814.

Benton, C.R., Y. Yoshida, J. Lally, X.-X. Han, H. Hatta, and A. Bonen. 2008. PGC-1α increases skeletal muscle lactate uptake by increasing the expression of MCT1 but not MCT2 or MCT4. *Physiological Genomics*. 35:45-54.

Berditchevski, F., S. Chang, J. Bodorova, and M.E. Hemler. 1997. Generation of Monoclonal Antibodies to Integrin-associated Proteins: Evidence that α3β1 complexes with EMMPRIN/BASIGIN/OX47/M6. *Journal of Biological Chemistry*. 272:29174-29180.

Besse, F., S. Mertel, R.J. Kittel, C. Wichmann, T.M. Rasse, S.J. Sigrist, and A. Ephrussi. 2007. The Ig cell adhesion molecule Basigin controls compartmentalization and vesicle release at *Drosophila melanogaster* synapses. *Journal of Cell Biology*. 177:843-855.

Biswas, C. 1984. Collagenase Stimulation in Cocultures of Human Fibroblasts and Human Tumor Cells. *Cancer Letters*. 24:201-207.

Biswas, C., and M.A. Nugent. 1987. Membrane Association of Collagenase Stimulatory Factor(s) From B-16 Melanoma Cells. *Journal of Cellular Biochemistry*. 35:247-258.

Biswas, C., Y. Zhang, R. DeCastro, H. Guo, T. Nakamura, H. Kataoka, and K. Nabeshima. 1995. The Human Tumor Cell-derived Collagenase Stimulatory Factor (Renamed EMMPRIN) Is a Member of the Immunoglobulin Superfamily. *Cancer Research*. 55:434-439.

Bodart, J.-F.L. 2010. Extracellular-Regulated Kinase-Mitogen-Activated Protein Kinase cascade: Unsolved Issues. *Journal of Cellular Biochemistry*. 109:850-857.

Botta, G.P., M.J. Reginato, M. Reichert, A.K. Rustgi, and P.I. Lelkes. 2011. Constitutive K-Ras^{G12D} Activation of ERK2 Specifically Regulates 3D Invasion of Human Pancreatic Cancer Cells via MMP-1. *Molecular Cancer Research*. 10:183-196.

Bougatef, F., S. Menashi, F. Khayati, B. Naimi, R. Porcher, M.-P. Podgorniak, G. Millot, A. Janin, F. Calvo, C. Lebbe, and S. Mourah. 2010. EMMPRIN Promotes Melanoma Cells Malignant Properties through a HIF-2alpha Mediated Up-regulation of VEGF-Receptor-2. *PLoS One*. 5:e12265.

Bougatef, F., C. Quemener, S. Kellouche, B. Naimi, M.-P. Podgorniak, G. Millot, E.E. Gabison, F. Calvo, C. Dosquet, C. Lebbe, S. Menashi, and S. Mourah. 2009. EMMPRIN promotes angiogenesis through hypoxia-inducible factor-2α-mediated regulation of soluble VEGF isoforms and their receptor VEGFR-2. *Blood*. 114:5547-5556.

Bourguignon, L.Y.W., E. Gilad, A. Brightman, F. Diedrich, and P. Singleton. 2006. Hyaluronan-CD44 Interaction with Leukemia-associated RhoGEF and Epidermal Growth Factor Receptor Promotes Rho/Ras Co-activation, Phospholipase Cε-Ca^{2+} Signaling, and Cytoskeleton Modification in Head and Neck Squamous Cell Carcinoma Cells. *Journal of Biological Chemistry*. 281:14026-14040.

Bourguignon, L.Y.W., E. Gilad, K. Rothman, and K. Peyrollier. 2005. Hyaluronan-CD44 Interaction with IQGAP1 Promotes Cdc42 and ERK Signaling, Leading to Actin Binding, Elk-

1/Estrogen Receptor Transcriptional Activation, and Ovarian Cancer Progression. *Journal of Biological Chemistry*. 280:11961-11972.

Braundmeier, A.G., A.T. Fazleabas, B.A. Lessey, H. Guo, B.P. Toole, and R.A. Nowak. 2006. Extracellular Matrix Metalloproteinase Inducer Regulates Metalloproteinases in Human Uterine Endometrium. *Journal of Clinical Endocrinology & Metabolism*. 91:2358-2365.

Brodersen, P., and O. Voinnet. 2009. Revisiting the principles of microRNA target recognition and mode of action. *Nature Reviews Molecular Cell Biology*. 10:141-148.

Brown, R.L., L.M. Reinke, M.S. Damerow, D. Perez, L.A. Chodosh, J. Yang, and C. Cheng. 2011. CD44 splice isoform switching in human and mouse epithelium is essential for epithelial-mesenchymal transition and breast cancer progression. *Journal of Clinical Investigation*. 121:1064-1074.

Buergy, D., T. Fuchs, P. Kambakamba, G. Mudduluru, G. Maurer, S. Post, Y. Tang, M.T. Nakada, L. Yan, and H. Allgayer. 2009. Prognostic impact of extracellular matrix metalloprotease inducer: immunohistochemical analyses of colorectal tumors and immunocytochemical screening of disseminated tumor cells in bone marrow from patients with gastrointestinal cancer. *Cancer*. 115:4667-4678.

Busco, G., R.A. Cardone, M.R. Greco, A. Bellizzi, M. Colella, E. Antelmi, M.T. Mancini, M.E. Dell'Aquila, V. Casavola, A. Paradiso, and S.J. Reshkin. 2010. NHE1 promotes invadopodial ECM proteolysis through acidification of the peri-invadopodial space. *FASEB Journal* 24:3903-3915.

Caldieri, G., G. Giacchetti, G. Beznoussenko, F. Attanasio, I. Ayala, and R. Buccione. 2009. Invadopodia biogenesis is regulated by caveolin-mediated modulation of membrane cholesterol levels. *Journal of Cellular and Molecular Medicine*. 13:1728-1740.

Camenisch, T.D., J.A. Schroeder, J. Bradley, S.E. Klewer, and J.A. McDonald. 2002. Heart-valve mesenchyme formation is dependent on hyaluronan-augmented activation of ErbB2-ErbB3 receptors. *Nature Medicine*. 8:850-855.

Camenisch, T.D., A.P. Spicer, T. Brehm-Gibson, J. Biesterfeldt, M.L. Augustine, J. Anthony Calabro, S. Kubalak, S.E. Klewer, and J.A. McDonald. 2000. Disruption of hyaluronan synthase-2 abrogates normal cardiac morphogenesis and hyaluronan-mediated transformation of epithelium to mesenchyme. *Journal of Clinical Investigation*. 106:349-360.

Campbell, P.M., and C.J. Der. 2004. Oncogenic Ras and its role in tumor cell invasion and metastasis. *Seminars in Cancer Biology*. 14:105-114.

Cao, X.-X., J.-D. Xu, J.-W. Xu, X.-L. Liu, Y.-Y. Cheng, W.-J. Wang, Q.-Q. Li, Q. Chen, Z.-D. Xu, and X.-P. Liu. 2010. RACK1 promotes breast carcinoma proliferation and invasion/metastasis in vitro and in vivo. *Breast Cancer Research and Treatment*. 123:375-386.

Castorino, J.J., S. Deborde, A. Deora, R. Schreiner, S.M. Gallagher-Colombo, E. Rodriguez-Boulan, and N.J. Philp. 2011. Basolateral Sorting Signals Regulating Tissue-Specific Polarity of Heteromeric Monocarboxylate Transporters in Epithelia. *Traffic*. 12:483-498.

Caudroy, S., M. Polette, J.-M. Tournier, H. Burlet, B.P. Toole, S. Zucker, and P. Birembaut. 1999. Expression of the Extracellular Matrix Metalloproteinase Inducer (EMMPRIN) and the Matrix Metalloproteinase-2 in Bronchopulmonary and Breast Lesions. *Journal of Histochemistry & Cytochemistry*. 47:1575-1580.

Chaffer, C.L., and R.A. Weinberg. 2011. A Perspective on Cancer Cell Metastasis. *Science*. 331:1559-1564.

Chen, L., R.J. Belton, and R.A. Nowak. 2009. Basigin-Mediated Gene Expression Changes in Mouse Uterine Stromal Cells During Implantation. *Endocrinology*. 150:966-976.

Chen, L., J. Bi, M. Nakai, D. Bunick, J.F. Couse, K.S. Korach, and R.A. Nowak. 2010. Expression of basigin in reproductive tissues of estrogen receptor-α or -β null mice. *Reproduction*. 139:1057-1066.

Chen, L., W. Zhang, N. Fregien, and M. Pierce. 1998. The *her*-2/*neu* oncogene stimulates the transcription of N-acetylglucosaminyltransferase V and expression of its cell surface oligosaccharide products. *Oncogene*. 17:2087-2093.

Chen, S., K. Kadomatsu, M. Kondo, Y. Toyama, K. Toshimori, S. Ueno, Y. Miyake, and T. Muramatsu. 2004. Effects of flanking genes on the phenotypes of mice deficient in basigin/CD147. *Biochemical and Biophysical Research Communications*. 324:147-153.

Chen, W.T., J.M. Chen, S.J. Parsons, and J.T. Parsons. 1985. Local degradation of fibronectin at sites of expression of the transforming gene product of pp60src. *Nature Reviews Molecular Cell Biology*. 316:156-158.

Chen, X., J. Lin, T. Kanekura, J. Su, W. Lin, H. Xie, Y. Wu, J. Li, M. Chen, and J. Chang. 2006a. A Small Interfering CD147-Targeting RNA Inhibited the Proliferation, Invasiveness, and Metastatic Activity of Malignant Melanoma. *Cancer Research*. 66:11323-11330.

Chen, Z.-N., L. Mi, J. Xu, F. Song, Q. Zang, Z. Zhang, J.-L. Xing, H.-J. Bian, J.-L. Jiang, X.-H. Wang, P. Shang, A.-R. Qian, S.-H. Zhang, L. Li, Y. Li, Q. Feng, X.-L. Yu, Y. Feng, X.-M. Yang, R. Tian, Z.-B. Wu, N. Leng, T.-S. Mo, A.-R. Kuang, T.-Z. Tan, Y.-C. Li, D.-R. Liang, W.-S. Lu, J. Miao, G.-H. Xu, Z.-H. Zhang, K.-J. Nan, J. Han, Q.-G. Liu, H.-X. Zhang, and P. Zhu. 2006b. Targeting radioimmunotherapy of hepatocellular carcinoma with iodine (^{131}I) Metuximab injection: Clinical Phase I/II Trials. *International Journal of Radiation Oncology Biology and Physics*. 65:435-444.

Cheng, C., M.B. Yaffe, and P.A. Sharp. 2006. A positive feedback loop couples Ras activation and CD44 alternative splicing. *Genes & Development*. 20:1715-1720.

Cheng, Y., X. Li, J. Kamholz, and F.R. Burns. 1994. Organization of the mouse GP42/Basigin gene: a member of the Ig superfamily. *Biochimica et Biophysica Acta*. 1217:307-311.

Chiampanichayakul, S., P. Peng-in, P. Khunkaewla, H. Stockinger, and W. Kasinrerk. 2006. CD147 contains different bioactive epitopes involving the regulation of cell adhesion and lymphocyte activation. *Immunobiology*. 211:167-178.

Chu, T., X. Chen, J. Yu, and Z. Fu. 2011. Extracellular matrix metalloproteinase inducer is a negative prognostic factor of pediatric medulloblastoma. *Pathology Oncology Research*. 17:705-711.

Clark, E.S., A.S. Whigham, W.G. Yarbrough, and A.M. Weaver. 2007. Cortactin is an Essential Regulator of Matrix Metalloproteinase Secretion and Extracellular Matrix Degradation in Invadopodia. *Cancer Research*. 67:4227-4235.

Cui, H.-Y., T. Guo, S.-J. Wang, P. Zhao, Z.-S. Dong, Y. Zhang, J.-L. Jiang, Z.-N. Chen, and X.-L. Yu. 2012. Dimerization is essential for HAb18G/CD147 promoting tumor invasion via MAPK pathway. *Biochemical and Biophysical Research Communications*:in press.

Curtin, K.D., I.A. Meinertzhagen, and R.J. Wyman. 2005. Basigin (EMMPRIN/CD147) interacts with integrin to affect cellular architecture. *Journal of Cell Science*. 118:2649-2660.

Curtin, K.D., R.J. Wyman, and I.A. Meinertzhagen. 2007. Basigin/EMMPRIN/CD147 Mediates Neuron-Glia Interactions in the Optic Lamina of Drosophila. *Glia*. 55:1542-1553.

Dai, J.-y., K.-f. Dou, C.-h. Wang, P. Zhao, W.B. Lau, L. Tao, Y.-m. Wu, J. Tang, J.-l. Jiang, and Z.-n. Chen. 2009. The interaction of HAb18G/CD147 with integrin $\alpha_6\beta_1$ and its implications for the invasion potential of human hepatoma cells. *BMC Cancer*. 9:337.

Dai, L., Z. Qin, M. Defee, B.P. Toole, K.L. Kirkwood, and C. Parsons. 2012. Kaposi sarcoma-associated herpesvirus (KSHV) induces a functional tumor-associated phenotype for oral fibroblasts. *Cancer Letters*. 318:214-220.

Dalberg, K., E. Eriksson, U. Enberg, M. Kjellman, and M. Backdahl. 2000. Gelatinase A, Membrane Type 1 Matrix Metalloproteinase, and Extracellular Matrix Metalloproteinase Inducer mRNA Expression: Correlation with Invasive Growth of Breast Cancer. *World Journal of Surgery*. 24:334-340.

Daniele, L.L., B. Sauer, S.M. Gallagher, J. Edward N. Pugh, and N.J. Philp. 2008. Altered visual function in monocarboxylate transporter 3 (*Slc16a8*) knockout mice. *American Journal of Physiology Cell Physiology*. 295:C451-457.

Dave, B., V. Mittal, N.M. Tan, and J.C. Chang. 2012. Epithelial-mesenchymal transition, cancer stem cells and treatment resistance. *Breast Cancer Research*. 14:202.

Davidson, B., I. Goldberg, A. Berner, G.B. Kristensen, and R. Reich. 2003a. EMMPRIN (extracellular matrix metalloproteinase inducer) is a novel marker of poor outcome in serous ovarian carcinoma. *Clinical and Experimental Metastasis*. 20:161-169.

Davidson, B., I. Goldberg, W.H. Gotlieb, J. Kopolovic, G. Ben-Baruch, and R. Reich. 2003b. PEA3 Is the Second Ets Family Transcription Factor Involved in Tumor Progression in Ovarian Carcinoma. *Clinical Cancer Research*. 9:1412-1419.

Davidson, B., S. Konstantinovsky, S. Nielsen, H.P. Dong, A. Berner, M. Vyberg, and R. Reich. 2004. Altered Expression of Metastasis-Associated and Regulatory Molecules in Effusions from Breast Cancer Patients: A Novel Model for Tumor Progression. *Clinical Cancer Research*. 10:7335-7346.

Dean, N.R., J.A. Knowles, E.E. Helman, J.C. Aldridge, W.R. Carroll, J.S. Magnuson, L. Clemons, B. Ziober, and E.L. Rosenthal. 2010. Anti-EMMPRIN antibody treatment of head and neck squamous cell carcinoma in an ex-vivo model. *Anti-Cancer Drugs*. 21:861-867.

Dean, N.R., J.R. Newman, E.E. Helman, W. Zhang, S. Safavy, D.M. Weeks, M. Cunningham, L.A. Snyder, Y. Tang, L. Yan, L.R. McNally, D.J. Buchsbaum, and E.L. Rosenthal. 2009. Anti-EMMPRIN Monoclonal Antibody as a Novel Agent for Therapy of Head and Neck Cancer. *Clinical Cancer Research*. 15:4058-4065.

Deaton, A.M., and A. Bird. 2011. CpG islands and the regulation of transcription. *Genes & Development*. 25:1010-1022.

Deborde, S., E. Perret, D. Gravotta, A. Deora, S. Salvarezza, R. Schreiner, and E. Rodriguez-Boulan. 2008. Clathrin is a key regulator of basolateral polarity. *Nature*. 452.

Deeg, H.J., B.R. Blazar, B.J. Bolwell, G.D. Long, F. Schuening, J. Cunningham, R.M. Rifkin, S. Havrilla, G. Schwab, and H.E. Heslop. 2001. Treatment of steroid-refractory acute graft-versus-host disease with anti-CD147 monoclonal antibody ABX-CBL. *Blood*. 98:2052-2058.

Deora, A.A., D. Gravotta, G. Kreitzer, J. Hu, D. Bok, and E. Rodriguez-Boulan. 2004. The Basolateral Targeting Signal of CD147 (EMMPRIN) Cosists of a Single Leucine and Is Not Recognized by Retinal Pigment Epithelium. *Molecular Biology of the Cell*. 15:4148-4165.

Deora, A.A., N. Philp, J. Hu, D. Bok, and E. Rodriguez-Boulan. 2005. Mechanisms regulating tissue-specific polarity of monocarboxylate transporters and their chaperone CD147 in kidney and retinal epithelia. *PNAS*. 102:16245-16250.

DesMarais, V., H. Yamaguchi, M. Oser, L. Soon, G. Mouneimne, C. Sarmiento, R. Eddy, and J. Condeelis. 2009. N-WASP and Cortactin Are Involved In Invadopodium-Dependent Chemotaxis to EGF In Breast Tumor Cells. *Cell Motility and the Cytoskeleton*. 66:303-316.

Eccles, S.A. 2011. The epidermal growth factor receptor/Erb-B/HER family in normal and malignant breast biology. *International Journal of Developmental Biology*. 55:685-696.

Eckert, L.B., G.A. Repasky, A.S. Ulku, A. McFall, H. Zhou, C.I. Sartor, and C.J. Der. 2004. Involvement of Ras Activation in Human Breast Cancer Cell Signaling, Invasion, and Anoikis. *Cancer Research*. 64:4585-4592.

Eckert, M.A., T.M. Lwin, A.T. Chang, J. Kim, E. Danis, L. Ohno-Machado, and J. Yang. 2011. Twist1-Induced Invadopodia Formation Promotes Tumor Metastasis. *Cancer Cell*. 19:372-386.

Eckert, M.A., and J. Yang. 2011. Targeting invadopodia to block breast cancer metastasis. *Oncotarget*. 2:562-568.

Edward, M., J.A. Quinn, and W. Sands. 2011. Keratinocytes stimulate fibroblast hyaluronan synthesis through the release of stratifin: a possible role in the suppression of scar tissue formation. *Wound Repair Regeneration*. 19:379-386.

Egawa, N., N. Koshikawa, T. Tomari, K. Nabeshima, T. Isobe, and M. Seiki. 2006. Membrane Type 1 Matrix Metalloproteinase (MT1-MMP/MMP-14) Cleaves and Releases a 22-kDa Extracellular Matrix Metalloproteinase Inducer (EMMPRIN) Fragment from Tumor Cells. *Journal of Biological Chemistry*. 281:37576-37585.

Ellis, S.M., K. Nabeshima, and C. Biswas. 1989. Monoclonal Antibody Preparation and Purification of a Tumor Cell Collagenase-stimulatory Factor. *Cancer Research*. 49:3385-3391.

Eyster, C.A., N.B. Cole, S. Petersen, K. Viswanathan, K. Fruh, and J.G. Donaldson. 2011. MARCH ubiquitin ligases alter the itinerary of clathrin-independent cargo from recycling to degradation. *Molecular Biology of the Cell*. 22:3218-3230.

Eyster, C.A., J.D. Higginson, R. Huebner, N. Porat-Shliom, R. Weigert, W.W. Wu, R.-F. Shen, and J.G. Donaldson. 2009. Discovery of New Cargo Proteins that Enter Cells through Clathrin-Independent Endocytosis. *Traffic*. 10:590-599.

Fadool, J.M., and P.J. Linser. 1993. 5A11 Antigen Is a Cell Recognition Molecule Which Is Involved in Neuronal-Glial Interactions in Avian Neural Retina. *Developmental Dynamics*. 196:252-262.

Fadool, J.M., and P.J. Linser. 1996. Evidence of the Formation of Multimeric Forms of 5A11/HT7 Antigen. *Biochemical and Biophysical Research Communications*. 229:280-286.

Faix, J., D. Breitsprecher, T.E.B. Stradal, and K. Rottner. 2009. Filopodia: Complex models for simple rods. *International Journal of Biochemistry and Cell Biology*. 41:1656-1664.

Fan, Y., S. Meng, Y. Wang, J. Cao, and C. Wang. 2011a. Visfatin/PBEF/Nampt induces EMMPRIN and MMP-9 production in macrophages via the NAMPT-MAPK (p38, ERK 1/2)-NF-kB signaling pathway. *International Journal of Molecular Medicine*. 27:607-615.

Fan, Y., J. Wang, L. Wei, B. He, C. Wang, and B. Wang. 2011b. Iron deficiency activates pro-inflammatory signaling in macrophages and foam cells via the p38 MAPK-NF-κβ pathway. *International Journal of Cardiology*. 152:49-55.

Fanelli, A., E.F. Grollman, D. Wang, and N.J. Philp. 2003. MCT1 and its accessory protein CD147 are differentially regulated by TSH in rat thyroid cells. *American Journal of Physiology Endocrinology and Metabolism*. 285:E1223-E1229.

Fillmore, C.M., and C. Kuperwasser. 2008. Human breast cancer cell lines contain stem-like cells that self-renew, give rise to phenotypically diverse progeny and survive chemotherapy. *Breast Cancer Research*. 10:R25.

Finch, N.A., P.J. Linser, and J.D. Ochrietor. 2009. Hydrophobic Interactions Stabilize the Basigin-MCT1 Complex. *Protein Journal*. 28:362-368.

Finnemann, S.C., A.D. Marmorstein, J.M. Neill, and E. Rodriguez-Boulan. 1997. Identification of the Retinal Pigment Epithelium Protein RET-PE2 as CE-9/OX-47, a member of the Immunoglobulin Superfamily. *Investigative Ophthalmology and Visual Science*. 38:2366-2374.

Fitzgerald, K.A., A.G. Bowie, B.S. Skeffington, and L.A.J. O'Neill. 2000. Ras, Protein Kinase Cζ, and IkB Kinases 1 and 2 Are Downstream Effectors of CD44 During the Activation of NF-kB by

Hyaluronic Acid Fragments in T-24 Carcinoma Cells. *Journal of Immunology*. 164:2053-2063.

Floch, R.L., J. Chiche, I. Marchiq, T. Naiken, K. Ilk, C.M. Murray, S.E. Critchlow, D. Roux, M.-P. Simon, and J. Pouyssegur. 2011. CD147 subunit of lactate/H^+ symporters MCT1 and hypoxia-inducible MCT4 is critical for energetics and growth of glycolytic tumors. *PNAS*. 108:16663-16668.

Fossum, S., S. Mallett, and A.N. Barclay. 1991. The MRC OX-47 antigen is a member of the immunoglobulin superfamily with an unusual transmembrane sequence. *European Journal of Immunology*. 21:671-679.

Foulkes, W.D., I.E. Smith, and J.S. Reis-Filho. 2010. Triple-Negative Breast Cancer. *NEJM*. 363:1938-1948.

Friedl, P., and K. Wolf. 2009. Plasticity of cell migration: a multiscale tuning model. *Journal of Cell Biology*. 188:11-19.

Frittoli, E., A. Palamidessi, A. Disanza, and G. Scita. 2011. Secretory and endo/exocytic trafficking in invadopodia formation: The MT1-MMP paradigm. *European Journal of Cell Biology*. 90:108-114.

Fu, T.-Y., C.-C. Chang, C.-T. Lin, C.-H. Lai, S.-Y. Peng, Y.-J. Ko, and P.-C. Tang. 2011a. Let-7b-mediated suppression of basigin expression and metastasis in mouse melanoma cells. *Experimental Cell Research*. 317:445-451.

Fu, T.-Y., C.-T. Lin, and P.-C. Tang. 2011b. Steroid Hormone-regulated *let-7b* Mediates Cell Proliferation and Basigin Expression in the Mouse Endometrium. *Journal of Reproduction and Development*. 57:627-635.

Gabison, E.E., E. Huet, C. Baudouin, and S. Menashi. 2009. Direct epithelial-stromal interaction in corneal wound healing: Role of EMMPRIN/CD147 in MMPs induction and beyond. *Progress in Retinal and Eye Research*. 28:19-33.

Gallagher, S.M., J.J. Castorino, D. Wang, and N.J. Philp. 2007. Monocarboxylate Transporter 4 Regulates Maturation and Trafficking of CD147 to the Plasma Membrane in the Metastatic Breast Cancer Cell Line MDA-MB-231. *Cancer Research*. 67:4182-4189.

Garraway, L.A., and P.A. Janne. 2012. Circumventing Cancer Drug Resistance in the Era of Personalized Medicine. *Cancer Discovery*. 2:214-226.

Ge, H., J.-f. Zhang, B.-s. Guo, Q. He, B.-y. Wang, B. He, and C.-q. Wang. 2007. Resveratrol inhibits macrophage expression of EMMPRIN by activating PPARγ. *Vascular Pharmacology*. 46:114-121.

Gerke, V., C.E. Creutz, and S.E. Moss. 2005. Annexins: Linking Ca^{2+} Signaling to Membrane Dynamics. *Nature Reviews Molecular Cell Biology*. 6:449-461.

Ghatak, S., S. Misra, and B.P. Toole. 2002. Hyaluronan oligosaccharides inhibit anchorage-independent growth of tumor cells by suppressing the phosphoinositide 3-kinase/Akt cell survival pathway. *Journal of Biological Chemistry*. 277:38013-38020.

Ghatak, S., S. Misra, and B.P. Toole. 2005. Hyaluronan Constitutively Regulates ErbB2 Phosphorylation and Signaling Complex Formation in Carcinoma Cells. *Journal of Biological Chemistry*. 280:8875-8883.

Gligorijevic, B., J. Wyckoff, H. Yamaguchi, Y. Wang, E.T. Roussos, and J. Condeelis. 2012. N-WASP-mediated invadopodium formation is involved in intravasation and lung metastasis of mammary tumors. *Journal of Cell Science*. 125:724-734.

Gordon, L.B., I.A. Harten, J. Anthony Calabro, G. Sugumaran, A.B. Coska, W.T. Brown, V. Hascall, and B.P. Toole. 2003. Hyaluronan is not elevated in urine or serum in Hutchinson-Gilford Progeria Syndrome. *Human Genetics*. 113:178-187.

Gou, X., Q. Ru, H. Zhang, Y. Chen, L. Li, H. Yang, J. Xing, and Z. Chen. 2009. HAb18G/CD147 inhibits starvation-induced autophagy in human hepatoma cell SMMC7721 with an involvement of Beclin 1 down-regulation. *Cancer Science*. 100:837-843.

Grass, G.D., M. Bratoeva, and B.P. Toole. 2012. Regulation of invadopodia formation and activity by CD147. *Journal of Cell Science*. 125:777-788.

Guo, H., R. Li, S. Zucker, and B.P. Toole. 2000. EMMPRIN (CD147), an Inducer of Matrix Metalloproteinase Synthesis, Also Binds Interstitial Collagenase to the Tumor Cell Surface. *Cancer Research*. 60:888-891.

Guo, H., G. Majmudar, T.C. Jensen, C. Biswas, B.P. Toole, and M.K. Gordon. 1998. Characterization of the gene for human EMMPRIN, a tumor cell surface inducer of matrix metalloproteinases. *Gene*. 220:99-108.

Guo, H., S. Zucker, M.K. Gordon, B.P. Toole, and C. Biswas. 1997. Stimulation of Matrix Metalloproteinase Production by Recombinant Extracellular Matrix Metalloproteinase Inducer from Transfected Chinese Hamster Ovary Cells. *Journal of Biological Chemistry*. 272:24-27.

Hagemann, T., J. Wilson, H. Kulbe, N.F. Li, D.L. Leinster, K. Charles, F. Klemm, T. Pukrop, C. Binder, and F.R. Balkwill. 2005. Macrophages Induce Invasiveness of Epithelial Cancer Cells Via NF-kB and JNK. *Journal of Immunology*. 175:1197-1205.

Halestrap, A.P. 2011a. The Monocarboxylate Transporter Family--Structure and Functional Characterization. *IUBMB Life*. 64:1-9.

Halestrap, A.P. 2011b. The Monocarboxylate Transporter Family-Structure and Functional Characterization. *IUBMB Life*. 64:1-9.

Hamilton, S.R., S.F. Fard, F.F. Paiwand, C. Tolg, M. Veiseh, C. Wang, J.B. McCarthy, M.J. Bissell, J. Koropatnick, and E.A. Turley. 2007. The Hyaluronan Receptors CD44 and Rhamm (CD168) Form Complexes with ERK1,2 That Sustain High Basal Motility in Breast Cancer Cells. *Journal of Biological Chemistry*. 282:16667-16680.

Han, Z.-d., X.-c. Bi, W.-j. Qin, H.-c. He, Q.-s. Dai, J. Zou, Y.-k. Ye, Y.-x. Liang, G.-h. Zeng, Z.-n. Chen, and W.-d. Zhong. 2009. CD147 Expression Indicates Unfavourable Prognosis in Prostate Cancer. *Pathology Oncology Research*. 15:369-374.

Hanna, S.M., P. Kirk, O.J. Holt, M.J. Puklavec, M.H. Brown, and A.N. Barclay. 2003. A novel form of the membrane protein CD147 that contains an extra Ig-like domain and interacts homophilically. *BMC Biochemistry*. 4.

Hashimoto, T., R. Hussien, and G.A. Brooks. 2006. Colocalization of MCT1, CD147, and LDH in mitochondrial inner membrane of L6 muscle cells: evidence of a mitochondrial lactate oxidation complex. *American Journal of Physiology Endocrinology and Metabolism*. 290:E1237-E1244.

Heller, M., M.v.d. Ohe, R. Kleene, M.H. Mohajeri, and M. Schachner. 2003. The immunoglobulin-superfamily molecule basigin is a binding protein for oligomannosidic carbohydrates: an anti-idiotypic approach. *Journal of Neurochemistry*. 84:557-565.

Hori, K., N. Katayama, S. Kachi, M. Kondo, K. Kadomatsu, J. Usukura, T. Muramatsu, S. Mori, and Y. Miyake. 2000. Retinal Dysfunction in Basigin Deficiency. *Investigative Ophthalmology and Visual Science*. 41:3128-3133.

Howard, J., N.A. Finch, and J.D. Ochrietor. 2010. Characterization of Monocarboxylate Transporter 1 (MCT1) Binding affinity for Basigin Gene Products and L1cam. *Cellular and Molecular Neurobiology*. 30:671-674.

Hsu, J.-M., C.-T. Chen, C.-K. Chou, H.-P. Kuo, L.-Y. Li, C.-Y. Lin, H.-J. Lee, Y.-N. Wang, M. Liu, H.-W. Liao, B. Shi, C.-C. Lai, M.T. Bedford, C.-H. Tsai, and M.-C. Hung. 2011. Crosstalk between

Arg 1175 methylation and Tyr 1173 phosphorylation negatively regulates EGFR-mediated ERK activation. *Nature Cell Biology*. 13:174-182.

Hu, J., A. Mukhopadhyay, P. Truesdell, H. Chandler, U.K. Mukhopadhyay, A.S. Mak, and A.W.B. Craig. 2011. Cdc42-interacting protein 4 is a Src substrate that regulates invadopodia and invasiveness of breast tumors by promoting MT1-MMP endocytosis. *Journal of Cell Science*. 124:1739-1751.

Hubbard, A.L., J.R. Bartles, and L.T. Braiterman. 1985. Identification of Rat Hepatocyte Plasma Membrane Proteins Using Monoclonal Antibodies. *Journal of Cell Biology*. 100:1115-1125.

Huber, O., R. Kemler, and D. Langosch. 1999. Mutations affecting transmembrane segment interactions impair adhesiveness of E-cadherin. *Journal of Cell Science*. 112:4415-4423.

Humphrey, M.B., L.L. Lanier, and M.C. Nakamura. 2005. Role of ITAM-containing adapter proteins and their receptors in the immune system and bone. *Immunological Reviews*. 208:50-65.

Hussien, R., and G.A. Brooks. 2011. Mitochondrial and plasma membrane lactate transporter and lactate dehydrogenase isoform expression in breast cancer cell lines. *Physiological Genomics*. 43:255-264.

Igakura, T., K. Kadomatsu, T. Kaname, H. Muramatsu, Q.-W. Fan, T. Miyauchi, Y. Toyama, N. Kuno, S. Yuasa, M. Takahashi, T. Senda, O. Taguchi, K.-i. Yamamura, K. Arimura, and T. Muramatsu. 1998. A Null Mutation in Basigin, an Immunoglobulin Superfamily Member, Indicates Its Important Roles in Peri-implantation Development and Spermatogenesis. *Developmental Biology*. 194:152-165.

Igakura, T., K. Kadomatsu, O. Taguchi, H. Muramatsu, T. Kaname, T. Miyauchi, K.-i. Yamamura, K. Arimura, and T. Muramatsu. 1996. Roles of Basigin, a Member of the Immunoglobulin Superfamily, in Behavior as to an Irritating Odor, Lymphocyte Response, and Blood-Brain Barrier. *Biochemical and Biophysical Research Communications*. 224:33-36.

Irwin, M.E., K.L. Mueller, N. Bohin, Y. Ge, and J.L. Boerner. 2010. Lipid Raft Localization of EGFR Alters the Response of Cancer Cells to the EGFR Tyrosine Kinase Inhibitor Gefitinib. *Journal of Cellular Physiology*. 226:2316-2328.

Jia, L., J. Cao, W. Wei, S. Wang, Y. Zuo, and J. Zhang. 2007. CD147 depletion down-regulates matrix metalloproteinase-11, vascular endothelial growth factor-A expression and the lymphatic metastasis potential of murine hepatocarcinoma Hca-F cells. *International Journal of Biochemistry and Cell Biology*. 39:2135-2142.

Jia, L., S. Wang, H. Zhou, J. Cao, Y. Hu, and J. Zhang. 2006. Caveolin-1 up-regulates CD147 glycosylation and the invasive capability of murine hepatocarcinoma cell lines. *International Journal of Biochemistry and Cell Biology*. 38:1584-1593.

Jian-Li, J., and T. Juan. 2007. CD147 and its interacting proteins in cellular functions. *Acta Physiologica Sinica*. 59:517-523.

Jiang, J.L., Q. Zhou, M.K. Yu, L.S. Ho, Z.N. Chen, and H.C. Chan. 2001. The Involvement of HAb18G/CD147 in Regulation of Store-operated Calcium Entry and Metastasis of Human Hepatoma Cells. *Journal of Biological Chemistry*. 276:46870-46877.

Jin, J.-S., D.-S. Hsieh, Y.-F. Lin, J.-Y. Wang, L.-F. Sheu, and W.-H. Lee. 2006. Increasing expression of extracellular matrix metalloprotease inducer in renal cell carcinoma: Tissue microarray analysis of immunostaining score with clinicopathological parameters. *International Journal of Urology*. 13:573-580.

Ju, X.-Z., J.-M. Yang, X.-Y. Zhou, Z.-T. Li, and X.-H. Wu. 2008. EMMPRIN Expression as a Prognostic Factor in Radiotherapy of Cervical Cancer. *Clinical Cancer Research*. 14:494-501.

Juin, A., C. Billottet, V. Moreau, O. Destaing, C. Albiges-Rizo, J. Rosenbaum, E. Genot, and F. Saltel. 2012. Physiological type I collagen organization induces the formation of a novel class of linear invadosomes. *Molecular Biology of the Cell*. 23:297-309.

Kalluri, R., and R.A. Weinberg. 2009. The basics of epithelial-mesenchymal transition. *Journal of Clinical Investigation*. 119:1420-1428.

Kamada, Y., Y. Arita, S.-i. Ogata, H. Muramatsu, and T. Muramatsu. 1987. Receptors for fucose-binding proteins of *Lotus tetragonolobus* isolated from mouse embryonal carcinoma cells: Structural characteristics of the poly(N-acetyllactosamine)-type glycan. *European Journal of Biochemistry*. 163:497-502.

Kaname, T., T. Miyauchi, A. Kuwano, Y. Matsuda, T. Muramatsu, and T. Kajiii. 1993. Mapping basigin (BSG), a member of the immunoglobulin superfamily, to 19p13.3. *Cytogenetic Cell Genetics*. 64:195-197.

Kanekura, T., T. Miyauchi, M. Tashiro, and T. Muramatsu. 1991. Basigin, a New Member of the Immunoglobulin Superfamily: Genes in Different Mammalian Species, Glycosylation Changes in the Molecule from Adult Organs and Possible Variation in the N-terminal Sequences. *Cell Structure and Function*. 16:23-30.

Karnoub, A.E., and R.A. Weinberg. 2008. Ras oncogenes: split personalities. *Nature Reviews Molecular Cell Biology*. 9:517-531.

Kasinrerk, W., E. Fiebiger, I. Stefanova, T. Baumruker, W. Knapp, and H. Stockinger. 1992. Human Leukocyte Activation Antigen M6, A Member of the Ig Superfamily, is the Species Homologue of Rat OX-47, Mouse Basigin, and Chicken HT7 Molecule. *Journal of Immunology*. 149:847-854.

Kataoka, H., R. DeCastro, S. Zucker, and C. Biswas. 1993. Tumor Cell-derived Collagenase-Stimulatory Factor Increases Expression of Interstitial Collagenase, Stromelysin, and 72-kDa Gelatinase. *Cancer Research*. 53.

Kato, N., T. Kosugi, W. Sato, T. Ishimoto, H. Kojima, Y. Sato, K. Sakamoto, S. Maruyama, Y. Yuzawa, S. Matsuo, and K. Kadomatsu. 2011. Basigin/CD147 Promotes Renal Fibrosis after Unilateral Ureteral Obstruction. *American Journal of Pathology*. 178:572-579.

Kawakami, T., T. Sameshima, H. Hojo, K. Koga, Y. Nakahara, B.P. Toole, J. Suzumiya, Y. Okada, A. Iwasaki, and K. Nabeshima. 2011. Synthetic emmprin peptides with chitobiose substitution stimulate MMP-2 production by fibroblasts. *BMC Cancer*. 11:300.

Keilhack, H., T. Tenev, E. Nyakatura, J. Godovac-Zimmermann, L. Nielsen, K. Seedorf, and F.-D. Bohmer. 1998. Phosphotyrosine 1173 Mediates Binding of the Protein-tyrosine Phosphatase SHP-1 to the Epidermal Growth Factor Receptor and Attenuation of Receptor Signaling. *Journal of Biological Chemistry*. 273:24839-24846.

Keller, S., A.-K. Konig, F. Marme, S. Runz, S. Wolterink, D. Koensgen, A. Mustea, J. Sehouli, and P. Altevogt. 2009. Systemic presence and tumor-growth promoting effects of ovarian carcinoma released exosomes. *Cancer Letters*. 278:73-81.

Kennedy, K.M., and M.W. Dewhirst. 2010. Tumor metabolism of lactate: the influence and therapeutic potential for MCT and CD147 regulation. *Future Oncology*. 6:127-148.

Kim, J.-Y., W.-J. Kim, H. Kim, K. Suk, and W.-H. Lee. 2009. The Stimulation of CD147 induces MMP-9 Expression through ERK and NF-kB in Macrophages: Implications for Atherosclerosis. *Immune Network*. 9:90-97.

Kirat, D., K. Kondo, R. Shimada, and S. Kato. 2009. Dietary pectin up-regulates monocarboxylate transporter 1 in th rat gastrointestinal tract. *Experimental Physiology*. 94:422-433.

Kirk, P., M.C. Wilson, C. Heddle, M.H. Brown, A.N. Barclay, and A.P. Halestrap. 2000. CD147 is tightly associated with lactate transporters MCT1 and MCT4 and facilitates their cell surface expression. *EMBO Journal*. 19:3896-3904.

Klein, C.A., S. Seidl, K. Petat-Dutter, S. Offner, J. Geigl, O. Schmidt-Kittler, N. Wendler, B. Passlick, R.M. Huber, G. Schlimok, P.A. Baeuerle, and G. Riethmuller. 2002. Combined transcriptome and genome analysis of single micrometastatic cells. *Nature Biotechnology*. 20:387-392.

Ko, M.H., and L. Puglielli. 2007. The Sterol Carrier Protein SCP-x/Pro-SCP-2 Gene Has Transcriptional Activity and Regulates the Alzheimer Disease γ-Secretase *Journal of Biological Chemistry*. 282:19742-19752.

Koho, N.M., A.K. Mykkanen, M. Reeben, M.R. Raekallio, M. Ilves, and A.R. Poso. 2012. Sequence variations and two levels of MCT1 and CD147 expression in red blood cells and gluteus muscle of horses. *Gene*. 491:65-70.

Kong, L.-M., C.-G. Liao, L. Chen, H.-S. Yang, S.-H. Zhang, Z. Zhang, H.-J. Bian, J.-L. Xing, and Z.-N. Chen. 2011a. Promoter hypomethylation up-regulates CD147 expression through increasing Sp1 binding and associates with poor prognosis in human hepatocellular carcinoma. *Journal of Cellular and Molecular Medicine*. 15:1415-1428.

Kong, L.-M., C.-G. Liao, F. Fei, X. Guo, J.-L. Xing, and Z.-N. Chen. 2011b. Transcription factor Sp1 regulates expression of cancer-associated molecule CD147 in human lung cancer. *Cancer Science*. 101:1463-1470.

Konig, B., S. Fischer, S. Schlotte, G. Wen, K. Eder, and G.I. Stangl. 2010. Monocarboxylate transporter 1 and CD147 are up-regulated by natural and synthetic peroxisome proliferator-activated receptor α agonists in livers of rodents and pigs. *Molecular Nutrition and Food Research*. 54:1248-1256.

Konishi, H., B. Karakas, A.M. Abukhdeir, J. Lauring, J.P. Gustin, J.P. Garay, Y. Konishi, E. Gallmeier, K.E. Bachman, and B.H. Park. 2007. Knock-in of mutant K-ras in nontumorigenic human epithelial cells as a new model for studying K-ras mediated transformation. *Cancer Research*. 67:8460-8467.

Kozma, S.C., M.E. Bogaard, K. Buser, S.M. Saurer, J.L. Bos, B. Groner, and N.E. Hynes. 1987. The human c-Kirsten *ras* gene is activated by a novel mutation in codon 13 in the breast carcinoma cell line MDA-MB-231. *Nucleic Acids Research*. 15:5963-5971.

Kuang, Y.-H., X. Chen, J. Su, L.-S. Wu, J. Li, J. Chang, Y. Qiu, Z.-S. Chen, and T. Kanekura. 2008. Proteome Analysis of Multidrug Resistance of Human Oral Squamous Carcinoma Cells Using CD147 Silencing. *Journal of Proteome Research*. 7:4784-4791.

Kuno, N., K. Kadomatsu, Q.-W. Fan, M. Hagihara, T. Senda, S. Mizutani, and T. Muramatsu. 1998. Female sterility in mice lacking the *basigin* gene, which encodes a transmembrane glycoprotein belonging to the immunoglobulin superfamily. *FEBS Letters*. 425:191-194.

Kuphal, S., H.G. Palm, I. Poser, and A.K. Bosserhoff. 2005. Snail-regulated genes in malignant melanoma. *Melanoma Research*. 15:305-313.

Lau, K.S., and J.W. Dennis. 2009. N-Glycans in cancer progression. *Glycobiology*. 18:750-760.

Lau, K.S., E.A. Partridge, A. Grigorian, C.I. Silvescu, V.N. Reinhold, M. Demetriou, and J.W. Dennis. 2007. Complex N-Glycan Number and Degree of Branching Cooperate to Regulate Cell Proliferation and Differentiation. *Cell*. 129:123-134.

Lee, J., S.K. Banu, T. Subbarao, A. Starzinski-Powitz, and J.A. Arosh. 2011. Selective inhibition of prostaglandin E2 receptors EP2 and EP4 inhibits invasion of human immortalized endometriotic epithelial and stromal cells through suppression of metalloproteinases. *Molecular and Cellular Endocrinology*. 332:306-313.

Lehmann, B.D., J.A. Bauer, X. Chen, M.E. Sanders, A.B. Chakravarthy, Y. Shyr, and J.A. Pietenpol. 2011. Identification of human triple-negative breast cancer subtypes and preclinical models for selection of targeted therapies. *Journal of Clinical Investigation*. 121:2750-2767.

Lemos, C., G. Jansen, and G.J. Peters. 2008. Drug transporters: recent advances concerning BCRP and tyrosine kinase inhibitors. *British Journal of Cancer*. 9:857-862.

Lescaille, G., S. Menashi, B. Cavelier-Balloy, F. Khayati, C. Quemener, M.P. Podgorniak, B. Naimi, C. Lebbe, and S. Mourah. 2012. EMMPRIN/CD147 up-regulates urokinase-type plasminogen activator: implications in oral tumor progression. *BMC Cancer*. 12:115.

Lesley, J., V.C. Hascall, M. Tammi, and R. Hyman. 2000. Hyaluronan Binding by Cell Surface CD44. *Journal of Biological Chemistry*. 275:26967-26975.

Li, A., J.C. Dawson, M. Forero-Vargas, H.J. Spence, X. Yu, I. Konig, K. Anderson, and L.M. Machesky. 2010. The Actin-Bundling Protein Fascin Stabilizes Actin in Invadopodia and Potentiates Protrusive Invasion. *Current Biology*. 20:339-345.

Li, Q.-Q., W.-J. Wang, J.-D. Xu, X.-X. Cao, Q. Chen, J.-M. Yang, and Z.-D. Xu. 2007a. Involvement of CD147 in regulation of multidrug resistance to P-gp substrate drugs and *in vitro* invasion in breast cancer cells. *Cancer Science*. 98:1064-1069.

Li, Q.-Q., W.-J. Wang, J.-D. Xu, X.-X. Cao, Q. Chen, J.-M. Yang, and Z.-D. Xu. 2007b. Up-regulation of CD147 and matrix metalloproteinase-2, -9 induced by P-glycoprotein substrates in multidrug resistant breast cancer cells. *Cancer Science*. 98:1767-1774.

Li, R., L. Huang, H. Guo, and B.P. Toole. 2001. Basigin (murine EMMPRIN) stimulates matrix metalloproteinase production by fibroblasts. *J Cell Physiol*. 186:371-379.

Li, Y., J. Wu, F. Song, J. Tang, S.-J. Wang, X.-L. Yu, Z.-N. Chen, and J.-L. Jiang. 2012. Extracellular Membrane-proximal Domain of HAb18G/CD147 Binds to Metal Ion-dependent Adhesion Site (MIDAS) Motif of Integrin β1 to Modulate Malignant Properties of Hepatoma Cells. *Journal of Biological Chemistry*. 287:4759-4772.

Li, Y., J. Xu, L. Chen, W.-D. Zhong, Z. Zhang, L. Mi, Y. Zhang, C.-G. Liao, H.-J. Bian, J.-L. Jiang, X.-M. Yang, X.-Y. Li, C.-M. Fan, P. Zhu, L. Fu, and Z.-N. Chen. 2009. HAb18G (CD147), a cancer-associated biomarker and its role in cancer detection. *Histopathology*. 54:677-687.

Liang, L., T. Major, and T. Bocan. 2002. Characterization of the promoter of human extracellular matrix metalloproteinase inducer (EMMPRIN). *Gene*. 282:75-86.

Liang, Q., H. Xiong, G. Gao, K. Xiong, X. Wang, Z. Zhao, H. Zhang, and Y. Li. 2005. Inhibition of Basigin Expression in Glioblastoma Cell Line via Antisense RNA Reduces Tumor Cell Invasion and Angiogenesis. *Cancer Biology & Therapy*. 4:759-762.

Liang, Y.X., H.C. He, Z.D. Han, X.C. Bi, Q.S. Dai, Y.K. Ye, W.J. Qin, G.H. Zeng, G. Zhu, C.L. Xu, and W.D. Zhong. 2009. CD147 and VEGF expression in advanced renal cell carcinoma and their prognostic value. *Cancer Investigation*. 27:788-793.

Liao, C.-G., L.-M. Kong, F. Song, J.-L. Xing, L.-X. Wang, Z.-J. Sun, H. Tang, H. Yao, Y. Zhang, L. Wang, Y. Wang, X.-M. Yang, Y. Li, and Z.-N. Chen. 2011. Characterization of Basigin Isoforms and the Inhibitory Function of Basigin-3 in Human Hepatocellular Carcinoma Proliferation and Invasion. *Molecular and Cellular Biology*. 31:2591-2604.

Lim, K.-H., and C.M. Counter. 2005. Reduction in the requirement of oncogenic Ras signaling to activation of PI3K/AKT pathway during tumor maintenance. *Cancer Cell*. 8:381-392.

Lim, M., T. Martinez, D. Jablons, R. Cameron, H. Guo, B.P. Toole, J.-d. Li, and C. Basbaum. 1998. Tumor-derived EMMPRIN (extracellular matrix metalloproteinase inducer) stimulates collagenase transcription through MAPK p38. *FEBS Letters*. 441:88-92.

Linder, S., C. Wiesner, and M. Himmel. 2011. Degrading devices: Invadosomes in Proteolytic Cell Invasion. *Annual Review of Cell and Developmental Biology*. 27:185-211.

Lintig, F.C.v., A.D. Dreilinger, N.M. Varki, A.M. Wallace, D.E. Casteel, and G.R. Boss. 2000. Ras activation in human breast cancer. *Breast Cancer Research and Treatment*. 62.

Liu, F.-T., and G. Rabinovich. 2005. Galectins as modulators of tumour progression. *Nature Reviews Cancer*. 5:29-41.

Liu, F., L. Cui, Y. Zhang, L. Chen, Y. Wang, Y. Fan, T. Lei, F. Gu, R. Lang, G.A. Pringle, X. Zhang, Z. Chen, and L. Fu. 2010. Expression of HAb18G is associated with tumor progression and prognosis in breast carcinoma. *Breast Cancer Research and Treatment*. 124:677-688.

Liu, J., P. Yue, V.V. Artym, S.C. Mueller, and W. Guo. 2009. The Role of the Exocyst in Matrix Metalloproteinase Secretion and Actin Dynamics during Tumor Cell Invadopodia Formation. *Molecular Biology of the Cell*. 20:3763-3771.

Liu, Z., Y.E. Hartman, J.M. Warram, J.A. Knowles, L. Sweeny, T. Zhou, and E.L. Rosenthal. 2011. Fibroblast Growth Factor Receptor Mediates Fibroblast-Dependent Growth in EMMPRIN-depleted Head and Neck Cancer Tumor Cells. *Molecular Cancer Research*. 9:1008-1017.

Luo, J., A. Teplyakov, G. Obmolova, T. Malia, S.-J. Wu, E. Beil, A. Baker, B. Swencki-Underwood, Y. Zhao, J. Sprenkle, K. Dixon, R. Sweet, and G.L. Gilliland. 2009. Structure of the EMMPRIN N-terminal domain 1: Dimerization via β-strand swapping. *Proteins*. 77:1009-1014.

Mader, C.C., M. Oser, M.A.O. Magalhaes, J.J. Bravo-Cordero, and J. Condeelis. 2011. An EGFR-Src-Arg-Cortactin Pathway Mediates Functional Maturation of Invadopodia and Breast Cancer Cell Invasion. *Cancer Research*. 71:1730-1741.

Magalhaes, M.A.O., D.R. Larson, C.C. Mader, J.J. Bravo-Cordero, H. Gil-Henn, M. Oser, X. Chen, A.J. Koleske, and J. Condeelis. 2011. Cortactin phosphorylation regulates cell invasion through a pH-dependent pathway. *Journal of Cell Biology*. 195:903-920.

Manoharan, C., M.C. Wilson, R.B. Sessions, and A.P. Halestrap. 2006. The role of charged residues in the transmembrane helices of monocarboxylate transporter 1 and its ancillary protein basigin in determining plasma membrane expression and catalytic activity. *Molecular Membrane Biology*. 23:486-498.

Marieb, E.A., A. Zoltan-Jones, R. Li, S. Misra, S. Ghatak, J. Cao, S. Zucker, and B.P. Toole. 2004. Emmprin promotes anchorage-independent growth in human mammary carcinoma cells by stimulating hyaluronan production. *Cancer Research*. 64:1229-1232.

Menashi, S., M. Serova, L. Ma, S. Vignot, S. Mourah, and F. Calvo. 2003. Regulation of Extracellular Matrix Metalloproteinase Inducer and Matrix Metalloproteinase Expression by Amphiregulin in Transformed Human Breast Epithelial Cells. *Cancer Research*. 63:7575-7580.

Mi, Z., T. Oliver, H. Guo, C. Gao, and P.C. Kuo. 2007. Thrombin-Cleaved COOH-Terminal Osteopontin Peptide Binds with Cyclophilin C to CD147 in Murine Breast Cancer Cells. *Cancer Research*. 67:4088-4097.

Millimaggi, D., M. Mari, S.D. Ascenzo, I. Giusti, A. Pavan, and V. Dolo. 2009. Vasculogenic mimicry of human ovarian cancer cells: Role of CD147. *International Journal of Oncology*. 35:1423-1428.

Millimaggi, D., M. Mari, S. D'Ascenzo, E. Carosa, E.A. Jannini, S. Zucker, G. Carta, A. Pavan, and V. Dolo. 2007. Tumor Vesicle-Associated CD147 Modulates the Angiogenic Capability of Endothelial Cells. *Neoplasia*. 9:349-357.

Misra, S., S. Ghatak, and B.P. Toole. 2005. Regulation of MDR1 Expression and Drug Resistance by a Positive Feeback Loop Involving Hyaluronan, Phosphoinositide 3-Kinase, and ErbB2. *Journal of Biological Chemistry*. 280:20310-20315.

Misra, S., S. Ghatak, A. Zoltan-Jones, and B.P. Toole. 2003. Regulation of Multidrug Resistance in Cancer Cells by Hyaluronan. *Journal of Biological Chemistry*. 278:25285-25288.

Misra, S., B.P. Toole, and S. Ghatak. 2006. Hyaluronan Constitutively Regulates Activation of Multiple Receptor Tyrosine Kinases in Epithelial and Carcinoma Cells. *Journal of Biological Chemistry*. 281:34936-34941.

Miyauchi, T., F. Jimma, T. Igakura, S. Yu, M. Ozawa, and T. Muramatsu. 1995. Structure of the Mouse Basigin Gene, a Unique Member of the Immunoglobulin Superfamily. *Journal of Biochemistry*. 118:717-724.

Miyauchi, T., T. Kanekura, A. Yamaoka, M. Ozawa, S. Miyazawa, and T. Muramatsu. 1990. Basigin, a New Broadly Distributed Member of the Immunoglobulin Superfamily, Has Strong Homology with Both the Immunoglobulin V Domain and the beta-chain of Major Histocompatability Complex Class II Antigen. *Journal of Biochemistry (Tokyo)*. 107:16-323.

Miyauchi, T., Y. Masuzawa, and T. Muramatsu. 1991. The Basigin Group of the Immunoglobulin Superfamily: Complete Conservation of a Segment in and around the Transmembrane Domains of Human and Mouse Basigin and Chicken HT7 Antigen. *Journal of Biochemistry*. 110:770-774.

Munro, M., Y. Akkam, and K.D. Curtin. 2010. Mutational analysis of *Drosophila basigin* function in the visual system. *Gene*. 449:50-58.

Muralidharan-Chari, V., J.W. Clancy, A. Sedgwick, and C. D'Souza-Schorey. 2010. Microvesicles: mediators of extracellular communication during cancer progression. *Journal of Cell Science*. 123:1603-1611.

Muramatsu, T., and T. Miyauchi. 2003. Basigin (CD147): a multifunctional transmembrane protein involved in reproduction, neural function, inflammation and tumor invasion. *Histology and Histopathology*. 18:981-987.

Murphy, D.A., and S.A. Courtneidge. 2011. The 'ins' and 'outs' of podosomes and invadopodia: characteristics, formation and function. *Nature Reviews Molecular Cell Biology*. 12:413-426.

Murphy, D.A., B. Diaz, P.A. Bromann, J.H. Tsai, Y. Kawakami, J. Maurer, R.A. Stewart, J.C. Izpisua-Belmonte, and S.A. Courtneidge. 2011. A Src-Tsk5 Pathway is Required for Neural Crest Cell Migration during Embryonic Development. *PLoS One*. 6:e22499.

Nabeshima, K., H. Iwasaki, K. Koga, H. Hojo, J. Suzumiya, and M. Kikuchi. 2006. Emmprin (basigin/CD147): Matrix metalloproteinase modulator and multifunctional cell recognition molecule that plays a critical role in cancer progression. *Pathology International*. 56:359-367.

Nakahara, H., L. Howard, E.W. Thompson, H. Sato, M. Seiki, Y. Yeh, and W.-T. Chen. 1997. Transmembrane/cytoplasmic domain-mediated membrane type 1-matrix metalloprotease docking to invadopodia is required for cell invasion. *PNAS*. 94:7959-7964.

Nakai, M., L. Chen, and R.A. Nowak. 2006. Tissue Distribution of Basigin and Monocarboxylate Transporter 1 in the Adult Male Mouse: A Study Using Wild-Type and Basigin Gene Knockout Mice. *The Anatomical Record Part A*. 288A:527-535.

Naruhashi, K., K. Kadomatsu, T. Igakura, Q.-W. Fan, N. Kuno, H. Muramatsu, T. Miyauchi, T. Hasegawa, A. Itoh, T. Muramatsu, and T. Nabeshima. 1997. Abnormalities of Sensory and Memory Functions in Mice Lacking *Bsg* Gene. *Biochemical and Biophysical Research Communications*. 236:733-737.

Neel, N.F., K.L. Rossman, T.D. Martin, T.K. Hayes, J.J. Yeh, and C.J. Der. 2012. The RalB Small GTPase Mediates Formation of Invadopodia through a GTPase-Activating Protein-Independent of the RalBP1/RLIP76 Effector. *Molecular and Cellular Biology*. 32:1374-1386.

Nehme, C.L., M.M. Cesario, D.G. Myles, D.E. Koppel, and J.R. Bartles. 1993. Breaching the Diffusion Barrier That Compartmentalizes the Transmembrane Glycoprotein CE9 to the

Posterior-Tail Plasma Membrane Domain of the Rat Spermatozoon. *Journal of Cell Biology*. 120:687-694.

Nehme, C.L., B.E. Fayos, and J.R. Bartles. 1995. Distribution of the integral plasma membrane glycoprotein CE9 (MRC OX-47) among rat tissues and its induction by diverse stimuli of metabolic activation. *Biochemical Journal*. 310:693-698.

Newman, J.R., I.A. Bohannon, W. Zhang, J.B. Skipper, W.E. Grizzle, and E.L. Rosenthal. 2008a. Modulation of Tumor Cell Growth In Vivo by Extracellular Matrix Metalloprotease Inducer. *Archives of Otolaryngology and Head and Neck Surgery*. 134:1218-1224.

Newman, J.R., J.P. Gleysteen, C.F. Baranano, J.R. Bremser, W. Zhang, K.R. Zinn, and E.L. Rosenthal. 2008b. Stereomicroscopic fluorescence imaging of head and neck cancer xenografts targeting CD147. *Cancer Biology & Therapy*. 7:1063-1070.

Newman, J.R., E.E. Helman, S. Safavy, W. Zhang, and E.L. Rosenthal. 2009. EMMPRIN expression is required for response to bevacizumab therapy in HNSCC xenografts. *Cancer Letters*. 274:313-318.

Niiya, D., N. Egawa, T. Sakamoto, Y. Kikkawa, T. Shinkawa, T. Isobe, N. Koshikawa, and M. Seiki. 2009. Identification and Characterization of Luthern Blood Group Glycoprotein as a New Substrate of Membrane-type 1 Matrix Metalloproteinase 1 (MT1-MMP): A systemic whole cell analysis of MT1-MMP-associating Proteins in A431 Cells. *Journal of Biological Chemistry*. 284:27360-27369.

Noguchi, Y., T. Sato, M. Hirata, T. Hara, K. Ohama, and A. Ito. 2003. Identification and Characterization of Extracellular Matrix Metalloproteinase Inducer in Human Endometrium during the Menstrual Cycle *in Vivo* and *in Vitro*. *Journal of Clinical Endocrinology & Metabolism*. 88:6063-6072.

Noordeen, N.A., F. Carafoli, E. Hohenester, M.A. Horton, and B. Leitinger. 2006. A Transmembrane Leucine Zipper Is Required for Activation of the Dimeric Receptor Tyrosine Kinase DDR1. *Journal of Biological Chemistry*. 281:22744-22751.

Ochrietor, J.D., and P.J. Linser. 2004. 5A11/Basigin Gene Products Are Necessary for Proper Maturation and Function of the Retina. *Developmental Neuroscience*. 26:380-387.

Ochrietor, J.D., T.M. Moroz, K. Kadomatsu, T. Muramatsu, and P.J. Linser. 2001. Retinal Degeneration Following Failed Photoreceptor Maturation in 5A11/Basigin Null Mice. *Experimental Eye Research*. 72:467-477.

Ochrietor, J.D., T.P. Moroz, M.F. Clamp, A.M. Timmers, T. Muramatsu, and P.J. Linser. 2002. Inactivation of the Basigin gene impairs normal retinal development and maturation. *Vision Research*. 42:447-453.

Ochrietor, J.D., T.P. Moroz, L.v. Ekeris, M.F. Clamp, S.C. Jefferson, A.C. deCarvalho, J.M. Fadool, G. Wistow, T. Muramatsu, and P.J. Linser. 2003. Retina-Specific Expression of 5A11/Basigin-2, a Member of the Immunoglobulin Gene Superfamily. *Investigative Ophthalmology and Visual Science*. 44:4086-4096.

Oikawa, T., T. Itoh, and T. Takenawa. 2008. Sequential signals toward podosome formation in NIH-src cells. *Journal of Cell Biology*. 182:157-169.

Olsson, E., G. Honeth, P.-O. Bendahi, L.H. Saal, S. Gruvberger-Saal, M. Ringner, J. Vallon-Christersson, G. Jonsson, K. Holm, K. Lovgren, M. Ferno, D. Grabau, A. Borg, and C. Hegardt. 2011. CD44 isoforms are heterogeneously expressed in breast cancer and correlate with tumor subtypes and cancer stem cell markers. *BMC Cancer*. 11:418.

Onder, T.T., P.B. Gupta, S.A. Mani, J. Yang, E.S. Lander, and R.A. Weinberg. 2008. Loss of E-Cadherin Promotes Metastasis via Multiple Downstream Transcriptional Pathways. *Cancer Research*. 68:3645-3654.

Oser, M., H. Yamaguchi, C.C. Mader, J.J. Bravo-Cordero, M. Arias, X. Chen, V. DesMarais, J.v. Rheenen, A.J. Koleske, and J. Condeelis. 2009. Cortactin regulates cofilin and N-WASp activities to control the stages of invadopodium assembly and maturation. *Journal of Cell Biology*. 186:571-587.

Pakula, R., A. Melchior, A. Denys, C. Vanpouille, J. Mazurier, and F. Allain. 2007. Syndecan-1/CD147 association is essential for cyclophilin B-induced activation of p44/p42 mitogen-activated protein kinases and promotion of cell adhesion and chemotaxis. *Glycobiology*. 17:492-503.

Papiewska-Pajak, I., J. Boncela, P. Przygodzka, and C.S. Cierniewski. 2010. Autocrine effects of VEGF-D on endothelial cells after transduction with AD-VEGF$^{\Delta N \Delta C}$ *Experimental Cell Research*. 316:907-914.

Paterson, D.J., W.A. Jefferies, J.R. Green, M.R. Brandon, P. Courthesy, M. Puklavec, and A.F. Williams. 1987. Antigens of activated rat T lymphocytes including a molecule of 50,000 M_r detected only on CD4 positive T blasts. *Molecular Immunology*. 24:1281-1290.

Philp, N.J., J.D. Ochrietor, C. Rudoy, T. Muramatsu, and P.J. Linser. 2003. Loss of MCT1, MCT3, and MCT4 Expression in the Retinal Pigment Epithelium and Neural Retina of the 5A11/Basigin-Null Mouse. *Investigative Ophthalmology and Visual Science*. 44:1305-1311.

Pituch-Noworolska, A., G. Drabik, R. Szantanek, M. Biatas, P. Kotodziejczyk, A. Szczepanik, J. Stachura, and M. Zembala. 2007. Immunophenotype of Isolated Tumor Cells in Blood, Bone Marrow and Lymph Nodes of Patients with Gastric Cancer. *Polish Journal of Pathology*. 58:93-97.

Polette, M., C. Gilles, V. Marchand, M. Lorenzato, B.P. Toole, J.-M. Tournier, S. Zucker, and P. Birembaut. 1997. Tumor Collagenase Stimulatory Factor (TCSF) Expression and Localization in Human Lung and Breast Cancers. *Journal of Histochemistry & Cytochemistry*. 45:703-709.

Pons, M., S.W. Cousins, O. Alcazar, G.E. Striker, and M.E. Marin-Castano. 2011. Angiotensin II-Induced MMP-2 Activity and MMP-14 and Basigin Protein Expression Are Mediated via the Angiotensin II Receptor Type 1-Mitogen-Activated Protein Kinase 1 Pathway in Retinal Pigment Epithelium. *American Journal of Pathology*. 178:2665-2681.

Pushkarsky, T., V. Yurchenko, A. Laborico, and M. Bukrinsky. 2007. CD147 stimultes HIV-1 infection in a signal-independent fashion. *Biochemical and Biophysical Research Communications*. 363:495-499.

Pushkarsky, T., V. Yurchenko, C. Vanpouille, B. Brichacek, I. Vaisman, S. Hatakeyama, K. Nakayama, B. Sherry, and M.I. Bukrinsky. 2005. Cell Surface Expression of CD147/EMMPRIN is Regulated by Cyclophilin 60. *Journal of Biological Chemistry*. 280:27866-27871.

Pylayeva-Gupta, Y., E. Grabocka, and D. Bar-Sagi. 2011. RAS oncogenes: weaving a tumorigenic web. *Nature Reviews Cancer*. 11:761-774.

Qian, A.-R., W. Zhang, J.-P. Cao, P.-F. Yang, X. Gao, Z. Wang, H.-Y. Xu, Y.-Y. Weng, and P. Shang. 2008. Downregulation of CD147 expression alters cytoskeleton architecture and inhibits gelatinase production and SAPK pathway in human hepatocellular carcinoma cells. *Journal of Experimental & Clinical Cancer Research*. 27:50.

Qin, Z., L. Dai, M. Bratoeva, M.G. Slomiany, B.P. Toole, and C. Parsons. 2011. Cooperative roles for emmprin and LYVE-1 in the regulation of chemoresistance for primary effusion lymphoma. *Leukemia*. 25:1598-1609.

Quemener, C., E.E. Gabison, B. Naimi, G. Lescaille, F. Bougatef, M.P. Podgorniak, G. Labarchede, C. Lebbe, F. Calvo, S. Menashi, and S. Mourah. 2007. Extracellular Matrix

Metalloproteinase Inducer Up-regulates the Urokinase-type Plasminogen Activator System Promoting Tumor Cell Invasion. *Cancer Research*. 67:9-15.

Ramos, D.M., and D. Dang. 2011. EMMPRIN Expression in Oral SCC Is Regulated by FYN Kinase. *Anticancer Research*. 31:1205-1210.

Reddy, V.S., S.D. Prabhu, S. Mummidi, A.J. Valente, B. Venkatesan, P. Shanmugam, P. Delafontaine, and B. Chandrasekar. 2010. Interleukin-18 induces EMMPRIN expression in primary cardiomyocytes via JNK/Sp1 signaling and MMP-9 in part via EMMPRIN and through AP-1 and NF-κB activation. *American Journal of Physiology Heart and Circulatory Physiology*. 299:H1242-H1254.

Reimers, N., K. Zafrakas, V. Assmann, C. Egen, L. Riethdorf, S. Riethdorf, J. Berger, S. Ebel, F. Janicke, G. Sauter, and K. Pantel. 2004. Expression of Extracellular Matrix Metalloproteinase Inducer on Micrometastatic and Primary Mammary Carcinoma Cells. *Clinical Cancer Research*. 10:3422-3428.

Ricardo, S., A.F. Vieira, R. Gerhard, D. Leitao, R. Pinto, J.F. Cameselle-Teijeiro, F. Milanezi, F. Schmitt, and J. Paredes. 2011. Breast cancer stem cell markers CD44, CD24 and ALDH1: expression distribution within intrinsic molecular subtype. *Journal of Clinical Pathology*. 64:937-946.

Ridley, A.J. 2011. Life at the Leading Edge. *Cell*. 145:1012-1022.

Riethdorf, S., N. Reimers, V. Assmann, J.-W. Kornfeld, L. Terracciano, G. Sauter, and K. Pantel. 2006. High incidence of EMMPRIN expression in human tumors. *International Journal of Cancer*. 119:1800-1810.

Risau, W., R. Hallmann, U. Albrecht, and S. Henke-Fahle. 1986. Brain induces the expression of an early cell surface marker for blood-brain barrier-specific endothelium. *EMBO Journal*. 5:3179-3183.

Rochlitz, C.F., G.K. Scott, J.M. Dodson, E. Liu, C. Dollbaum, H.S. Smith, and C.C. Benz. 1989. Incidence of Activating *ras* Oncogene Mutations Associated with Primary and Metastatic Human Breast Cancer. *Cancer Research*. 49:357-360.

Rojas, M., S. Yao, and Y.-Z. Lin. 1996. Controlling Epidermal Growth Factor (EGF)-stimulated Ras Activation in Intact Cells by a Cell-permeable Peptide Mimicking Phosphorylated EGF Receptor. *Journal of Biological Chemistry*. 271:27456-27461.

Rosenthal, E.L., S. Shreenivas, G.E. Peters, W.E. Grizzle, R. Desmond, and C.L. Gladson. 2003. Expression of Extracellular Matrix Metalloproteinase Inducer in Laryngeal Squamous Cell Carcinoma. *Laryngoscope*. 113:1406-1410.

Ruan, W., V. Becker, U. Klingmuller, and D. Langosch. 2004. The Interface between Self-assembling Erythropoietin Receptor Transmembrane Segments Corresponds to a Membrane-spanning Leucine Zipper. *Journal of Biological Chemistry*. 279:3273-3279.

Rucci, N., D. Millimaggi, M. Mari, A.D. Fattore, M. Bologna, A. Teti, A. Angelucci, and V. Dolo. 2010. Receptor Activator of NF-kB Ligand Enhances Breast Cancer-induced Osteolytic Lesion Through Upregulation of Extracellular Matrix Metalloproteinase Inducer/CD147. *Cancer Research*. 70:6150-6160.

Ruiz, S., A. Castro-Castro, and X.R. Bustelo. 2008. CD147 Inhibits the Nuclear Factor of Activated T-cells by Impairing Vav1 and Rac1 Downstream Signaling. *Journal of Biological Chemistry*. 283:5554-5566.

Sahai, E. 2005. Mechanisms of cancer invasion. *Current Opinion in Genetics and Development*. 15:87-96.

Sakaguchi, K., Y. Okabayashi, Y. Kido, S. Kimura, Y. Matsumura, K. Inushima, and M. Kasuga. *1998. Shc Phosphotyrosine-Binding Domain Dominantly Interacts with Epidermal*

Growth Factor Receptors and Mediates Ras Activation in Intact Cells. *Molecular Endocrinology*. 12:536-543.

Saksena, S., S. Theegala, N. Bansal, R.K. Gill, S. Tyagi, W.A. Alrefai, K. Ramaswamy, and P.K. Dudeja. 2009. Mechanisms underlying modulaton of monocarboxylate transporter 1 (MCT1) by somatostatin in human intestinal epithelial cells. *American Journal of PHysiology Gastrointestinal and Liver Physiology*. 297:G878-G885.

Sakurai-Yageta, M., C. Recchi, G.L. Dez, J.-B. Sibarita, L. Daviet, J. Camonis, C. D'Souza-Schorey, and P. Chavrier. 2008. The interaction of IQGAP1 with the exocyst complex is required for tumor cell invasion downstream of Cdc42 and RhoA. *Journal of Cell Biology*. 181:985-998.

Sameshima, T., K. Nabeshima, B.P. Toole, K. Yokogami, Y. Okada, T. Goya, M. Koono, and S. Wakisaka. 2000. Glioma cell extracellular matrix metalloproteinase inducer (EMMPRIN) (CD147) stimulates production of membrane-type matrix metalloproteinases and activated gelatinase A in co-cultures with brain-derived fibroblasts. *Cancer Letters*. 157:177-184.

Sanz-Moreno, V., G. Gadea, J. Ahn, H. Paterson, P. Marra, S. Pinner, E. Sahai, and C.J. Marshall. 2008. Rac Activation and Inactivation Control Plasticity of Tumor Cell Movement. *Cell*. 135:510-523.

Sanz-Moreno, V., and C.J. Marshall. 2009. Rho-GTPase signaling drives melanoma cell plasticity. *Cell Cycle*. 8:1484-1487.

Schlosshauer, B., H. Bauch, and R. Frank. 1995. Neurothelin: amino acid sequence, cell surface dynamics and actin colocalization. *European Journal of Cell Biology*. 68:159-166.

Schmidt, R., A. Bultmann, S. Fischel, A. Gillitzer, P. Cullen, A. Walch, P. Jost, M. Ungerer, N.D. Tolley, S. Lindemann, M. Gawaz, A. Schomig, and A.E. May. 2008. Extracellular Matrix Metalloproteinase Inducer (CD147) Is a Novel Receptor on Platelets, Activates Platelets, and Augments Nuclear Factor kB-Dependent Inflammation in Monocytes. *Circulation Research*. 102:302-309.

Schmidt, R., A. Bultmann, M. Ungerer, N. Joghetaei, O. Bulbul, S. Thieme, T. Chavakis, B.P. Toole, M. Gawaz, A. Schomig, and A.E. May. 2006. Extracellular Matrix Metalloproteinase Inducer Regulates Metalloproteinase Activity in Cardiovascular Cells: Implications in Acute Myocardial Infarction. *Circulation Research*. 113:834-841.

Schneiderhan, W., M. Scheler, K.H. Holzmann, M. Marx, J.E. Gschwend, M. Bucholz, T.M. Gress, T. Seufferlein, G. Adler, and F. Oswald. 2009. CD147 Silencing inhibits lactate transport and reduces malignant potential of pancreatic cancer cells in in vivo and in vitro models. *Gut*. 58.

Schoumacher, M., R.D. Goldman, D. Louvard, and D.M. Vignjevic. 2010. Actin, microtubules, and vimentin intermediate filaments cooperate for elongation of invadopodia. *Journal of Cell Biology*. 189:541-556.

Schuster, V.L., R. Lu, N. Kanai, Y. Bao, S. Rosenberg, D. Prie, P. Ronco, and M.L. Jennings. 1996. Cloning of the rabbit homologue of mouse 'basigin' and rat 'OX-47': kidney cell type-specific expression, and regulation in collecting duct cells. *Biochimica et Biophysica Acta*. 1311:13-19.

Seales, E.C., G.A. Jurado, A. Singhal, and S.L. Bellis. 2003. Ras oncogene directs expression of a differentially sialylated, functionally altered β1 integrin. *Oncogene*. 22:7137-7145.

Seizer, P., T. Schonberger, M. Schott, M.R. Lang, H.F. Langer, B. Bigalke, B.F. Kramer, O. Borst, K. Daub, O. Heidenreich, R. Schmidt, S. Lindemann, Y. Herouy, M. Gawaz, and A.E. May. 2010. EMMPRIN and its ligand cyclophilin A regulate MT1-MMP, MMP-9 and M-CSF during foam cell formation. *Atherosclerosis*. 209:51-57.

Serbulea, M., S. Kakumu, A.A. Thant, K. Miyazaki, K. Machida, T. Senga, S. Ohta, K. Yoshioka, N. Hotta, and M. Hamaguchi. 1999. Hyaluronan activates mitogen-activated protein kinase via Ras-signaling pathway. *International Journal of Oncology*. 14:733-738.

Seulberger, H., F. Lottspeich, and W. Risau. 1990. The inducible blood-brain barrier specific molecule HT7 is a novel immunoglobulin-like cell surface glycoprotein. *EMBO Journal*. 9:2151-2158.

Shah, N., G. Zhai, J.A. Knowles, C.R. Stockard, W.E. Grizzle, N. Fineberg, T. Zhou, K.R. Zinn, E.L. Rosenthal, and H. Kim. 2011. ^{18}F-FDG PET/CT Imaging Detects Therapy Efficacy of Anti-EMMPRIN Antibody and Gemcitabine in Orthotopic Pancreatic Tumor Xenografts. *Molecular Imaging and Biology*. 14:237-244.

Si, A.I.C., L. Huang, J. Xu, S.-M. Kumta, D. Wood, and M.H. Zheng. 2003. Expression and Localization of Extracellular Matrix Metalloproteinase Inducer in Giant Cell Tumor of Bone. *Journal of Cellular Biochemistry*. 89:1154-1163.

Sidhu, S.S., A.T. Mengistab, A.N. Tauscher, J. LaVail, and C. Basbaum. 2004. The microvesicle as a vehicle for EMMPRIN in tumor-stromal interactions. *Oncogene*. 23:956-963.

Sidhu, S.S., R. Nawroth, M. Retz, H. Lemjabbar-Alaoui, V. Dasari, and C. Basbaum. 2010. EMMPRIN regulates the canonical Wnt/β-catenin signaling pathway, a potential role in accelerating lung tumorigenesis. *Oncogene*. 29:4145-4156.

Sienel, W., B. Polzer, K. Elshawi, M. Linder, A. Morresi-Hauf, C. Vay, F. Eder, B. Passlick, and C.A. Klein. 2008. Cellular localization of EMMPRIN predicts prognosis of patients with operable lung adenocarcinoma independent from MMP-2 and MMP-9. *Modern Pathology*. 21:1130-1138.

Siwik, D.A., G.M. Kuster, J.V. Brahmbhatt, Z. Zaidi, J. Malik, H. Ooi, and G. Ghorayeb. 2008. EMMPRIN mediates β-adrenergic receptor-stimulated matrix metalloproteinase activity in cardiac myocytes. *Journal of Molecular and Cellular Cardiology*. 44:210-217.

Slomiany, M.G., L. Dai, P.A. Bomar, T.J. Knackstedt, D.A. Kranc, L. Tolliver, B.L. Maria, and B.P. Toole. 2009a. Abrogating drug resistance in malignant peripheral nerve sheath tumors by disrupting hyaluronan-CD44 interactions with small hyaluronan oligosaccharides. *Cancer Research*. 69:4992-4998.

Slomiany, M.G., G.D. Grass, A.D. Robertson, X.Y. Yang, B.L. Maria, C. Beeson, and B.P. Toole. 2009b. Hyaluronan, CD44, and emmprin regulate lactate efflux and membrane localization of monocarboxylate transporters in human breast carcinoma cells. *Cancer Research*. 69:1293-1301.

Sluijter, J.P.G., W.P.C. Pulskens, A.H. Schoneveld, E. Velema, C.F. Strijder, F. Moll, J.-P.d. Vries, J. Verheijen, R. Hanemaaijer, D.P.V.d. Kleijn, and G. Pasterkamp. 2005. Matrix Metalloproteinase 2 Is Associated With Stable and Matrix Metalloproteinase 8 and 9 With Vulnerable Carotid Atherosclerotic Lesions: A Study in Human Endarterectomy Specimen Pointing to a Role for Different Extracellular Matrix Metalloproteinase Inducer Glycosylation Forms. *Stroke*. 37:235-239.

Soderberg, O., M. Gullberg, M. Jarvius, K. Ridderstrale, K.-J. Leuchowius, J. Jarvius, K. Wester, P. Hydbring, F. Bahram, L.-G. Larsson, and U. Landegren. 2006. Direct observation of individual endogenous protein complexes *in situ* by proximity ligation. *Nature Methods*. 3:995-1000.

Sohara, Y., N. Ishiguro, K. Machida, H. Kurata, A.A. Thant, T. Senga, S. Matsuda, K. Kimata, H. Iwata, and M. Hamaguchi. 2001. Hyaluronan Activates Cell Motility of v-Src-transformed Cells via Ras-Mitogen-activated Protein Kinase and Phosphoinositide 3-Kinase-Akt in a Tumor-specific Manner. *Molecular Biology of the Cell*. 12:1859-1868.

Sonveaux, P., F. Vegran, T. Schroeder, M.C. Wergin, J. Verrax, Z.N. Rabbani, C.J.D. Saedeleer, K.M. Kennedy, C. Diepart, B.F. Jordan, M.J. Kelley, B. Gallez, M.L. Wahl, O. Feron, and M.W. Dewhirst. 2008. Targeting lactate-fueled respiration selectively kills hypoxic tumor cells in mice. *Journal of Clinical Investigation*. 118:3930-3942.

Soule, H.D., T.M. Maloney, S.R. Wolman, W.D.P. Jr., R. Brenz, C.M. McGrath, J. Russo, R.J. Pauley, R.F. Jones, and S.C. Brooks. 1990. Isolation and Characterization of a Spontaneously Immortalized Human Breast Epithelial Cell Line, MCF-10. *Cancer Research*. 50:6075-6086.

Spring, F.A., C.H. Holmes, K.L. Simpson, W.J. Mawby, M.J. Mattes, Y. Okubo, and S.F. Parsons. 1997. The Ok^a blood group antigen is a marker for the M6 leukocyte activation antigen, the human homolog of OX-47 antigen, basigin and neurothelin, an immunoglobulin superfamily molecule that is widely expressed in human cells and tissues. *European Journal of Immunology*. 27:891-897.

Staffler, G., A. Szekeres, G.J. Schutz, M.D. Saemann, E. Prager, M. Zeyda, K. Drbal, G.J. Zlabinger, T.M. Stulnig, and H. Stockinger. 2003. Selective Inhibition of T Cell Activation Via CD147 Through Novel Modulation of Lipid Rafts. *Journal of Immunology*. 171:1707-1714.

Stamatakos, M., C. Stefanaki, K. Kontzoglou, S. Masouridi, G. Sakorafas, and M. Safioleas. 2010. Recapitulation of Ras Oncogene Mutations in Breast Cancer. *Onkologie*. 33:540-544.

Staubach, S., and F.-G. Hanisch. 2011. Lipid rafts: signaling and sorting platforms of cells and their roles in cancer. *Expert Review of Proteomics*. 8:263-277.

Stoorvogel, W., M.J. Kleijmeer, H.J. Geuze, and G. Raposo. 2002. The Biogenesis and Functions of Exosomes. *Traffic*. 3:321-330.

Su, J., X. Chen, and T. Kanekura. 2009. A CD147-targeting siRNA inhibits the proliferation, invasiveness, and VEGF production of human malignant melanoma cells by down-regulating glycolysis. *Cancer Letters*. 273:140-147.

Sun, J., and M.E. Hemler. 2001. Regulation of MMP-1 and MMP-2 Production through CD147/Extracellular Matrix Metalloproteinase Inducer Interactions. *Cancer Research*. 61:2276-2281.

Tan, H., K. Ye, Z. Wang, and H. Tang. 2008. CD147 expression as a significant prognostic factor in differentiated thyroid carcinoma. *Translational Research*. 152:143-149.

Tang, J., Y.-M. Wu, P. Zhao, X.-M. Yang, J.-L. Jiang, and Z.-N. Chen. 2008. Overexpression of HAb18G/CD147 promotes invasion and metastasis *via* $\alpha 3\beta 1$ integrin mediated FAK-paxillin and FAK-PI3K-Ca^{2+} pathways. *Cellular and Molecular Life Sciences*. 65:2933-2942.

Tang, W., S.B. Chang, and M.E. Hemler. 2004a. Links between CD147 Function, Glycosylation, and Caveolin-1. *Molecular Biology of the Cell*. 15:4043-4050.

Tang, W., and M.E. Hemler. 2004. Caveolin-1 Regulates Matrix Metalloproteinase-1 Induction and CD147/EMMPRIN Cell Surface Clustering. *Journal of Biological Chemistry*. 279:11112-11118.

Tang, Y., P. Kesavan, M.T. Nakada, and L. Yan. 2004b. Tumor-Stroma Interaction: Positive Feedback Regulation of Extracellular Matrix Metalloproteinase Inducer (EMMPRIN) Expression and Matrix Metalloproteinase-Dependent Generation of Soluble CD147. *Molecular Cancer Research*. 2:73-80.

Tang, Y., M.T. Nakada, P. Kesavan, F. McCabe, H. Millar, P. Rafferty, P. Bugelski, and L. Yan. 2005. Extracellular Matrix Metalloproteinase Inducer Stimulates Tumor Angiogenesis by Elevating Vascular Endothelial Cell Growth Factor and Matrix Metalloproteinases. *Cancer Research*. 65:3193-3199.

Tang, Y., M.T. Nakada, P. Rafferty, J. Laraio, F.L. McCabe, H. Millar, M. Cunningham, L.A. Snyder, P. Bugelski, and L. Yan. 2006. Regulation of Vascular Endothelial Growth Factor

Expression by EMMPRIN via the PI3K-Akt Signaling Pathway. *Molecular Cancer Research*. 4:371-378.

Tarin, C., B. Lavin, M. Gomez, M. Saura, A. Diez-Juan, and C. Zaragoza. 2011. The extracellular matrix metalloproteinase inducer EMMPRIN is a target of nitric oxide in myocardial ischemia/reperfusion. *Free Radical Biology and Medicine*. 51:387-395.

Taylor, P.M., R.J. Woodfield, M.N. Hodgkin, T.R. Pettitt, A. Martin, D.J. Kerr, and M.J.O. Wakelam. 2002. Breast cancer cell-derived EMMPRIN stimulates fibroblast MMP2 release through a phospholipase A_2 and 5-lipoxygenase catalyzed pathway. *Oncogene*. 21:5765-5772.

Teng, Y., M. Zeisberg, and R. Kalluri. 2007. Transcriptional regulation of epithelial-mesenchymal transition *Journal of Clinical Investigation*. 117:304-306.

Tolde, O., D. Rosel, P. Vesely, P. Folk, and J. Brabek. 2010. The structure of invadopodia in a complex 3D environment. *European Journal of Cell Biology*. 89:674-680.

Toole, B.P. 2004. Hyaluronan: from extracellular glue to pericellular cue. *Nature Reviews Cancer*. 4:528-539.

Toole, B.P. 2009. Hyaluronan-CD44 Interactions in Cancer: Paradoxes and Possibilities. *Clinical Cancer Research*. 15:7462-7468.

Toole, B.P., and M.G. Slomiany. 2008. Hyaluronan, CD44 and Emmprin: partners in cancer cell chemoresistance. *Drug Resistance Updates*. 11:110-121.

Tsai, W.-C., L.-F. Sheu, S. Nieh, C.-P. Yu, G.-H. Sun, Y.-F. Lin, A. Chen, and J.-S. Jin. 2007. Association of EMMPRIN and fascin expression in renal cell carcinoma: correlation with clinicopathological parameters. *World Journal of Urology*. 25:73-80.

Ueda, K., K. Yamada, M. Urashima, Y. Ishibashi, M. Shirai, T. Nikaido, H. Takahashi, A. Okamoto, M. Saito, M. Yasuda, K. Ohkawa, and T. Tanaka. 2007. Association of extracellular matrix metalloproteinase inducer in endometrial carcinoma with patient outcomes and clinicopathogenesis using monoclonal antibody 12C3. *Oncology Reports*. 17:731-735.

Ullmann, U., C. Gilles, M.D. Rycke, H.V.d. Velde, K. Sermon, and I. Liebaers. 2008. GSK-3-specific inhibitor-supplemented hESC medium prevents the epithelial-mesenchymal transition process and the up-regulation of matrix metalloproteinases in hESCs cultured in feeder-free conditions. *Molecular Human Reproduction*. 14:169-179.

Umar, A., H. Kang, A.M. Timmermans, M.P. Look, M.E.M.-v. Gelder, M.A.d. Bakker, N. Jaitly, J.W.M. Martens, T.M. Luider, J.A. Foekens, and L. Pasa-Tolic. 2009. Identification of a Putative Protein Profile Associated with Tamoxifen Therapy Resistance in Breast Cancer. *Molecular and Cellular Proteomics*. 8:1278-1294.

Underhill, C.B., and B.P. Toole. 1979. Binding of Hyaluronate to the Cell Surface of Cultured Cells. *Journal of Cell Biology*. 82:475-484.

Vander, M.G., L.C. Cantley, and C.B. Thompson. 2009. Understanding the Warburg Effect: The Metabolic Requirements of Cell Proliferation. *Science*. 324:1029-1033.

VanMeter, A.J., A.S. Rodriguez, E.D. Bowman, J. Jen, C.C. Harris, J. Deng, V.S. Calvert, A. Silvestri, C. Fredolini, V. Chandhoke, E.F.P. III, L.A. Liotta, and V. Espina. 2008. Laser Capture Microdissection and Protein Microarray Analysis of Human Non-small Cell Lung Cancer. *Molecular and Cellular Proteomics*. 7:1902-1924.

Venkatesan, B., A.J. Valente, S.D. Prabhu, P. Shanmugam, P. Delafontaine, and B. Chandrasekar. 2010. EMMPRIN activates multiple transcription factors in cardiomyocytes, and induces interleukin-18 expression via Rac1-dependent PI3K/Akt/IKK/NF-kappaB and MKK7/JNK/AP-1 signaling. *Journal of Molecular Cardiology*. 49:655-663.

Venkatesan, B., A.J. Valente, V.S. Reddy, D.A. Siwik, and B. Chandrasekar. 2009. Resveratrol blocks interleukin-18-EMMPRIN cross-regulation and smooth muscle cell migration. *American Journal of Physiology Heart and Circulatory Physiology*. 297:H874-H886.

Vigil, D., J. Cherfils, K.L. Rossman, and C.J. Der. 2010. Ras superfamily GEFs and GAPs: validated and tractable targets for cancer therapy? *Nature Reviews Cancer*. 10:842-857.

Vignjevic, D., M. Schoumacher, N. Gavert, K.-P. Janssen, G. Jih, M. Lae, D. Louvard, A. Ben-Ze'ev, and S. Robine. 2007. Fascin, a Novel Target of B-Catenin-TCF Signaling, Is Expressed at the Invasive Front of Human Colon Cancer. *Cancer Research*. 67:6844-6853.

Visvader, J.E., and G.J. Lindeman. 2008. Cancer stem cells in solid tumours: accumulating evidence and unresolved questions. *Nature Reviews Cancer*. 8:755-768.

Voduc, K.D., M.C.U. Cheang, S. Tyldesley, K. Gelmon, T.O. Nielsen, and H. Kennecke. 2010. Breast Cancer Subtypes and the Risk of Local and Regional Relapse. *Journal of Clinical Oncology*. 28:1684-1691.

Voigt, H., C.S. Vetter-Kauczok, D. Schrama, U.B. Hofmann, J.C. Becker, and R. Houben. 2009. CD147 Impacts Angiogenesis and Metastasis Formation. *Cancer Investigation*. 27:329-333.

Vrijsen, K.R., J.P. Sluijter, M.W.L. Schuchardt, B.W.M.v. Balkom, W.A. Noort, S.A.J. Chamuleau, and P.A.F.M. Doevendans. 2010. Cardiomyocyte progenitor cell-derived exosomes stimulate migration of endothelial cells. *Journal of Cellular and Molecular Medicine*. 14:1064-1070.

Wadhwa, R., K. Taira, and S.C. Kaul. 2002. An Hsp70 family chaperone, mortalin/mthsp70/PBP74/Grp75: what, when, and where? *Cell Stress & Chaperones*. 7:309-316.

Wang, J., L. Fu, F. Gu, and Y. Ma. 2011a. Notch1 is involved in migration and invasion of human breast cancer cells. *Oncology Reports*. 26:1295-1303.

Wang, L., X.-M. Ku, Y. Li, H.-J. Bian, S.-H. Zhang, H. Ye, X.-Y. Yao, B.-H. Li, X.-M. Yang, C.-G. Liao, and Z.-N. Chen. 2006. Regulation of Matrix Metalloproteinase Production and Tumor Cell Invasion by Four Monoclonal Antibodies Against Different Epitopes of HAb18G/CD147 Extracellular Domain. *Hybridoma*. 25:60-67.

Wang, S.J., and L.Y.W. Bourguignon. 2006. Hyaluronan and the Interaction Between CD44 and Epidermal Growth Factor Receptor in Oncogenic Signaling and Chemotherapy Resistance in Head and Neck Cancer. *Archives of Otolaryngology and Head and Neck Surgery*. 132:771-778.

Wang, W.-J., Q.-Q. Li, J.-D. Xu, X.-X. Cao, H.-X. Li, F. Tang, Q. Chen, J.-M. Yang, Z.-D. Xu, and X.-P. Liu. 2008. Interaction between CD147 and P-Glycoprotein and Their Regulation by Ubiquitination in Breast Cancer Cells. *Chemotherapy*. 54:291-301.

Wang, Y., Z.-Q. Huang, C.-Q. Wang, L.-S. Wang, S. Meng, Y.-C. Zhang, T. Chen, and Y.-Q. Fan. 2011b. Artemisinin inhibits extracellular matrix metalloproteinase inducer (EMMPRIN) and matrix metalloproteinase-9 expression via a protein kinase Cδ/p38/extracellular signal-regulated kinase pathway in phorbol myristate acetate-induced THP-1 macrophages. *Clinical and Experimental Pharmacology and Physiology*. 38:11-18.

Warburg, O. 1956. On the origin of cancer cells. *Science*. 123:309-314.

Weaver, A.M. 2009. Regulation of Cancer Invasion by Reactive Oxygen Species and Tks Family Scaffold Proteins. *Science Signaling*. 2:pe56.

Weidle, U.H., W. Scheuer, D. Eggle, S. Klostermann, and H. Stockinger. 2010. Cancer-related Issues of CD147. *Cancer Genomics & Proteomics*. 7:157-170.

Welton, J.L., S. Khanna, P.J. Giles, P. Brennan, I.A. Brewis, J. Staffurth, M.D. Mason, and A. Clayton. 2010. Proteomics analysis of bladder cancer exosomes. *Molecular and Cellular Proteomics*. 9:1324-1338.

Wierstra, I. 2008. Sp1: Emerging roles --Beyond constitutive activation of TATA-less housekeeping genes. *Biochemical and Biophysical Research Communications*. 372:1-13.

Wilson, M.C., D. Meredith, and A.P. Halestrap. 2002. Fluorescence Resonance Energy Transfer Studies on the Interaction between the Lactate Transporter MCT1 and CD147 Provide Information on the Topology and Stoichiometry of the Complex *in Situ*. *Journal of Biological Chemistry*. 277:3666-3672.

Wilson, M.C., D.C. Meredith, C. Bunnun, R.B. Sessions, and A.P. Halestrap. 2009. Studies of the DIDS-binding site of Monocarboxylate Transporter 1 Suggest a Homology Model of the Open Conformation and a Plausible Translocation Cycle. *Journal of Biological Chemistry*. 284:20011-20021.

Wu, J., N.-Y. Ru, Y. Zhang, Y. Li, D. Wei, Z. Ren, X.-F. Huang, Z.-N. Chen, and H. Bian. 2011a. HAb18G/CD147 promotes epithelial-mesenchymal transition through TGF-beta signaling and is transcriptionally regulated by Slug. *Oncogene*. 30:4410-4427.

Wu, L.-S., F.-F. Li, L.-D. Sun, D. Li, J. Su, Y.-H. Kuang, G. Chen, X.-P. Chen, and X. Chen. 2011b. A miRNA-492 binding-site polymorphism in BSG (*basigin*) confers risk to psoriasis in Central South Chinese population. *Human Genetics*. 130:749-757.

Xiao, L.-J., H.-L. Diao, X.-H. Ma, N.-Z. Ding, K. Kadomatsu, T. Muramatsu, and Z.-M. Yang. 2002. Basigin expression and hormonal regulation in the rat uterus during the peri-implantation period. *Reproduction*. 124:219-225.

Xie, H., L. Liu, W. Shi, X. Xiao, L. Tian, D. Jian, X. Chen, and J. Li. 2011. Down regulation of CD147 boosts the premature senescence in human skin fibroblasts by destroying the redox balance and inhibiting klotho. *Journal of Dermatological Science*. 64:237-248.

Xu, D., and M.E. Hemler. 2005. Metabolic Activation-related CD147-CD98 Complex. *Molecular and Cellular Proteomics*. 4:1061-1071.

Xu, H.-Y., A.-R. Qian, P. Shang, J. Xu, L.-M. Kong, H.-J. Bian, and Z.-N. Chen. 2007. siRNA targeted against HAb18G/CD147 inhibits MMP-2 secretion, actin and FAK expression in hepatocellular carcinoma cell line via ERK1/2 pathway. *Cancer Letters*. 247:336-344.

Xu, J.-W., Q.-Q. Li, L.-L. Tao, Y.-Y. Cheng, J. Yu, Q. Chen, X.-P. Liu, and Z.-D. Xu. 2011. Involvement of EGFR in the promotion of malignant properties in multidrug resistant breast cancer cells. *International Journal of Oncology*. 39:1501-1509.

Xue, Y.-J., Q. Lu, and Z.-X. Sun. 2011. CD147 overexpression is a prognostic factor and a potential therapeutic target in bladder cancer. *Medical Oncology*. 28:1363-1372.

Yamaguchi, H., Y. Takeo, S. Yoshida, Z. Kouchi, Y. Nakamura, and K. Fukami. 2009. Lipid Rafts and Caveolin-1 Are Required for Invadopodia Formation and Extracellular Matrix Degradation by Human Breast Cancer Cells. *Cancer Research*. 69:8594-8602.

Yamaguchi, H., S. Yoshida, E. Muroi, N. Yoshida, M. Kawamura, Z. Kouchi, Y. Nakamura, R. Sakai, and K. Fukami. 2011. Phosphoinositide 3-kinase signaling pathway mediated by p110α regulates invadopodia formation. *Journal of Cell Biology*. 193:1275-1288.

Yamaoka, T., M.R. Frey, R.S. Dise, J.K. Bernard, and D.B. Polk. 2011. Specific epidermal growth factor receptor autophosphorylation sites promote mouse colon epithelial cell chemotaxis and restitution. *American Journal of Physiology Gastrointestinal and Liver Physiology*. 301:G368-376.

Yan, L., S. Zucker, and B.P. Toole. 2005. Roles of the multifunctional glycoprotein, emmprin (basigin;CD147), in tumour progression. *Thromb Haemost*. 93:199-204.

Yang, H., W. Zou, Y. Li, B. Chen, and X. Xin. 2007. Bridge Linkage Role Played by CD98hc of Anti-Tumor Drug Resistance and Cancer Metastasis on Cisplatin-Resistant Ovarian Cancer Cells. *Cancer Biology & Therapy*. 6:942-947.

Yang, J.-M., P. O'Neill, W. Jin, R. Foty, D.J. Medina, Z. Xu, M. Lomas, G.M. Arndt, Y. Tang, M. Nakada, L. Yan, and W.N. Hait. 2006. Extracellular Matrix Metalloproteinase Inducer (CD147) Confers Resistance of Breast Cancer Cells to Anoikis through inhibition of Bim. *Journal of Biological Chemistry*. 281:9719-9727.

Yang, J.-M., Z. Xu, H. Wu, H. Zhu, X. Wu, and W.N. Hait. 2003. Overexpression of Extracellular Matrix Metalloproteinase Inducer in Multidrug Resistant Cancer Cells. *Molecular Cancer Research*. 1:420-427.

Yang, L.-x., J.-s. Ye, R.-w. Guo, H. Liu, X.-m. Wang, F. Qi, and C. Guo. 2010a. The effect of the expression of angiotensin II on extracellular matrix metalloproteinase inducer (EMMPRIN) in macrophages is mediated via the ATI/COX-2/PGE_2 pathway. *Inflammation Research*. 59:1033-1040.

Yang, L., J.O. Nyalwidhe, S. Guo, R.R. Drake, and O.J. Semmes. 2011. Targeted Identification of Metastasis-associated Cell-surface Sialoglycoproteins in Prostate Cancer. *Molecular and Cellular Proteomics*. 10:M110.007294.

Yang, X., J. Dai, T. Li, P. Zhang, Q. Ma, Y. Li, J. Zhou, and D. Lei. 2010b. Expression of EMMPRIN in adenoid cystic carcinoma of salivary glands: correlation with tumor progression and patients' prognosis. *Oral Oncology*. 46:755-760.

Yilmaz, M., and G. Christofori. 2009. EMT, the cytoskeleton, and cancer cell invasion. *Cancer Metastasis Review*. 28:15-33.

Yoshida, S., M. Shibata, S. Yamamoto, M. Hagihara, N. Asai, M. Takahashi, S. Mizutani, T. Muramatsu, and K. Kadomatsu. 2000. Homo-oligomer formation by basigin, an immunoglobulin superfamily member, via its N-terminal immunoglobulin domain. *European Journal of Biochemistry*. 267:4372-4380.

Yu, X.-L., T. Hu, J.-M. Du, J.-P. Ding, X.-M. Yang, J. Zhang, B. Yang, X. Shen, Z. Zhang, W.-D. Zhong, N. Wen, H. Jiang, P. Zhu, and Z.-N. Chen. 2008. Crystal Structure of HAb18G/CD147: Implications for Immunoglobulin Superfamily Homophilic Adhesion. *Journal of Biological Chemistry*. 283:18056-18065.

Yurchenko, V., S. Constant, E. Eisenmesser, and M. Bukrinsky. 2010. Cyclophilin-CD147 interactions: a new target for anti-inflammatory therapeutics. *Clinical and Experimental Immunology*. 160:305-317.

Yurchenko, V., T. Pushkarsky, J.-H. Li, W.W. Dai, B. Sherry, and M. Bukrinsky. 2005. Regulation of CD147 Cell Surface Expression: Involvement of the proline residue in the CD147 transmembrane domain. *Journal of Biological Chemistry*. 280:17013-17019.

Zeng, C., B.P. Toole, S.d. Kinney, J.-w. Kuo, and I. Stamenkovic. 1998. Inhibition of tumor growth *in vivo* by hyaluronan oligomers. *International Journal of Cancer*. 77:396-401.

Zhang, H., J.S. Berg, Z. Li, Y. Wang, P. Lang, A.D. Sousa, A. Bhaskar, R.E. Cheney, and S. Stromblad. 2004. Myosin-X provides a motor-based link between integrins and the cytoskeleton. *Nature Cell Biology*. 6.

Zhang, J., X. Liu, A. Datta, K. Govindarajan, W.L. Tam, J. Han, J. George, C. Wong, K. Ramnarayanan, T.Y. Phua, W.Y. Leong, Y.S. Chan, N. Palanisamy, E.T.-B. Liu, K.M. Karuturi, B. Lim, and L.D. Miller. 2009. *RCP* is a human breast cancer-promoting gene wtih Ras-activating function. *Journal of Clinical Investigation*. 119:2171-2183.

Zhang, Q., X. Chen, J. Zhou, L. Zhang, Q. Zhao, G. Chen, J. Xu, F. Qian, and Z. Chen. 2006. CD147, MMP-2, MMP-9 and MVD-CD34 are significant predictors of recurrence after liver

transplantation in hepatocellular carcinoma patients. *Cancer Biology & Therapy*. 5:808-814.

Zhang, W., M. Erkan, I. Abiatari, N.A. Giese, K. Felix, H. Kayed, M.W. Buchler, H. Friess, and J. Kleeff. 2007. Expression of Extracellular Matrix Metalloproteinase Inducer (EMMPRIN/CD147) in Pancreatic Neoplasm and Pancreatic Stellate Cells. *Cancer Biology & Therapy*. 6:e1-e10.

Zhang, X., P. Liu, B. Zhang, A. Wang, and M. Yang. 2010. Role of STAT3 decoy oligodeoxynucleotides on cell invasion and chemosensitivity in human epithelial ovarian cancer cells. *Cancer Genetics and Cytogenetics*. 197:46-53.

Zhao, P., W. Zhang, J. Tang, X.-K. Ma, J.-Y. Dai, Y. Li, J.-L. Jiang, S.-H. Zhang, and Z.-N. Chen. 2010. Annexin II promotes invasion and migration of human hepatocellular carcinoma cells *in vitro* via its interaction with HAb18G/CD147. *Cancer Science*. 101:387-395.

Zhao, P., W. Zhang, S.-J. Wang, X.-L. Yu, J. Tang, W. Huang, Y. Li, H.-Y. Cui, Y.-S. Guo, J. Tavernier, S.-H. Zhang, J.-L. Jiang, and Z.-N. Chen. 2011. HAb18G/CD147 Promotes Cell Motility by Regulating Annexin II-Activated RhoA and Rac1 Signaling Pathways in Hepatocellular Carcinoma Cells. *Hepatology*. 54:2012-2024.

Zheng, H.-c., W. Wang, X.-y. Xu, P. Xia, M. Yu, T. Sugiyama, and Y. Takano. 2011. Up-regulated EMMPRIN/CD147 protein expression might play a role in colorectal carcinogenesis and its subsequent progression without an alteration of its glycosylation and mRNA level. *Journal of Cancer Research and Clinical Oncology*. 137:585-596.

Zheng, H.C., H. Takahashi, Y. Murai, Z.G. Cui, K. Nomoto, S. Miwa, K. Tsuneyama, and Y. Takano. 2006. Upregulated EMMPRIN/CD147 might contribute to growth and angiogenesis of gastric carcinoma: a good marker for local invasion and prognosis. *British Journal of Cancer* 95:1371-1378.

Zhou, F.X., H.J. Merianos, A.T. Brunger, and D.M. Engelman. 2001. Polar residues drive association of polyleucine transmembrane helices. *PNAS*. 98:2250-2255.

Zhou, Q., Y. Zhu, Z. Deng, H. Long, S. Zhang, and X. Chen. 2011. VEGF and EMMPRIN expression correlates with survival of patients with osteosarcoma. *Surgical Oncology*. 20:13-19.

Zhu, H., B. Evans, P. O'Neill, X. Ren, Z. Xu, W.N. Hait8, and J.-M. Yang. 2009. A role for p53 in the regulation of extracellular matrix metalloproteinase inducer in human cancer cells. *Cancer Biology & Therapy*. 8:1722-1728.

Zhu, H., J. Zhao, B. Zhu, J. Collazo, J. Gal, P. Shi, L. Liu, A.-L. Strom, X. Lu, R.O. McCann, M. Toborek, and N. Kyprianou. 2011. EMMPRIN Regulates Cytoskeleton Organization and Cell Adhesion in Prostate Cancer. *Prostate*. 72:72-81.

Zoltan-Jones, A., L. Huang, S. Ghatak, and B.P. Toole. 2003. Elevated Hyaluronan Production Induces Mesenchymal and Transformed Properties in Epithelial Cells. *Journal of Biological Chemistry*. 278:45801-45810.

Zucker, S., M. Hymowitz, C.E. Conner, E.A. DiYanni, and J. Cao. 2002. Rapid Trafficking of Membrane Type 1-Matrix Metalloproteinase to the Cell Surface Regulates Progelatinase A Activation. *Laboratory Investigation*. 82:1673-1684.

Zucker, S., M. Hymowitz, E.E. Rollo, R. Mann, C.E. Conner, J. Cao, H.D. Foda, D.C. Tompkins, and B.P. Toole. 2001. Tumorigenic Potential of Extracellular Matrix Metalloproteinase Inducer. *American Journal of Pathology*. 158:1921-1928.